ABSTRACT

FILPPONEN, ILARI. The Synthetic Strategies for Unique Properties in Cellulose Nanocrystal Materials. (Under the direction of Dr. Dimitris S. Argyropoulos and Dr. Lucian A. Lucia).

Cellulose is renewable, biodegradable and widely available natural biopolymer which upon acid hydrolysis yields highly crystalline rod-like rigid hydrophilic particles having nanoscale dimensions. The acid hydrolysis of cellulose fibers is a heterogeneous acid diffusion process wherein acid penetrates the less ordered amorphous regions and causes the cleavage of glycosidic bonds while leaving the highly organized crystalline regions undamaged. The penetration and the glycosidic bond breakage are known to depend on the hydrolysis conditions, the acid type, hydrolysis temperature, and acid concentration. Acid hydrolysis is typically done using either hydrochloric acid or sulfuric acid. The effect of reaction conditions to the production of cellulose nanocrystals (CNCs) was investigated in the present research. It was demonstrated that the use of ultrasonic energy during the acidic hydrolysis (HBr) elevates the yields of cellulose nanocrystals at lower reaction temperatures (80°C). At higher reaction temperatures (100°C), the ultrasonication was not seen to improve the yields of CNCs. The optimum conditions for the hydrolysis reaction, at given experimental set up, were found to be 2.5 M HBr, 3 hours at 100°C applying the ultrasonic energy in the course of the reaction.

A novel quantitative ^{31}P NMR methodology has been developed to determine the amount of reactive hydroxyl groups in cellulose. It was then used for the monitoring the amount of accessible hydroxyl groups in relation with the mechanical treatment and moisture content of cellulose.

Cellulose nanocrystals were modified starting either from the reducing end aldehyde or the surface hydroxyl groups. TEMPO-mediated oxidation was applied to selectively oxidize the primary hydroxyl groups on the surface of cellulose nanocrystals. The produced carboxylic sites were used for the grafting reactions with various amine bearing compounds using coupling agents such as N-hydroxysuccinimide (NHS) and 1-Ethyl-3-(3-dimethylaminopropyl)-carbodiimide (EDC). Moreover, suitable CNC precursors for the 1,3-dipolar cycloaddition reaction ("Click"-reaction) were developed. As a result, the cross linking of cellulose nanocrystals accompanied with the gel formation was demonstrated. Moreover, the "Click"-chemistry was successfully used for the creation of fluorescence cellulose nanocrystals.

The Synthetic Strategies for Unique Properties in Cellulose Nanocrystal Materials

by
Ilari Filpponen

A dissertation submitted to the Graduate Faculty of
North Carolina State University
In partial fulfillment of the
Requirements for the degree of
Doctor of Philosophy

Wood & Paper Science

Raleigh, North Carolina

July 2009

APPROVED BY:

Dr. Dimitris S. Argyropoulos Chair of Advisory Committee	Dr. Lucian A. Lucia Co-chair of Advisory Committee
Dr. Orlando J. Rojas Member of Advisory Committee	Dr. David C. Tilotta Member of Advisory Committee

BIOGRAPHY

Ilari Filpponen received a M. S. degree in Organic Chemistry from University of Helsinki, Finland in 2003

After graduation, he worked as a research assistant in the Laboratory of Organic Chemistry at University of Helsinki for 16 months until September, 2004. From October 2004 to July 2006 he worked as a research assistant in the Department of Wood & Paper Science, NCSU.

In August of 2006, he began the Ph. D. program in the Department of Wood and Paper Science under the guidance of Dr. Dimitris S. Argyropoulos and Dr. Lucian A. Lucia.

ACKNOWLEDGEMENTS

I would like to express my grateful and sincere appreciation to Dr. Dimitris S. Argyropoulos, Dr. Lucian A. Lucia and Dr. Orlando J. Rojas, co-chairmen of my advisory committee, for their inspiring and encouraging guidance, invaluable advice in my research, and their insightful comments during the entire process of this dissertation.

Sincere thanks also go to Dr. David C. Tilotta for his guidance, suggestions and assistance. I would also like to give thanks to Drs. Armindo Ribeiro Gaspar, Anderson de Almeida Guerra, Alistair King, Luca Zoia, Xingwu Wang, Bin Li, Nestor Urian Soriano, Jr., Haibo Xie, Carl Saquing, Qirong Fu, Hongyang Li, Ms. Barbara Ann White and Irma Sofia Contreras for their suggestions, discussions and friendships.

I would also like to thank all of my faculty members, colleagues and friends for their support and friendships during my three years at North Carolina State University.

In giving appreciation, I must acknowledge my parents for their unwavering love and support all through my life. I extend my appreciation to my in-laws and all relatives who have provided me an encouraging atmosphere and have been patient in waiting for me to finish this task. Above all, I thank my loving wife, Hanna-Kaisa, without whom this would not have been possible.

TABLE OF CONTENTS

LIST OF TABLES

LIST OF FIGURES

LIST OF SCHEMES

1. Introduction

1.1 Cellulose Chemistry

1.1.1 Origin

Cellulose is a renewable, biodegradable and the most abundant organic biopolymer on the Earth with more than 1 x 10^{11} tons produced and also destroyed each year.[1] It is the primary structural component of the cell wall of higher plants and it can be obtained from various sources like wood, some bacteria, fungi and some algae.[2,3] Grasses such as papyrus and bamboo are also important sources. The cellulose content in different plants and trees varies significantly. The highest content of cellulose can be found in cotton bolls (90-99%). Wood which is the most abundant lignocellulosics resource on the earth contains approximately 40-50% of cellulose. It is also a major component of jute (60-70%) and flax fibers (80%). Besides plant sources cellulose is also produced by tunicates, a class of sea animals.[4]

Besides being extremely important to the natural world, cellulose is also extremely important to human beings. Being derived from cellulose cottons and woods, this compound benefits human beings in the most basic ways, like clothing and writing. Cellulose is one of the oldest polymers and has a long history of industrial applications for making paper, textiles, plastics and food additives.[1] As a matter of fact, it has a large impact for the comfort and quality of our life. Although the development and

utilization of cellulose have a long history, the understanding of its chemistry and structure is relatively new. Most of the important developments took place between 1920 and 1940 but the research maintain to make progress as the scientists continue to publish papers on the structure, solubility and applications of cellulose and its derivatives.

1.1.2 Molecular Structure

In 1838, a French chemist Anselm Payen succeeded to isolate cellulose from various plant matters and determined its chemical formula by using elemental analysis.[5,6,7] However it required another fifty years for the basic cellulose formula to be established by Weillstatter and Zechmeister.[8] The early steps in the structural characterization of cellulose took place in the 1920's by the German chemist Hermann Staudinger who determined the polymer structure of cellulose.[9] It was due to his contribution that the macromolecular nature of cellulose was finally recognized and accepted.[10] The work by Irvine and Hirst and then Freudenberg and Braun showed that the carbon atoms 2, 3 and 6 in cellulose have free hydroxyls group available for reaction.[11,12] The investigations revealed that 2,3,6-trimethyl glucose was the only product from the methylation and hydrolysis of cellulose. In 1926 Dore *et al* proposed a cellulose structure which was closely followed by the discovery of the cellobiose structure by Haworth *et al.*[13] In 1930, Haworth *et al.* were able to prove that cellobiose is the only building block for cellulose polymer.[14] Crystallographic studies of D-glucose and cellobiose clearly established that the D-glucose residues had the $^{4}C_{1}$chair conformation.[15]

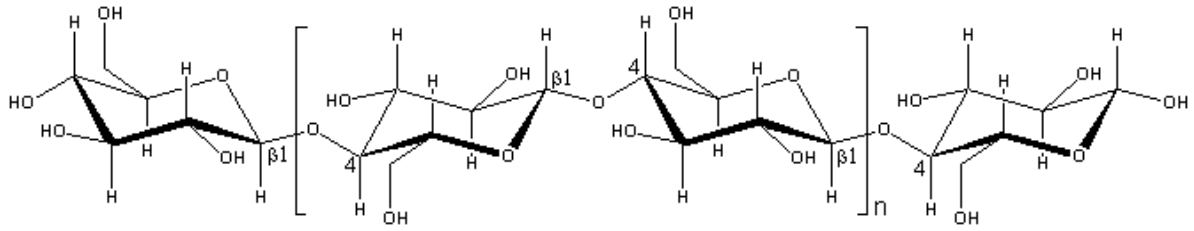

Figure 1.1 Chemical structure of cellulose

Cellulose is a high molecular-weight (10^6 or more) linear homopolymer of D-anhydroglucopyranose monomeric units connected through ß-(1,4) glycosidic linkages in the $^4C_1$ conformation (Figure 1.1). The fully equatorial conformation of ß-linked glucopyranose residues stabilizes the chair structure, minimizing its flexibility. The glucose units in cellulose polymer are referred to as anhydroglucose units when an alcohol and a hemiacetal react to form an acetal. Glucose anhydride, which is formed via the removal of water from each glucose molecule, is polymerized into long cellulose chains that contain 5000-10000 glucose units. The basic repeating unit of the cellulose polymer consists of two glucose anhydride units, called a cellobiose unit.

Each monomeric residue is oriented 180° to the next with the chain synthesized two residues at a time which identifies the disaccharide cellobiose. The orientation of the glycosidic linkages between the glucose monomers builds the glucose rings in cellulose polymer in a flip-flop manner which in turn generates a long straight rigid molecule. The stereochemistry at C-1 (acetal linkages) has an important role on the macromolecular properties of cellulose polymer. The hemiacetal formation between the hydroxyl at C-4 and

the carbonyl at C-1 can result in two different stereocenters at C-1 as the hydroxyl group at C-4 can attack the C-1 carbonyl from both sides of glucose. The resulting hydroxyl group at C-1 has two possible configurations, α and β. In cellulose the hydroxyl group at C-1 is on the same side of the ring with the C-6 carbon giving it β configuration. Starch on the other hand has α configuration and the hydroxyl group at C-1 is on the opposite side of the ring compared to C-6 carbon. As mentioned above the configuration at C-1 has large impact on the properties of the resulting polymer as the cellulose molecule have all of the larger groups in the equatorial positions. As a result of the bond angles in the β acetal linkage, cellulose is mostly a linear chain whereas the α acetal linkage gives starch a spiral much like a coiled spring form.

The two chain ends of cellulose polymer are chemically different (Figure 1.1). One end has a D-glucopyranose unit in which the anomeric carbon atom is involved in a closed ring structure (glycosidic linkage) whereas the other end has a D-glucopyranose unit in which the anomeric carbon atom is part of a cyclic hemiacetal functionality. The terminal hemiacetal group is in an equlibrium in which a small proportion is an aldehyde group which can act as a reducing group (can engage in a 2 electron reduction and transform to a carboxylic acid group) properties and hence called the terminal reducing end. The opposite end with closed ring structure is termed as the non-reducing end.

Plant-derived cellulose is usually contaminated with hemicelluloses, lignin, pectin and other substances, while microbial cellulose is quite pure, has much higher water content, and

consists of long chains. Four different crystalline allomorphs have been identified for cellulose: I, II, III and IV.[16] Each of these forms has its characteristic X-ray diffraction pattern. The characterization of cellulose ultrastructure has revealed the existence of subgroups within these four allomorphic forms. Cellulose that is produced by plants, called cellulose I or native cellulose, apparently is the most abundant form. However, its highly complex, three-dimensional structure comprising two distinct crystalline forms, cellulose I_α (triclinic) and I_β (monoclinic), has not yet been fully resolved.[17,18,19] The proportions of triclinic and monoclinic cellulose varies depending on its origin; I_α being found more in algae and bacteria whilst I_β is the major form in higher plants (woody tissues, cotton, ramie etc..). Cellulose II, generally occurring in marine algae, is a crystalline form obtained by regeneration of cellulose I from solution or by mercerization.[20,21,22] Cellulose II is often referred as a "regenerated" cellulose and the transition from cellulose I to cellulose II is irreversible indicating that cellulose II is thermodynamically more stable than metastable cellulose I**.** Cellulose I has all the cellulose strands arranged in a parallel fashion whilst cellulose II possesses an antiparallel strand arrangement.[23,24] Cellulose III is formed when cellulose I or cellulose II is treated with liquid ammonia or with certain amines such as ethylene diamine.[25,26,27] Cellulose III is similar to cellulose II but with the parallel chain arrangement, as in cellulose I_α and cellulose I_β.[28] The treatment of cellulose III at high temperature in the presence of glycerol generates cellulose IV crystalline form.[29]

The free hydroxyl groups present in the equatorial position in the cellulose macromolecule are likely to be involved in a number of *intra* and *inter* molecular hydrogen bonds which

gives rise to a variety of ordered crystalline arrangements. The hydrogen bonding organizes the chains together in highly ordered crystal-like structures which minimizes the flexibility and increases the strength of cellulose polymer by hindering the free rotation of the pyranose rings to their adjacent glycoside bonds. Part of a cellulose preparation is amorphous between these crystalline sections. The overall structure is of aggregated particles with extensive pores capable of holding relatively large amounts of water by capillarity (Figure 1.2).

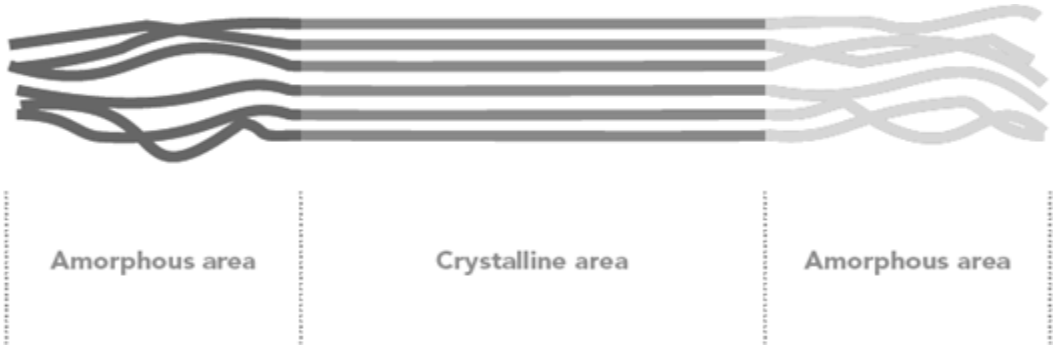

Figure 1.2 Crystalline and amorphous regions in cellulose microfibril. Reprinted from source: http://www.cottoninc.com/Cotton-Nonwoven-Technical-Guide/

Cellulose is insoluble in most common solvents due to the extensive and strong *inter*- and *intra*-molecular hydrogen bonding within the crystalline regions of polymer (Figure 1.3).[30,31] The *intra* chain hydrogen bonding between the C3-OH and endocyclic oxygen (O5) and/or the primary hydroxyl (C6-OH) and C2-OH are similar for both cellulose I and cellulose II However, the *inter* chain hydrogen bonding differs for cellulose I and II. In cellulose I, the inter chain hydrogen bonding occurs between the primary hydroxyl (C6-OH) of one chain and the C3-OH of the neighboring chain whereas in cellulose II shows the bonding takes place between C6-OH and C2-OH. The hydrogen bonding network also

increases the thermal durability of cellulose. Despite the comprehensive efforts by many investigators the exact structure of the strong hydrogen bonding network between the hydroxyl groups has not been fully resolved.

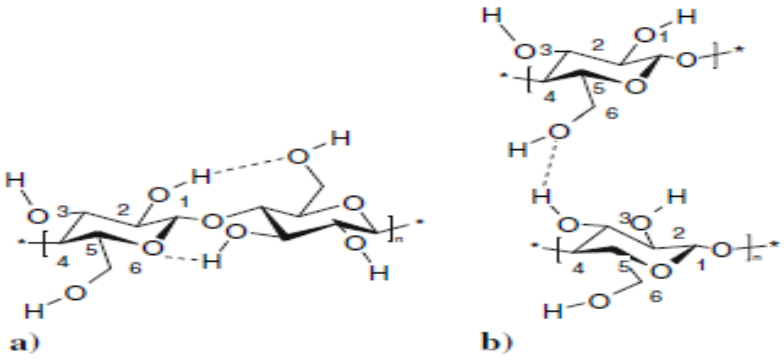

Figure 1.3 Intramolecular hydrogen bonding (a) and intermolecular hydrogen bonding (b) of cellulose (Krässig, 1993)

In the amorphous or less ordered regions the cellulose chains are not so tightly packed making them more available for hydrogen bonding to other molecules, such as water (Figure 1.4). Aqueous solutions are not capable to dissolve cellulose. However, the hydrogen bonding with water makes cellulose swell, i.e., to absorb rather large quantities of water.

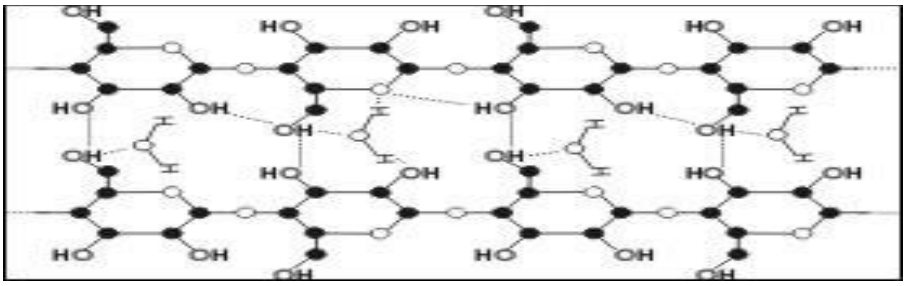

Figure 1.4 Hydrogen bonding between cellulose and water. Reprinted from source: http://www.lla.de/en/index.php/content/view/18/46/

The degree of polymerization (DP) of native celluloses depends on the source and it is not well established because the purification and separation process of cellulose involves various steps including pulping, partial hydrolysis, dissolution, re-precipitation and extraction with organic solvents. Such procedures generally cause the scission of the cellulose chain leading to underestimated values of DP depending on the methods used.[32] As a matter of fact, the reported DP values are ranging from hundreds to several tens of thousands.[33] The difficulties on the accurate determination of the DP of cellulose are accompanied with the challenges to verify the distribution of the chain lengths of cellulose polymer. However, it has been suggested by some researchers that the molecular mass distribution of cellulose has to be homogeneous within a given source.[34]

The structural analysis of cellulose is typically carried out by using techniques such as X-ray diffraction, electron microscopy, neutron diffraction and solid-state ^{13}C NMR spectroscopy.[35,36,37,38,39] Electron microscopy has been used to establish the microfibrillar structure of cellulose.[40,41] However, great variations in dimensions, depending on origin, have been reported.[42,43,44] Nevertheless, the utilization of the transmission electron microscopy has firmly established that the microfibril is the basic crystalline element of native cellulose.[45,46,47] Depending on their origin cellulose microfibrils have diameters from 2-20 nm while their length can achieve several micrometers.[48,49,50]

The structural investigations of native crystalline cellulose (Ramie) were initiated by Meyer *et al.* at in 1928.[51,52,53] It was proposed that the structure is made up of a monoclinic unit

cell of two polysaccharide chains oriented in antiparallel direction. It is worth mentioning here, that the early investigations were based on the assumption of all the native cellulose having similar structure (cellulose I). Only careful infrared spectroscopic studies by Mann *et al.* revealed the difference in cellulose structures obtained from the different sources.[54,55] Yet, the two distinct crystalline phases of cellulose remained unidentified. The results of Meyer *et al.* on the antiparallel orientation of cellulose chains were contradicted by Sarko *et al.* who proposed a model of parallel packing fashion of the cellulose chains.[56]

The development of new structural analysis methods led to the discovery of two distinct crystalline phases of native cellulose I named I_α and I_β, respectively. The existence of these two families was confirmed by the application of solid-state ^{13}C NMR to a variety of cellulose samples from different sources.[18,57,58] The occurrence of the dimorphism in native cellulose has been further evaluated by systematic investigations of a wide range of samples by X-ray diffraction, Raman spectroscopy and electron diffraction.[59,60,61,62] As a result the crystal forms of cellulose I_α and cellulose I_β are nowadays well established. Cellulose I_α has a triclinic unit cell containing one chain whereas cellulose I_β has a monoclinic unit cell containing two parallel chains, similar to the approximate unit cell proposed previously for cellulose I by Sarko *et al*. (Figure 1.5).

a) 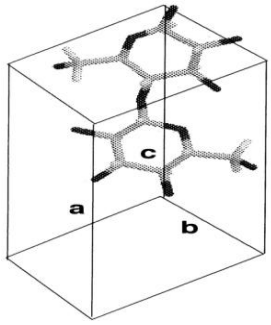

b) 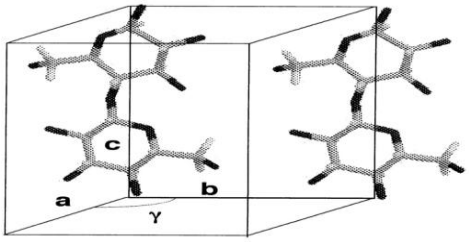

Figure 1.5 Schematic representation of chain packing in the unit cell of cellulose. Triclinic unit cell (a) and monoclinic unit cell (b). Reprinted from source: http://www.pnas.org/content/94/17/9091/F5.expansion

The celluloses produced by primitive organisms (bacteria, algae etc.) are enriched in the I_α phase whereas the cellulose of higher plants (woody tissues, cotton, ramie etc.) consists mainly of the I_β phase.[63,64] Cellulose I_α can be transformed to more thermodynamically stable form I_β by annealing the cellulose in the solid state.[65,66] The discovery of the crystalline dimorphism of cellulose has initiated a number of research projects endeavoring to evaluate the properties of each allomorph and methods for their interconversion.[64,67,68,69,,70]

1.1.3 Cellulose Properties

Cellulose has no taste, is odourless, is hydrophilic, is insoluble in water and most organic solvents, is chiral and is biodegradable. It is a long chain colloidal carbohydrate polymer that can be broken down into its glucose units by treating it with certain enzymes or concentrated acids at high temperature. As we know, cellulose has more crystalline

structure compared to starch. Whereas starch undergoes a crystalline to amorphous transition when heated beyond 60-70 °C in water (as in cooking), cellulose requires a temperature of 320 °C and pressure of 25 MPa to become amorphous in water.[71]

Table 1.1 Average DP of cellulose obtained from different sources. Reprinted from the reference 73.

Source	$*DP_w$ (10^3)
Wood	8-9
Cotton	8-15
Valonia	25-27
Acetobacter xylinum	2-6
Pulp	2.1
Flax	7-8

$*DP_w$ weight average DP determined by viscometric methods.[72]

Many properties of cellulose depend on its chain length or degree of polymerization (DP). For instance, cellulose from wood pulp typically has chain lengths between 300 and 2500 units whereas cotton and other plant fibers as well as bacterial celluloses have chain lengths ranging from 2000 to 27,000 units (Table 1.1).[73] Molecules with very small chain length resulting from the breakdown of cellulose are known as cellodextrins; in contrast to long-chain cellulose, cellodextrins are typically soluble in water and organic solvents.

The strong hydrogen bonding network within the cellulose molecules greatly affects to the properties of cellulose polymer. For instance, properties such as swelling, absorption and

optical behavior are influenced by the hydrogen bonding.[74] Swelling of cellulose is to a certain extent reversible when the surrounding humidity level is increased or decreased. However, there is a distinct hysteresis effect in the absorption/desorption curves. The desorption curves typically show higher moisture content values than absorption curves.[62] Hysteresis is caused by the inaccessible hydroxyl groups of the cellulose in the dry state that can become accessible only after more water is absorbed, i.e., at dry state hydroxyl groups satisfy each other through adjacent free hydroxyl groups but as the moisture increases the hydrogen bonding breaks while more water is absorbed.

Cellulose's tendency to form crystals utilizing extensive intramolecular and intermolecular hydrogen bonding makes it completely insoluble in normal aqueous solutions. However, it is soluble in more exotic solvents, such as aqueous N-methylmorpholine-N-oxide (NMNO), CdO/ethylenediamine (cadoxen), or LiCl/N,N'-dimethylacetamide, or near supercritical water and in some ionic liquids.[75,76,77]

1.1.4 Cellulose Derivatives

The history of cellulosic materials contains numerous technologies for chemical and mechanical modification of cellulose. Some of these technologies have been applied to produce modified cellulosic materials for our daily and industrial needs.[78] Cellulosic materials are generally strong, hydrophilic, biodegradable, recyclable and insoluble in

water. Typically, the purpose of the modifications is either to reinforce the original properties of cellulose or to add new functionalities in order to create a cellulosic product with specific properties.

By virtue of the hydroxyl groups of cellulose polymer it can be partially or fully reacted with various reagents to yield derivatives with industrial and commercial potential. Due to the fact that cellulose is insoluble in most common solvents derivatization reactions are typically carried out in heterogeneous media which limits the accessibility of reagents thus decreasing the overall reaction efficiency. In general, it is easier for the reagents and solvents to penetrate into the amorphous region than the crystalline region of cellulose. As we know, cellulose is a homopolymer comprised of anhydroglucopyranose monomers connected by β-1-4-glycosidic linkages. This type of structure consists of three different kinds of anhydroglucopyranose units. The reducing end of the cellulose contains three hydroxyl groups and a free hemi-acetal group at C-1 whereas the non reducing end contains four hydroxyl groups at C-2, C-3, C-4 and C-6. Moreover, each of the anhydroglucopyranose repeating units contains three hydroxyl groups at C-2, C-3 and C-6. The hydroxyl groups at C-2 and C-3 are secondary while the one in C-6 is primary.

Due to the large presence of hydroxyl groups in the cellulose polymer the main derivatization reactions are based on alcohol chemistry. Reactions like etherification and esterification are the most typical approaches for the cellulose modification. However, steric factors, as a result of the crystalline structure of cellulose, diminish the reactivity of a

preponderance of the hydroxyl groups. The degree of substitution (DS) is a value used to characterize the reactivity of cellulose. It ranges from 0 to 3 based on the three hydroxyl groups in anhydroglucopyranose repeat units. In many cases, because of the poor accessibility of crystalline regions, the DS is notably lower than 3 indicating partial reactions in the less ordered amorphous regions of cellulose. Reaction conditions that are able to disrupt the extensive *inter*- and *intra*-molecular hydrogen bonding network (crystalline region) generate products with higher DS values thus making them soluble in more common solvents.

Cellulose derivatives can be used as adhesives, explosives, thickening agents in food, and moisture-proof coatings. The most important commercial materials are cellulose esters and cellulose ethers. Among the esters are cellulose acetate and cellulose triacetate that are used in wide variety of applications such as film- and fiber-forming materials, tools, toys and packaging materials. Cellulose acetate was first introduced in the 1930s by reacting cellulose, acetic acid, acetic anhydride and a catalyst. In 1833, Henri Braconnot discovered that nitric acid when combined with the plant substances produced a lightweight combustible material which he named xyloidine.[79] This invention was the beginning of the nitrocellulose chemistry. Years later, in 1846, a German-Swiss chemist Christian Friedrich Schönbein introduced a more practical solution to prepare cellulose nitrate.[80] He immersed cotton in the equal mixture of sulfuric acid and nitric acids resulting in a more versatile reaction because of the catalytic effect of sulfuric acid. Cellulose nitrate was initially used

as an explosive and was an early film forming material. Also, it was extensively used in the automobile industry for 30 years when the nitrocellulose lacquers were developed in 1920s.

As mentioned above, the typical cellulose modifications reactions are esterification and etherification at the hydroxyl groups of cellulose. Esterifications include acetylations with acetic acid or acetic anhydride which produce cellulose derivatives with different properties depending on the degree of substitution. Etherifications are carried out using different types of alkylating reagents such as chloroacetic acid, methyl chloride, benzyl chloride and ethylene oxide. Other type of modification reactions are ionic and radical grafting, oxidation and deoxyhalogenation. The main aim of the derivatization reactions is to change the original properties of cellulose. Properties such as hydrophobicity and solubility, both in water and organic solvents can be tailored by installing different functionalities onto cellulose. Many of the cellulose derivatives have found commercial use including ethyl cellulose, carboxymethyl cellulose, methyl cellulose and hydroxypropyl cellulose.

It has been known for a while that certain room temperature ionic liquids (ILs), consisting of organic cations and organic or inorganic anions, can efficiently dissolve cellulosic materials at mild temperatures.[77,81,82,83,84] The poor solubility of cellulose in common solvents is due to the strong inter- and intramolecular hydrogen- bonding network.[85] It has been difficult to achieve a homogeneous solution of cellulose without using harsh conditions, which in turn often affects negatively to the degree of polymerization (DP). In addition, the hydrogen-bonding pattern diminishes the reactivity of cellulose, and often the

DS values achieved from heterogeneous modifications reactions have ranged from poor to moderate. The ionic liquid is capable of disrupting the hydrogen bonds between different polysaccharide chains. This interaction decreases the crystallinity of cellulose and makes the carbohydrate fraction more susceptible to derivatization reactions. The chemical modification of cellulose in ILs is relatively straightforward and products such as cellulose acetates, tosylates and benzoates have been achieved with high degrees of substitutions.[86,87,88,89]

1.1.5 Industrial Applications

Undoubtedly, paper manufacture is one of the major discoveries in human history.[90] Its birth goes far back to the beginning of our current era (100 AD) when it was found in China that paper sheets can be prepared by using cellulosic fibers. Since then cellulose has become one of the most important materials for writing documents. The significance of paper and paper products is apparent to everyone. Annually, around 300 million metric tons of paper and paperboard is produced world-wide. Approximately 45% of the paper production is used for printing and writing grades, 40% for packaging and 15% for hygienic, health care and other specialized products.

About a third of the world's production of purified cellulose is used as the base material for a number of water-soluble derivatives with pre-designed and wide-ranging properties dependent on groups involved and the degree of derivatization.[91] Derivatizing cellulose

interferes with the orderly crystal-forming hydrogen bonding, as described above, so that even hydrophobic derivatives may increase the apparent solubility in water. Methyl cellulose (made by methylating about 30% of the hydroxyl groups) is thermogelling, forming gels above a critical temperature due to hydrophobic interactions between high-substituted regions and consequentially stabilized intermolecular hydrogen bonding. Such gels break down on cooling. In a manner similar to that causing the solubility minimum for non-polar gases; hydrophobic saccharides become less soluble as the temperature increases.[92] This property is useful in forming films as barriers to water loss and for holding on to small gas bubbles. Methylcellulose finds uses as thickener and emulsifier, lubricant, glue and binder, artificial tears and saliva

Hydroxypropylmethylcellulose (HPMC) has similar properties and uses but with added water interaction and surface activity.[93] Both methylcellulose and HPMC may be used in gluten-free bakery products as gluten substitutes. Hydroxypropyl cellulose possesses good surface activity but does not gel as it forms open helical coils. It is a water-soluble thickener, emulsifier and film-former often used in tablet coating. Another important derivative of cellulose is carboxymethylcellulose.

Cellulose has many uses as an anticake agent, emulsifier, stabilizer, dispersing agent, thickener, and gelling agent but these are generally subsidiary to its most important use of holding on to water.[94,95] Water cannot penetrate crystalline cellulose but dry amorphous cellulose absorbs water becoming soft and flexible. Some of this water is non-freezing but

most is simply trapped. Less water is bound by direct hydrogen bonding if the cellulose has high crystallinity but some fibrous cellulose products can hold on to considerable water in pores and its typically straw-like cavities; water holding ability correlating well with the amorphous (surface area effect) and void fraction (that is, the porosity). As such water is supercoolable (remains liquid below its freezing point), this effect may protect against ice damage. Cellulose can give improved volume and texture particularly as a fat replacer in sauces and dressings but its insolubility means that all products will be cloudy.

The inorganic ester nitrocellulose was initially used as an explosive and was an early film forming material. Cellulose nitrate was the first successful plastic made in 1869 by converting alcoholic cellulose into nitrate esters. Cellulose nitrate also helped the automotive industry, when polishers were developed in the 1920s. Now, it is used in making toilet pieces, membranes, lacquers and other industrial items.

Ethylcellulose, a water-insoluble commercial thermoplastic used in coatings, inks, binders, and controlled-release drug tablets; is produced when alkali cellulose is treated with ethyl chloride or ethyl sulfate. This compound is used in making flashlight cases, fire extinguishers and electrical appliance parts. It is the lightest and the most expensive of the cellulosics.

Hydroxypropyl cellulose (HPC) is a cellulose derivative with both water and organic solubility. It is used as a lubricant for artificial eyes as well as thickener and emulsion

stabiliser in food industry. In pharmaceutical industry it can be used as a disintegrant and binder in tablet preparations.[96,97] HPC also has applications in analytical chemistry as it is used as a sieving matrix for DNA separations by capillary and microchip electrophoresis[98]. HPC forms liquid crystals and many mesophases according to its concentration in water. Such mesophases include isotropic, anisotropic, nematic and cholesteric. The last one gives many colors such as violet, green and red.

Carboxymethylcellulose (CMC), which is prepared from the pure cellulose of cotton or wood, absorbs up to fifty times its own weight of water to form a stable colloidal mass. It is a non-toxic high viscosity product which is used in food science as a viscosity modifier or thickener, and to stabilize emulsions in various products including ice cream. It is also a constituent of many non-food products, such as toothpaste, water-based paints, detergents, textile sizing and various paper products. Table 1.2 summarizes some of the uses of cellulose derivatives.

The most recent developments in the cellulose industry have taken place in the production of artificial fibers. Such fibers can be prepared by spinning or drawing the solutions of cellulose or derivatives. These artificial fibers are produced in three different methods. The first method utilizes cellulose nitrates which are first dissolved in ether-alcohol. The resulting solution is then spun through fine glass jets into air or water, where the unit threads are twisted together comprising the thread used for weaving. Another method is somewhat similar as it employs the cupro-ammonium solution of cellulose which is being

spun or drawn into a strong acid bath regenerating cellulose hydrate in continuous length.[99] The third method, developed for viscose cellulose solutions, is used in the production of artificial silk. In this technique the alkaline solution of the cellulose derivative is drawn either into concentrated ammonium salt solutions or into acid baths producing artificial silk as the product. In addition, the viscose solution of cellulose has industrial importance in several applications including paper-sizing, paper-coating and textile finishes.

Table 1.2 Summary of some common cellulose derivatives. Reprinted from source: http://www.herc.com/aqualon/product_data/aq_bro_cmc_appendix.html

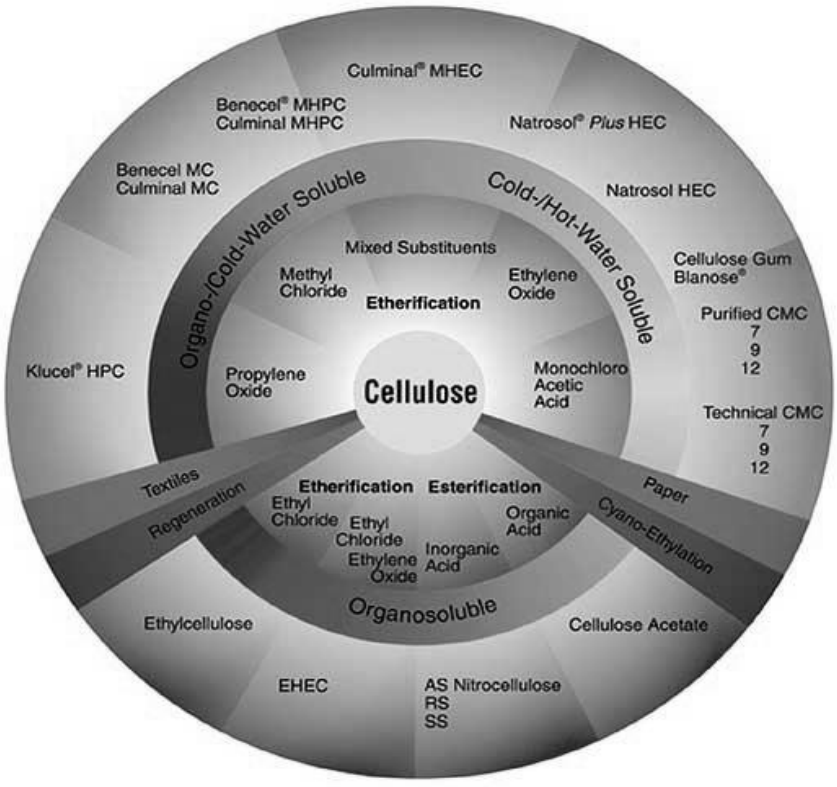

1.2 Cellulose Nanocrystals (CNCs)

1.2.1 Introduction

Nanotechnology, though still in an emerging stage, is currently one of the most promising venues of technological development and is expected to grow enormously in coming years.[100] Probably the most cited definition is found from the NASA's website where nanotechnology is recognized as "creation of functional materials, devices and systems through control of matter on the nanometer length scale (1-100 nanometers), and exploitation of novel phenomena and properties (physical, chemical, biological) at that length scale."[101] The unique properties of nanomaterials and of structures at the nanometer scale (at least one dimension is < 100 nm) have sparked the attention of scientists and engineers in diverse areas, such as, physics, chemistry, materials, information technology, and even bioscience.[102]

Manipulating matter at a nanoscale level has been shown to offer enhanced product performance, examples include, fillers in plastics, coatings on surfaces, and UV-protectors in cosmetics.[103] Particularly, the incorporation of nanoscale materials into the conventional polymer matrices has created a broad range of novel applications. Albeit the idea of adding fillers into the polymers is not a new one nanoscale materials can offer further improvements in mechanical, thermal, electrical and barrier properties compared to conventional composites.[104] These advantages are mainly derived from their high aspect

ratio, high interfacial area and their extent of dispersion and percolation, which takes place when the filler particles start physically interacting and form a continuous network.[105] In addition, some nano-sized fillers can provide composites with preferred properties at far less filler content when compared to conventional fillers. This in turn will contribute to the overall density of composites and desired materials with significantly reduced weight can be achieved.[106]

Nanomaterials and nanotechnology could pervade almost any industry--including medicine, plastics, energy, electronics, and aerospace. Nanomaterials and nanoscale engineering will play a critical role in the future of information technology and biotechnology. Indeed, they are already an integral part of today's data storage media, semiconductor manufacturing, biomedical research and emerging memory, computing, optical, and sensing devices. Nanoparticles, quantum dots, nanowires, nanotubes, and nanoscale films along with new nanofabrication technologies, such as chemical self-assembly and novel soft lithography techniques, will allow for continued advancements in a diverse range of products, from drug delivery systems to chemical sensors. Nanocrystalline materials are exceptionally strong and hard at high temperatures, and offer great resistant to wear, erosion, and corrosion.

Cellulose is one of the most abundant natural biopolymers which upon acid hydrolysis yields highly crystalline rod-like hydrophilic particles at the nanoscale level.[107,108,109] Compared to other nanomaterials it is low in cost and density (Table 1.3). Cellulose

nanocrystals have high aspect ratio (length/diameter) varying between 30 – 150 depending on the source from which it is obtained.[110,111]

Table 1.3 Density and cost of some frequently used reinforcing fillers.

Materials	Density (g/cm3)	Cost ($/kg)
Cellulose nanocrystal	1.5	1.8-2.0
Glass fiber	2.6	1.3-2.0
Aramid	1.45	22-33
Flax	1.5	0.22-1.1
Boron	2.45	330-440

The advantage for the applications of cellulose nanocrystals, besides them being relatively cheap biodegradable materials is their competitive mechanical properties. For example, cellulose nanocrystals can be considered stronger than steel and stiffer than aluminum. Their elastic modulus and tensile strength have been reported to be 145 GPa and 7.5 GPa, respectively (Table 1.4).[112,113]

Table 1.4 Strength and stiffness of cellulose nanocrystals compared to other materials. Reprinted from the source: http://woodscience.oregonstate.edu/faculty/simonsen/

Material	Tensile strength (GPa)	Modulus (GPa)
Cellulose nanocrystal	7.5	145
Steel wire	4.1	207
Glass fiber	4.8	86
Carbon nanotubes	11-73	270-970

1.2.2 Preparation, Structure and Properties

Cellulose is a biopolymer of D-anhydroglucopyranose monomeric units linked together by β-1, 4-glycosidic bonds that can be easily cleaved by mineral acids.[114] Natural cellulose is a semi-crystalline polymer composed of amorphous and crystalline domains.[115] Cellulose nanocrystals are the crystalline portion of cellulose. The highly ordered, hydrogen bonded and extended macromolecular packing within the crystalline domains limits access of chemicals, and therefore such regions are much more stable to acid hydrolysis treatments compared to their amorphous counterparts. Proper selection of the reaction conditions can selectively degrade and remove the amorphous cellulose without significantly affecting the crystalline domains. The hydrolysis process, which was first described by Ranby at 1951, is also known to cleave the elemental microfibrils of cellulose into smaller particles at the nanoscale level (Figure 1.6).[116]

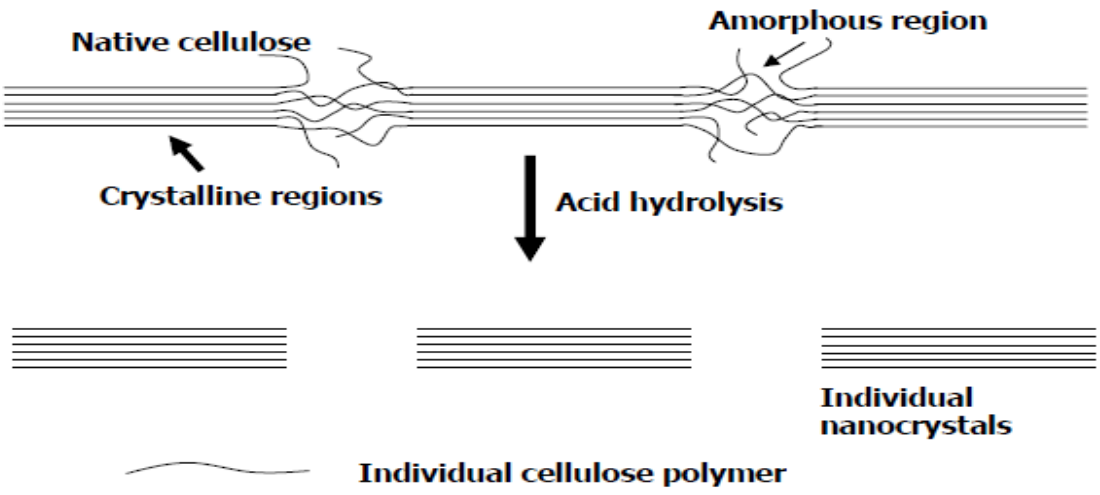

Figure 1.6 Acid hydrolysis of cellulose to form cellulose nanocrystals

The acid hydrolysis of cellulose fibers is considered to be a heterogeneous acid diffusion process where the less ordered amorphous regions are attacked by acid resulting in the cleavage of glycosidic bonds. The overall efficiency of the hydrolysis process is affected by several factors such as acid type, hydrolysis temperature, and acid concentration.[117] The reaction continues until all the amorphous region is hydrolyzed to glucose and then slows down significantly as the remaining acid attacks to the surface of the residual crystalline regions as well as the reducing end groups of cellulose. The selection of hydrolysis conditions plays an important role in the production of cellulose nanocrystals. On the one hand the amorphous region needs to be hydrolyzed but the conditions should be mild enough to avoid complete hydrolysis of cellulose to glucose or even carbonization. A vast majority of the research has been done by using either hydrochloric acid or sulfuric acid. For example, Dong *et al.* studied the optimum conditions for the production of cellulose nanocrystals and it was concluded that a hydrolysis temperature of 45 °C and hydrolysis time of 60 min completely hydrolyzes the amorphous regions leaving behind crystalline particles with the length of approximately 200 nm.[118] Cellulose nanocrystals have high specific strength and stiffness but they are fairly brittle when used by themselves. Due to their prominent strength properties cellulose nanocrystals have been advantageously incorporated in the polymer matrixes as reinforcing fillers. Moreover, the dispersion of cellulose nanocrystals can be used as a vapor-proof barrier for diffusing vapor as vapors are not able pass through the crystal structure.[119]

The dimensions of the cellulose nanocrystals depend on several factors, including the cellulose source, the hydrolysis conditions, and ionic strength.[120] For example, the dimensions for crystallites obtained from cotton, bleached softwood Kraft pulp and *Valonia* have found to be 7 x (100 – 300) nm, (3 – 5) x 180 ± 75 nm and 20 x (100 – 2000) nm, respectively.[118,121,122] Moreover, the high aspect (length to width) ratio is an important factor in contribution of the formation of anisotropic phase in cellulose nanocrystal suspensions.[123]

The ultrastructure of individual cellulose nanocrystals has been studied with several techniques such as small angle neutron scattering (SANS), atomic force microscopy (AFM), high resolution solid-state NMR spectroscopy and small angle X-ray scattering (SAXS).[124,125,126,127] The scattering data was in agreement with the electronic microscopic investigations and showed the cellulose nanocrystals as rod-shaped particles with a high aspect ratio (*L*/*d*). Cellulose whiskers from tunicin were studied by small angle neutron scattering (SANS) and it was concluded that the crystals have cross-sectional rectangular shape with the lateral dimensions of 88 × 182 Å.[128] It is worth to note that these results correlated well with the previous crystallographic data.[129] Recently, Leppanen *et al.* used small angle X-ray scattering (SAXS) technique to investigate the ultrastructures of microcrystalline celluloses (MCC) achieved from different sources.[130] For example, MCC from cotton linters was found to have rectangular shape with the cross-sectional dimensions of 40±18 Å. Topographical high-resolution AFM images of cellulose crystallites derived from a green alga, *Valonia*, have revealed a detailed description of spacings between the

cellulose chains within the crystalline unit cell.[125] The images showed approximately 6 Å intermolecular spacing between the individual cellulose chains inside the crystallite.

In suspension, cellulose nanocrystals have a strong propensity to align along a vector director because of their rigid rod-like shape. This alignment produces a macroscopic birefringence that can be directly observed through crossed polarizers. The first observation of the birefringent nature of cellulose nanocrystals was made by Marchessault et al.[131] When the cellulose nanocrytals suspension reaches a critical concentration a chiral nematic ordered phase displaying optical characteristics can be formed.[132,133] The chiral nematic, or cholesteric, phase is formed by virtue of the self-alignment of the particles along a vector director in a packed nematic plane (*n)* with the orientation of each director rotated about the perpendicular axis from one plane to the next, as shown in Figure 1.7a. It has been postulated that the chiral interaction arises from the packing of screw-like rods (see Figure 1.7b). It is important to note here that the chiral nematic orders can be preserved after evaporation of the solvent (normally water) to produce iridescent films of cellulose I. The reflected color of films can be controlled by changing either salt content of the suspension or by applying an electric field.[134,135]

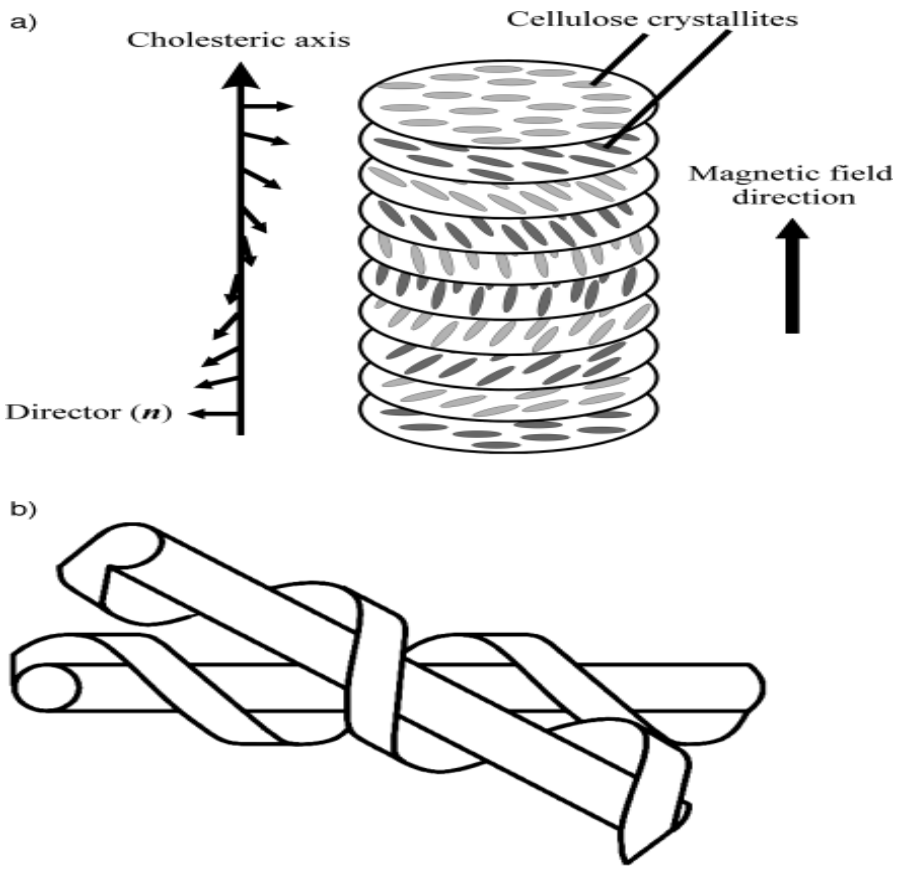

Figure 1.7 a) Schematic representation of the chiral nematic phase of cellulose nanocrystals. b) Schematic model of the tight packing of screw-like rods. Reprinted from source: http://www3.interscience.wiley.com/cgi-bin/fulltext/80002079/HTMLSTART

1.2.3 Derivatization Reactions

The rigid rod-like cellulose nanocrystals offer various unique features by virtue of their structure. Firstly, they are molecular constructions whose nano dimensions can be altered in accordance with the cellulose hydrolysis conditions. Secondly, the cellulose chains are known to be uni-directionally oriented and as such the nanocrystals contain a site of

concentrated reducing end groups on one end of the crystal. This asymmetric structural characteristic of cellulose nanocrystals provides an opportunity to create novel nanomaterials by selectively grafting polymer chains to one end of these rigid rods. In fact, the viability of the selective grafting has been demonstrated by Saglam *et al*. who anchored various small molecules at the end of cellulose micro-crystals.[136] Subsequently, the anchored sites were coupled with polydimethylsiloxanes resulting in block polymers that displayed a pronounced tendency to form specific super-structures in slurries and films made from it. In addition, cellulose nanocrystals, similarly with the cellulose polymer contain a variety of hydroxyl functionalities on their surface. The validity of using these hydroxyl groups as reactive sites for the creation of new nanomaterials has already been widely explored.[137,138,139,140,141]

Based on the aforementioned properties of cellulose nanocrystals it is logical to assume that the properties of such nanomaterials can be tailored and accordingly tuned by simply varying the size of cellulose nanocrystals, the structure of the polymer blocks (such as chain length, polymer architecture and type), as well as the location and density of the grafting. Furthermore, the individual properties of the grafted polymer precursors (such as chain flexibility, hydrophobicity, binding capacity, thermal behavior etc) will have a significant impact to the properties of new materials. Such properties can be controlled and tuned by altering the nature of the grafted polymers as well as the coupling chemistry utilized. The opportunities provided by such designs are exceptional with numerous potential applications. It is worth to mention here that adding stimuli responsive functionalities to the

selectively grafted polymers or other molecules coupled to the nanocrystals could lead to novel nanodevices.

1.2.4 Applications

Cellulose nanocrystals have been used as reinforcing materials in polymeric nanocomposites displaying enhanced properties when compared to conventional fillers.[142,143,144,145] Several studies have demonstrated the utility of cellulose nanocrystals in enhancing the mechanical properties of polyoxyethylene based polymer electrolyte systems.[146,147,148] However, the high hydrophilicity of cellulose has set limitations to its applications in non-polar composites. To overcome this deficiency, a variety of methods have been proposed for the surface modification of cellulose nanocrystals. These modifications include the use of surfactants possessing polar heads and long hydrophobic tails,[149] as well as the grafting of various hydrophobic moieties on the surface of cellulose nanocrystals.[140,150,151] The surface modifications produced cellulose nanocrystals dispersible in non-polar solvents but their utility toward aqueous media was diminished. Therefore, modification of the cellulose nanocrystals with hydrophobic blocks while retaining their hydrophilic character can greatly expand their application areas toward both polar and non-polar environments. Moreover, selective grafting of the hydrophobic polymer chains at specific locations on the cellulose nanocrystals should further promote their utility. The weak boundary layers between the individual components are often responsible for the composite failures that are typically occuring between polar and non-polar materials.

However, strong boundary adhesion can be achieved by surface modification and crosslinking reactions. Therefore, a site-spesific and uniform grafting of cellulose nanocrystals with hydrophobic polymer chains, should offer strong interactions with both polar and non-polar components, and thus provide strong boundary binding. Furthermore, the high melting temperature of the cellulose nanocrystals may further benefit the thermal transition properties of any covalently attached functional polymers on them. It is therefore likely that the increase in the overall thermal stability of the composites will expand the application temperature ranges of such composites.

In fact, cellulose has been covalently grafted with various synthetic polymers aiming to various applications. Kim *et al.* grafted polyallylamine to porous cellulose gels in order to enhance the ion exchange capacity of columns that are used as packing material in liquid chromatography.[152,153] Another study introduced the grafting of poly(ethylene glycol) to cellulose microcrystals to increase the stability of such suspensions by establishing steric stabilizing effects.[154] However, in all cases these grafting reactions were random with no particular site specificity on the morphology and nanocrystal architecture.

The potential applications utilizing the self-assembly of chiral nematic phases of cellulose nanocrystal suspensions have lately sparked an increased amount of attention. It has been known for a long time that cellulose derivatives can form iridescent liquid and solid phases.[155] Therefore, it is possible to prepare colored cellulose nanocrystal films by adding small quantities of electrolytes in to the suspension before the evaporation.[135] The intensity

of the reflected colors depends primarily of the uniformity and direction of the chiral nematic phase. Possible areas of application include security paper including bank notes, passports, and certificates because the optical properties cannot be reproduced by printing or photocopying.[156] They can also be used to form optically variable ink pigments whose colors depend on the viewing angle.[135]

Polysaccharides have recently gained increased attention as surface coatings for drug carriers.[157] Moreover, the possibility to use cellulose nanocrystals in pharmaceutical applications has been realized and substantial amount of research has been put for cellulose nanocrystal based drug delivery systems.[158] The properties required for suitable delivery systems are preferred biodistribution, an efficient delivery of the therapeutic agent to the targeted tissue, and sufficient rate for the departure from the host.[159] The blood circulation time of the drug carriers is a sum of several factors. It has been proposed that features such as small size, biocompatibility and hydrophilicity can extend the blood circulation times of the potential carriers.[160] Another advantage, besides the prolonged circulation time, is the presence of reactive hydroxyl groups on the surface of polysaccharides. This can be beneficial as far as the chemical coupling of functional agents is taken into a consideration. The several reported properties of cellulose nanocrystals show potential to be efficiently utilized in the development of new drug delivery systems[120,161,162]

1.3 References

1. Hon, D. N. S. (1994). "Cellulose: a random walk along its historical path," *Cellulose*, 1994, 1(1), 1-25.

2. Shibazaki, H., Kuga, S., Onabe, F., and Brown, R. M. J. (1995). "Acid hydrolysis behaviour of microbial cellulose II," *Polymer*, 36(26), 4971-4976.

3. Robyt, J. F. Essentials of Carbohydrate Chemistry. 1998, XV, 399 p. 370, ISBN: 978-0-387-94951-2.

4. Kimura, S. and Itoh, T. (1995). "Evidence for the role of the glomerulocyte in cellulose synthesis in the tunicate, *Metandrocarpa uedai*," *Protoplasma, 186(1)*, 24-33.

5. Payen, A. (1838). *Compt. Rend, 7*, 1052-1125.

6. Crawford, R. L. (1981). Lignin biodegradation and transformation. New York: John Wiley and Sons.

7. Young, Raymond (1986). Cellulose structure modification and hydrolysis. New York: Wiley.
8. Willstätter, R. and Ber, Z. L. (1913). Zur Kenntnis der Hydrolyse von cellulose. I, 46, 2401-2412.

9. Staudinger, H. (1920). "Über Polymerisation". *Ber. Deut. Chem. Ges.*, 53, 1073.

10. Staudinger, H. (1926). "Die Chemie der hochmolekularen organischen Stoffe im Sinne der Kekulèschen Strukturlehre," *Ber. Deut. Chem. Ges.*, 59, 3019-3043.

11. Irvine, J. C. and Hirst, E. L. (1923). "The constitution of polysaccharides. Part VI. The molecular structure of cotton cellulose," *J. Chem. Soc.*, 123, 518-532.

12. Freudenberg, K. and Braun, E. (1928). Mitteilung über Lignin und Cellulose Ann., Methylcellulose 5, 460, 288-304.

13. Dore, W. H. and Sponsler, O.L. (1926). *Colloid Symposium Monogr*. *4*, 174-202.

14. Hirst, E. L., Thomas, H.A. and Haworth, W. N. (1930). "The existence of the cellobiose residue in cellulose," *Nature, 126(3177)*, 438.

15. Chu, S. S. C. and Jeffrey, G. A. (1968). "The refinement of the crystal structures of β-D-glucose and cellobiose," *Acta Cryst.*, 24, 830-838.

16. Howsmon, J. A. and Sisson, W. A. (1963). "High polymers, structure and properties of cellulose fibers. B-submicroscopic structure, in cellulose and cellulose derivatives," Part I, V, 231-346.

17. Kuga, S.; Brown, R. M. J. (1988). "Silver labeling of the reducing ends of bacterial cellulose," *Carbohydr. Res.,180,* 345-350.

18. Atalla, R. H. and VanderHart, D.L. (1984). "Native cellulose: a composite of two distinct crystalline forms," *Science*, 223, 283-285.

19. VanderHart, D. L. and Atalla, R. H. (1984). "Studies of microstructure in native celluloses using solid state ^{13}C NMR," *Macromolecules,* 17(8), 1465-1472.

20. Andress, K. R. Z. (1929) *Phys. Chem. Abt*. B, *4*, 190.

21. Blackwell, J. and Kolpak, F. J. (1976). "Packing analysis of carbohydrates and polysaccharides. Molecular and crystal structure of regenerated cellulose II," *Macromolecules, 9,* 851-857.

22. Chanzy, H., Nishiyama, Y., and Langan, P. (1999). "A Revised Structure and Hydrogen-Bonding System in Cellulose II from a Neutron Fiber Diffraction Analysis" J. *Am. Chem. Soc., 121(43),* 9940-9946.

23. Langan, P., Chanzy, H., and Nishiyama, Y. (2000). "X-ray Structure of Mercerized Cellulose II at 1 Å Resolution," *Biomacromolecules* 2000, 2(2), 410-416.

24. Langan, P., Chanzy, H., and Nishiyama, Y. (2002). "Crystal Structure and Hydrogen-Bonding System in Cellulose Iβ from Synchrotron X-ray and Neutron Fiber Diffraction," *J. Am. Chem. Soc., 124(31),* 9074-9082.

25. Watanabe, S., Ohkita, J., Hayashi, J., and Sufoka, A. (1975). "The confirmation of existences of cellulose III_I, III_{II}, IV_I, and IV_{II} by the x-ray method," *J. Polym. Sci., Polym. Lett.,* 13, 23-27.

26. Southwick, J., Hayashi, J., and Sarko, A. (1976). "Packing Analysis of Carbohydrates and Polysaccharides. 7. Crystal Structure of Cellulose IIII and Its Relationship to Other Cellulose Polymorphs," *Macromolecules.,* 9(5), 857-863.

27. Tanner, S. F., Belton, P.S., Chanzy, H., Vincendon, M., and Henrissat, B. (1987). "Solid-state ^{13}C-N.M.R. and electron microscopy study on the reversible cellulose I→cellulose III_I transformation in *Valonia*," *Carbohydrate Res.,* 160, 1-11.

28. Wada, M., Chanzy, H., Nishiyama, Y., and Langan, P. (2004). "Cellulose IIII crystal structure and hydrogen bonding by synchrotron X-ray and neutron fiber diffraction," *Macromolecules*, 37(23), 8548 -8555.

29. Chanzy, H. and Buleon, A. J. (1980). "Single crystals of cellulose IV_{II}, Preparation and properties," *Polym. Sci. Polym. Phys. Ed*., 18, 1209-1217.

30. Rowell, R. M. The Chemistry of Solid Wood. (1984). American Chemical Society: Washington, DC.

31. Krässig, H. A. In: Huglin, M. B. (ed), (1993). Cellulose, 1st edn, vol 11. Gordon and Breach Science Publishers, Amsterdam, 31.

32. B. Philipp, K.-J. Linow, (1960). "Untersuchungen zur Kettenlangendifferenz zwischen Nitrat- und Cuoxam-DP der Cellulose and ihrer Änderung im Viskoseprozelb," *Papier*, 20, 649-657.

33. R. E. Mark, (1981). "Adhesion in Cellulosic and Wood-based Composites, Molecular and cell wall structure of wood," 7-51, (Oliver, J.F. ed.,) Plenum Press, New-York.

34. Marx-Figini, M. (1964). "Über die Kinetik der Biosynthese der Cellulose in der Baumwolle," Papier, 18, 546-549.

35. Hayashi, J., Hiroshi, K., Takai, M., Hatano, M., and Nozawa, T. (1987). In *The Structures of Cellulose*; Atalla, R. H., Ed.; ACS Symposium Series 340; American Chemical Society: Washington, DC. 135.

36. O'Sullivan, A. C. (1997). "Cellulose: the structure slowly unravels," *Cellulose*, 4(3), 173-207.

37. Zugenmaier, P. (2001). "Conformation and packing of various crystalline cellulose fibers," *Prog. Polym. Sci*., 26(9), 1341-1417.

38. Herbert, J. J. and Muller, L. L. (1974). "An electron diffraction study of the crystal structure of native cells," *J. Appl. Polymer Sci.,* 18, 3373-3377.

39. Fischer, D. G. and Mann, J. (1960). "Crystalline modifications of cellulose. Part VI. Unit cell and molecular symmetry of cellulose I," *J. Polymer Sci.,* 62, 189-194.

40. Preston, R. D., Nicolai, E., Reed, R., and Mallard, A. (1948). "Electron-microscopic study of cellulose in the wall of Valonia ventricosa," *Nature*, 162, 665-667.

41. Frey-Wyssling, A., Miihlethaler, K., Wyckoff, R. W. G. (1948). "Mikrofibrillenbau der pflanzlichen Zellwände," *Experientia,* 4, 475-476.

42. Chanzy, H., Imada, K., and Vuong, R. (1978) "Electron diffraction from the primary wall of cotton fibers," *Protoplasma,* 94, 299-306.

43. Chanzy, H., Imada, K., Mollard, A., Vuong, R., and Barnoud, F. (1979). "Crystallographic aspects of sub-elementary cellulose fibrils occurring in the wall of rose cells cultured in vitro," *Protoplasma,* 100, 303-316.

44. Preston, R. D. (1975). "X-ray analysis and the structure of the components of plant cell walls," *Physic Reports,* 21, 183-226.

45. Revol, J. F. (1985). "Change of the d-spacing in cellulose crystals during lattice imaging," *J. Mat. Sci. Letters,* 4, 1347-1349.

46. Sugiyama, J., Harada, H., Fujiyoshi, Y., and Uyeda, N. (1985). "High resolution observations of cellulose microfibrils," *Mokuzai Gakkaishi,* 30, 98-99.

47. Marchessault, R. H. (1989). Cellulose and Wood-Chemistry and technology, Cellulosics as advanced materials, 1-20.

48. Chanzy, H. (1990) Cellulose Sources and Exploitation, Aspects of Cellulose Structure, 3-12. (Kennedy, J.F., Phillips, G.O. & Williams P.A. eds., Ellis Horwood Ltd., N.Y.).

49. Conrad, C. and Tripp, V. W.; O'Connor, R. T. (Ed) (1972). "*Instrumental Analysis of Cotton Cellulose and Modified Cotton Cellulose*," Marcel Dekker: New York.

50. Cannizzaro, A. M., Goynes, W. R., and Rollins, M. L.; O'Connor, R. T., (Ed) (1972). "*Instrumental Analysis of Cotton Cellulose and Modified Cotton Cellulose,*" Marcel Dekker: New York, 1972.

51. Mark, H. and Meyer, K. H. (1929) "Structure of the Crystalline Part of Cellulose II," Z. *Phys. Chem*. Abt B.,2, 115.

52. Mark, H. and Meyer, K. H. (1928). "The Structure of the Crystallized Components of Cellulose,"*Chem. Ber., B61,* 593.

53. Meyer, K. H. and Misch, L. (1937). "Position des atomes dans le nouveau module spatial de la cellulose," *Helv. Chim. Acta,* 20, 232-244.

54. Marrinan, H. J. and Mann, J. (1956). "Infrared spectra of the crystalline modifications of cellulose," *J. Polymer Sci.*, 21, 301-311.

55. Mann, J. and Marrinan, H. J. (1958). "Crystalline modifications of cellulose. Part II. A study with plane-polarized infrared radiation," *J. Polymer Sci.*, 32, 357-370.

56. Sarko, A. and Woodcock, C. (1980). "Packing Analysis of Carbohydrates and Polysaccharides. 11. Molecular and Crystal Structure of Native Ramie Cellulose," *Macromolecules*, *13*, 1183-1187.

57. VanderHart, D. L. A. and Atalla R.H. (1987). "The structures of Cellulose, Characterization of the Solid States, Further 13C NMR evidence for the co-existence of two crystallines forms in native celluloses," *ACS Symposium Series,* 340, 88-118.

58. VanderHart, D. L. and Atalla, R. H. (1984). "Studies of microstructure in native celluloses using solid state 13C NMR," *Macromolecules*, 17, 1465-1472.

59. Wiley, J. H. and Atalla, R. H. (1987). "Bands assignments in the Raman spectra of celluloses," *Carbohydr. Res.*, 160, 113-129.

60. Wiley, J. H. and Atalla, R. H. (1987). "The Structures of Cellulose. Characterization of the Solid States, The Raman spectra of celluloses," *ACS Symposium Series,* 340, 151-168.

61. Imai, T., Sugiyama, J., Itoh, T., and Horii, F. (1999). "Almost Pure I□ Cellulose in the Cell Wall of Glaucocystis," *J. Struct. Biol.*, 127(3), 248-257.

62. Sugiyama, J., Vuong, R., and Chanzy, H. (1999). "Electron diffraction study on the two crystalline phases occurring in native cellulose from an algal cell wall," *Macromolecules*, 24(14), 4168-4175.

63. Imai, T. and Sugiyama, J. (1999). "Aspects of Native Cellulose Microfibrils at Molecular Resolution," *Trends in Glycoscience and Glycotechnology*, 11(57), 23-31.

64. Persson, J., Chanzy, H., and Sugiyama, J. (1991). "Combined infrared and electron diffraction study of the polymorphism of native celluloses," *Macromolecules,* 24(9), 2461-2466.

65. Tekely, P., Chanzy, H., Excoffier, G., Debzi, E. M., and Sugiyama, J. (1991). "The Iα →Iβ transformation of highly crystalline cellulose by annealing in various mediums," *Macromolecules*, 24(26), 6816-6822

66. Odani, H.; Yamanoto, H.; Horii, F. (1989). "Structural changes of native cellulose crystals induced by annealing in aqueous alkaline and acidic solutions at high temperatures," *Macromolecules,* 22(10), 4130-4132.

67. Chanzy, H., Henrissat, B., Vincendon, M., Tanner, S., and Belton, P. S. (1987) "Solid-state 13C-NMR and electron microscopy study on the reversible cellulose I → cellulose IIII transformation in Valonia," *Carbohydr. Res.,* 160, 1-11.

68. Hirai, A. Horii, F. Kitamaru, R. (1987). "Transformation of native cellulose crystals from cellulose I_b to cellulose I_a through solid-state chemical reactions," *Macromolecules,* 20(6), 1440-1442.

69. Atalla, R. H. and VanderHart, D. L. (1989). "Studies on the structure of cellulose using Raman spectroscopy and solid state 13C NMR," Cellulose and Wood -Chemistry and Technology, 169-188, John Wiley & Sons Inc.

70. Yamamoto, H. and Horii, F. (1993). "CP/MAS 13C NMR analysis of the crystal transformation induced for Valonia cellulose by annealing at high temperatures," *Macromolecules,* 26(6), 1313-1317.

71. Deguchi, S. Tsujii K., and Horikoshi, K. (2006). "Cooking cellulose in hot and compressed water " *Chem. Commun.*, 31, 3293 – 3295.

72. Conner, A. H. (1995). Size Exclusion Chromatography of Cellulose and Cellulose Derivatives. In *Handbook of Size Exclusion Chromatography*; Wu, C., Eds.; Chromatographic Science Series; Marcel Dekker: New York.

73. Klemm, D., Heublein, B., Fink, H-P., and Bohn A. (2005). "Cellulose: Fascinating Biopolymer and Sustainable Raw Material," *ChemInform,* 36, 3358-3393.

74. Philipp, B., Heinze, T., Klemm, D., Wagenknecht, W., and Heinze, U. (1998). *Comprehensive Cellulose Chemistry*; Wiley VCH: Weinheim.

75. Stenius, Per. (2000). Papermaking Science and Technology 3 Finland: Fapet OYp, *Forest Products Chemistry,* ISBN 952-5216-03-9.

76. Turner, M. B., Spear, S. K., Holbrey, J. D., and Rogers, R. D. (2004). "Production of Bioactive Cellulose Films Reconstituted from Ionic Liquids," *Biomacromolecules,* 5 (4), 1379-1384.

77. Swatloski, R. P., Spear, S. K., Holbrey, J. D., and Rogers, R. D. (2002). Dissolution of Cellose with Ionic Liquids," *J.Am. Chem. Soc.,* 124 (18), 4974-4975.

78. Hon, D. N.-S., Shiraishi, N. (2001), "Wood and Cellulose Chemistry*,"* Marcel Dekker, New York.

79. Braconnot, H. (1833). "Idem," *Ann.Chim. Phys,*. 52, 290-293.

80. Cameron, S. J. (2000). "Practical haemodialysis began with cellophane and heparin: the crucial role of William Thalhimer (1884–1961)," *Nephrol. Dial. Transplant*, 15, 1086-1091.

81. Fort, D. A., Remsing, R. C., Swatloski, R. P., Moyna, P., Moyna, G., and Rogers. R.D. (2007). "Can ionic liquids dissolve wood? Processing and analysis of lignocellulosic materials with 1-n-3-methylimidazolium chloride," *Green Chemistry*, 9, 63-69.

82. Kilpelainen, I. Xie, H. King, A. Granstrom, M., Heikkinen, S., and Argyropoulos, D. S. (2007). "Dissolution of Wood in Ionic Liquids," *J. Agric. Food Chem.*, 55, 9142-9148.

83. Zhang, H., Wu, J., Zhang, J., and He, J. (2005). « 1-Allyl-3-methylimidazolium Chloride Room Temperature Ionic Liquid: A New and Powerful Nonderivatizing Solvent for Cellulose," *Macromolecules* 38, 8272-8277.

84. El Seoud, O. A., Koschella, A., Fidale, L. C., Dorn, S., and Heinze, T. (2007). "Applications of Ionic Liquids in Carbohydrate Chemistry: A Window of Oppertunities," *Biomacromolecules*, 8(9), 2629–2647.

85. Kondo, T. (1997). "The relationship between intramolecular hydrogen bonds and certain physical properties of regioselectively substituted cellulose derivatives," *J Polym Sci B Polym Phys*, 35(7), 717–723.

86. Granstrom, M., Kavakka, J., King, A., Majoinen, J., Makela, V., Helaja, J., Hietala, S., Virtanen, T., Maunu, S.-L., Argyropoulos, D. S., and Kilpelainen, I. (2008). "Tosylation and acylation of cellulose in 1-allyl-3-methylimidazolium chloride," *Cellulose*, 15, 481–488.

87. Kadokawa, M. Murakami, Y., and Kaneko, Y. (2008). "A facile preparation of gel materials from a solution of cellulose in ionic liquid," *Carbohydrate research*, 343, 769-772.

88. Heinze, T., Schwikal, K., Barthel, S. (2005). "Ionic Liquids as Reaction Medium in Cellulose Functionalization," *Macromolecular Bioscience*, 5, 520-525.

89. Xie, H., King, A., Kilpelainen, I., Granstrom, M., and Argyropoulos, D. S. (2007). "Thorough Chemical Modification of Wood-Based Lignocellulosic Material in Ionic Liquids," *Biomacromolecules*, 8(12), 3740-3748.

90. Smook, G., A. (2002). Handbook for Pulp and Paper Technologists. 3rd ed. Angus Wilde, Vancouver.

91. Clasen C. and Kulicke, W.-M. (2001). "Determination of viscoelastic and rheo-optical material functions of water-soluble cellulose derivatives," *Prog. Polym. Sci.*, 26, 1839-1919.

92. Starikov, E. B., Brasicke, K., Knapp E. W., and Saenger, W. (2001). "Negative solubility coefficient of methylated cyclodextrins in water: a theoretical study," *Chem. Phys. Lett.*, 336, 504-510.

93. Pérez, O. E., Sánchez, C. C., Pilosof A. M. R., and Patino, J. M. R. (2008). "Dynamics of adsorption of hydroxypropyl methylcellulose at the air–water interface," *Food Hydrocolloids* 22, 387-402.

94. Kennedy, J. F., Phillips, G. O., Wedlock, D. J., and Williams, P. A. (1985). Cellulose and its derivatives, chemistry, biochemistry and applications, Halsted Press: New York.

95. Tonnesen, H. H. and Karlsen, J. (2002). "Alginate in drug delivery systems," *Drug Development & Industrial Pharmacy,* 28(6), 621-630.

96. Liebermann, H. A., Lachman, L., and Schwartz, J. B. (1990). Pharmaceutical Dosage Forms: tablets. Marcel Dekker, ISBN: 0-8247-8300-X.

97. Weiner, M. L., Kotkoskie, L. A. (1999). Excipient Toxicity and Safety. Marcel Dekker, New York, ISBN: 0-8247-8210-0.

98. Sanders, J. C., Breadmore, M. C., Kwok, Y. C., Horsman, K. M., and Landers, J. P. (2003). "Hydroxypropyl cellulose as an adsorptive coating sieving matrix for DNA separations: artificial neural network optimization for microchip analysis," *Anal. Chem.*, 75(4), 986-994.

99. Plunguian, M. (1943). Cellulose Chemistry; Chemical Publishing Co., Inc., New York.

100. Havancsak, K. (2003). "Nanotechnology at present and its promises in the future," *Material Science Forum*, Vols. 414-415, 85-94.

101. NASA., http://www.ipt.arc.nasa.gov/nanotechnology.html.

102. Foster, L. E. (2006). Nanotechnology: Science, Innovation and Opportunity; Publish: Upper Saddle River, NJ.

103. Gogotsi, Y. (2006). Handbook of Nanomaterials; Publish: Baco Raton; CRC/Taylor & Francis.

104. Bor, J. (1994). Advanced polymer composites; ASM International: Materials Park, 1-279.

105. Brechet, Y., Cavaille, J., Chabert, E., Chazeau, L., Dendievel, R., Flandin, L., and Gauthier, C. (2001). "Polymer based nanocomposites: Effect of filler-filler and filler-matrix interactions," *Advanced engineering materials,* 3(8), 571-578.

106. Giannelis, E. (1998). "Polymer-Layered silicate nanocomposites: Synthesis, properties and applications," *Applied organometallic chemistry,* 12, 675-680.

107. Beck-Candanedo, S., Roman, M., and Gray, D. G. (2005). "Effect of Reaction Conditions on the Properties and Behavior of Wood Cellulose Nanocrystal Suspensions," *Biomacromolecules*, 6(2), 1048-1054.

108. Dong, X. M., Kimura, T., Revol, J., and Gray, D. G. (1996). "Effects of Ionic Strength on the Phase Separation of Suspensions of Cellulose Crystallites," *Langmuir,* 12, 2076-2082.

109. Araki, J., Wada, M., Kuga, S., and Okano, T. (1999). "Influence of surface charge on viscosity behavior of cellulose microcrystal suspension," *J. Wood Sci.,* 45(3), 258-261.

110. Favier, V. J. C. (1995). "Polymer Nanocomposites reinforced by cellulose whiskers," *Macromolecules,* 28(18), 6365-6367.

111. Dufresne, A., Kellerhals, M., and Witholt B. (1999). "Transcrystallization in Mcl-PHAs/Cellulose whiskers composites," *Macromolecules*, 32(22), 7396-7401.

112. Eichhorn, S., Baillie, C., Zafereiropoulos, N., Mwaikambo, L., Ansell, M., Dufresne, A., Entwistle, K., Herrera-Franco, P., Escamilla, G., Groom, L., Hughes, M., Hill, C., and Rials, T. (2001). "Review- Current international research into cellulosic fibres and composites," *Journal of Material Science,* 36, 2107-2131.

113. Marks R. (1967). Cell wall mechanics of tracheids. Yale University press: New Haven.

114. Fan, L. T., Gharpuray, M. M., and Lee, Y.-H. (1987). Biotechnology Monographs: Cellulose Hydrolysis; Springer-Verlag.

115. Hon D. (1996). Chemical modification of lignocellulosic materials; Marcel Dekker Inc., New York.

116. Ranby G. (1951). "The colloidal properties of cellulose micelles," *Discussions Faraday Society,* 11, 158-164.

117. Millet, M., Moore, W., and Saeman, J. (1954). "Preparation and properties of hydrocelluloses," *Industrial Engineering Journal,* 46, 1493-1497.

118. Dong, X., Revol, J., and Gray, D. (1998). "Effect of microcrystallite preparation conditions on the formation of colloid crystals of cellulose," *Cellulose,* 5(1), 19-32.

119. Crank, J. and Park, G. (1968). Diffusion in polymers; Academic Press: New York.

120. Fleming, K., Gray, D. G., and Matthews, S. (2001). "Cellulose Crystallites," *Chem. Eur. J.,* 7(9), 1831-1836.

121. Araki, J., M. Wada, S. Kuga and T. Okano, (1998) "Flow Properties of Microcrystalline Cellulose Suspension Prepared by Acid Treatment of Native Cellulose," *Colloid Surfaces A,* 142(1), 75-82.

122. Imai, T., Boisset, C., Samejima, M., Igarashi, K., and Sugiyama, J. (1998). "Unidirectional Processive Action of Cellobiohydrolase Cel7A on Valonia Cellulose Microcrystals," *FEBS Letters,* 432(3), 113-116.

123. Revol, J.-F., Bradford, H., Giasson, J., Marchessault, R. H., and Gray, D. G. (1992). "Helicoidal Self-Ordering of Cellulose Microfi brils in Aqueous Suspension," Int. J. Biol. Macromol. 14(3), 170-172.

124. Heux, L., Dinand, E., and Vignon, M. R. (1999). "Structural aspects in ultrathin cellulose microfibrils followed by ^{13}C CP-MAS NMR," *Carbohydr. Polym.*, 40(2), 115-124.

125. Baker, A. A., Helbert, J. Sugiyama, J., and Miles, M. J. (2000). "New Insight into Cellulose Structure by Atomic Force Microscopy Shows the Iα Crystal Phase at Near-Atomic Resolution," *Biophys. J.*, 79, 1139-1145.

126. Orts, W. J., Godbout, L., Marchessault, R. H., and Revol, J. F. (1998). "Enhanced ordering of liquid crystalline suspensions of cellulose microfibrils: A small-angle neutron scattering study," *Macromolecules*, 31(17), 5717-5725.

127. Ebeling, T., Paillet, M., Borsali, R., Diat, O., Dufresne, A., Cavaille, J. Y., and Chanzy, H. (1999). "Shear-Induced Orientation Phenomena in Suspensions of Cellulose Microcrystals, Revealed by Small Angle X-ray Scattering," *Langmuir*, 15(19), 6123-6126.

128. Terech, P., Chazeau, L., and Cavaille, J. Y. (1999). "A Small-Angle Scattering Study of Cellulose Whiskers in Aqueous Suspensions," *Macromolecules*, 32(6), 1872-1875.

129. Sugiyama, J., Vuong, R., and Chanzy, H. (1991). "Electron diffraction study on the two crystalline phases occurring in native cellulose from an algal cell wall, "*Macromolecules*, 24(14), 4168-4175.

130. Leppänen, K., Andersson, S., Torkkeli, M., Knaapila, M., Kotelnikova, N., and Serimaa, R. (2009). "Structure of cellulose and microcrystalline cellulose from various wood species, cotton and flax studied by X-ray scattering," *Cellulose*, ASAP Article, Published online 13 may 2009.

131. Marchessault, R. H., Morehead, F. F., and Walter, N. M. (1959). "Liquid Crystal Systems from Fibrillar Polysaccharides," *Nature*, 184, 632-633.

132. Marchessault, R. H., Morehead, F. F., and Koch, M. Jean. (1961). "Hydrodynamic properties of neutral suspensions of cellulose crystallites as related to size and shape," *J. Colloid Sci.*, 16, 327-344.

133. Dong, X. M., Kimura, T., Revol, J. F., and Gray, D. G. (1996). "Effects of Ionic Strength on the Isotropic−Chiral Nematic Phase Transition of Suspensions of Cellulose Crystallites," *Langmuir*, 12(8), 2076-2082.

134. Revol, J. F., Godbout, L., Dong, X. M., and Gray, D. G. (1994). "Chiral nematic suspension of cellulose crystallites: Phase separation and magnetic field orientation," *Liq. Cryst.*, 16(1), 127-134.

135. Revol, J. F., Godbout, L., and Gray, D. G. (1998). "Solid self-assembled films of cellulose with chiral nematic order and optically variable properties," *J. Pulp Paper Sci.*, 24(5), 146-149.

136. Sipahi-Saglam, E., Gelbrich, M., and Gruber, E. (2003). "Topochemically Modified Cellulose," *Cellulose* 10(3), 237–250.

137. Buining, P. A., Veldhuizen, Y. S., Pathmamanoharan, C., and Lekkerkerker, H. N. W. (1992). "Preparation of a non-aqueous dispersion of sterically stabilized boehmite rods," *Colloids Surf.*, 64(1), 47-55.

138. van der Zande, B. M. I., Bohmer, M. R., Fokkink, L. G. J., and Schonenberger, C. (1997). "Aqueous Gold Sols of Rod-Shaped Particles," *J. Phys. Chem. B*, 101(6), 852-854.

139. van der Zande, B. M. I., Bohmer, M. R. Fokkink, L. G. J., and Schonenberger, C. (2000). "Colloidal Dispersions of Gold Rods: Synthesis and Optical Properties," *Langmuir*, 16(2), 451-458.

140. Goussé, C., Chanzy, H., Excoffier, G., Soubeyrand, L., and Fleury, E. (2002). "Stable suspensions of partially silylated cellulose whiskers dispersed in organic solvents," *Polymer*, 43(9), 2645-2651.

141. Morandi, G., Heath, L., and Thielemans, W. (2009). "Cellulose Nanocrystals Grafted with Polystyrene Chains through Surface-Initiated Atom Transfer Radical Polymerization (SI-ATRP)," *Langmuir*, ASAP article.

142. Grunert, M. and Winter, W. T. (2000). "Progress in the development of cellulose reinforced nanocomposites," *Polymeric Materials Science and Engineering*, 82, 232-238.

143. Favier, V., Chanzy, H., and Cavaille, J. Y. (1995). "Polymer Nanocomposites Reinforced by Cellulose Whiskers," *Macromolecules*, 28(18), 6365-6367.

144. Favier, V., Canova, G. R., Shrivastava, S. C., and Cavaille, J. Y. (1997). "Mechanical percolation in cellulose whisker nanocomposites," *Polymer Engineering and Science*, 37(10), 1732-1739.

145. Podsiadlo, P., Choi, S. Y., Shim, B., Lee, J., Cuddihy, M., and Kotoy, P. P. (2005). "Molecularly Engineered Nanocomposites: Layer-by-Layer Assembly of Cellulose Nanocrystals," *Biomacromolecules*, 6(6), 2914-2918.

146. Samir, M. A. S. A., Alloin, F., Sanchez, J., and Dufresne A. (2004). "Cellulose nanocrystals reinforced poly(oxyethylene)," *Polymer*; 45(12), 4149–4157.

147. Samir, M. A. S. A., Alloin, F., Gorecki, W., Sanchez, J., and Dufresne A. (2004). "Nanocomposite Polymer Electrolytes Based on Poly(oxyethylene) and Cellulose Nanocrystals," *J. Phys. Chem. B,* 108(30), 10845-10852.

148. Schroers, M., Kokil, A., and Weder, C. (2004). "Solid polymer electrolytes based on nanocomposites of ethylene oxide-epichlorohydrin copolymers and cellulose whiskers," *J. Appl. Polym. Sci., 93*, 2883−2888.

149. Heux, L., Chauve, G., and Bonnini, C. (2000). "Nonflocculating and Chiral-Nematic Self-ordering of Cellulose Microcrystals Suspensions in Nonpolar Solvents," *Langmuir,* 16(21), 8210-8212.

150. Grunert, M. and Winter, W. T. (2002). "Nanocomposites of Cellulose Acetate Butyrate Reinforced with Cellulose Nanocrystals," *Journal of Polymers and the Environment,* 10(1-2), 27-30.

151. Sassi, J. F., and Chanzy, H. (1995). "Ultrastructural aspects of the acetylation of cellulose," *Cellulose,* 2(2), 111-127.

152. Kim, U. J. and Kuga, S. (2002). "Polyallylamine-grafted cellulose gel as high-capacity anion-exchanger," *Journal of Chromatography A,* 946(1-2), 283–289.

153. Kim, U. J. and Kuga, S. (2002). "Ion-exchange separation of proteins by polyallylamine-grafted cellulose gel," *Journal of Chromatography A,* 955(2), 191–196.

154. Araki, J., Wada, M. and Kuga, S. (2001). "Steric Stabilization of a Cellulose Microcrystal Suspension by Poly(ethylene glycol) Grafting," *Langmuir,* 17(1), 21-27.

155. Harkness, B. R. and Gray D. G. (1994). Liquid Crystalline and Mesomorphic Polymers (Eds.: V. Shibaev, L. Lam), Springer, New York. 298.

156. Revol, J. F., Godbout, L., and Gray, D. G. US-P 5629 055, 1997.

157. Lemarchand, C., Gref, R., and Couvreur, P. (2004). "Polysaccharide-decorated nanoparticles," *Eur. J. Pharm. Biopharm.,* 58(2), 327−341.

158. Emerich, D. F., and Thanos, C. G. (2007). "Targeted nanoparticle-based drug delivery and diagnosis," *J. Drug Target.,* 15(3), 163−183.

159. Liu, Y., Miyoshi, H., and Nakamura, M. (2007). "Nanomedicine for drug delivery and imaging: A promising avenue for cancer therapy and diagnosis using targeted functional nanoparticles," *Int. J. Cancer*., 120(12), 2527−2537.

160. Vonarbourg, A., Passirani, C., Saulnier, P., and Benoit, J.-P. (2006). "Parameters influencing the stealthiness of colloidal drug delivery systems," *Biomaterials*, 27(24), 4356−4373.

161. De Souza Lima, M. M. and Borsali, R. (2004). "Rodlike Cellulose Microcrystals: Structure, Properties, and Applications," *Macromol. Rapid Commun.*, 25(7), 771−787.

162. Azizi Samir, M. A. S., Alloin, F., and Dufresne, A. (2005). "Review of Recent Research into Cellulosic Whiskers, Their Properties and Their Application in Nanocomposite Field," *Biomacromolecules*, 6(2), 612−626.

2. Research Objectives

The production and synthetic modifications of cellulose nanocrystals are investigated in this study, with the main focus on developing synthetic strategies. There are three major objectives in the present study: (a) Optimization of the reaction conditions for the efficient production of cellulose nanocrystals (reaction time, temperature and the effect of ultrasonication); (b) Study the reactivity of the hydroxyl groups in cellulose; (c) Synthetically modify cellulose nanocrystals by using various approaches.

The first part of this research involves the production and characterization of cellulose nanocrystals related to the reaction conditions (Chapter 3). The second part of this research focuses on the development of the novel ^{31}P NMR methodology for determining the reactive hydroxyl groups on cellulose (Chapter 4). The third part of this research provides different approaches to modify cellulose nanocrystals starting either from the reducing end aldehyde or the surface hydroxyl groups (Chapters 5, 6, 7 and 8).

3. Optimization Study for the Production of Cellulose Nanocrystals

3.1 Abstract

Cellulose nanocrystals were prepared in our laboratory by acidic hydrolysis of cotton fibers (Whatman #1 filter paper). In our efforts to select conditions in which the hydrolysis media does not install labile protons on the cellulose crystals, mineral acid other than sulfuric acid (H_2SO_4) was used. Furthermore, in our attempts to increase the yields of nanocrystals ultrasonic energy was applied during the hydrolysis reaction. The primary objective was to develop hydrolysis reaction conditions for the optimum and reproducible cellulose nanocrystal production. As such, hydrobromic acid (HBr) with concentrations of 1.5 M, 2.5 M and 4.0 M, at 80^{o}C or 100^{o}C, for a period of time varying from 1 hour to 4 hours, applying the ultrasonic energy either during or after the reaction was selected as hydrolysis media. The combination of 2.5 M HBr, 100^{o}C, and 3 hours with ultrasonication during the reaction generated the highest nanocrystal yield.

3.2 Introduction

Perhaps the earliest technical work on microcrystalline cellulose, or MCC, was documented in a journal article by O.A. Battista in 1949.[1] Battista exposed native and regenerated cellulose to hydrochloric acid, measuring the degree of polymerization of the polymer at different points in time. A decrease in degree of polymerization was observed, but the decrease leveled off after approximately five hours. Battista proposed that this was evidence to two separate amorphous and crystalline regions in the cellulose. Since then, a

vast amount of research has been conducted into the properties of and the processes producing micro- and nano-sized cellulose crystals.

In 1997, Dong, Revol, and Gray published a paper studying the effects of acid hydrolysis conditions on microcrystalline cellulose size and other properties.[2] They used reaction conditions of 45°C and 62% sulfuric acid and it was found out that the size of the particles decreased sharply as the reaction time was lengthened. Dong *et al.*, on the other hand, found that the average sizes of the crystalline particles levels off after 1 hour reaction having lengths approximately of 175 nm. They concluded that the particle sizes decreased sharply at first as the easily reached glycosidic linkages in the amorphous region of cellulose are broken. Moreover, after the amorphous region is hydrolyzed, it became significantly more difficult for the acid to reach and break the remaining glycosidic linkages in the crystalline region of cellulose.

Dong *et al.* also introduced a relationship for the reaction time and particle size distribution. It was found that by increasing the reaction time from 20 minutes to 4 hours the particle size distribution was significantly reduced. The study also established a discrepancy between the particle sizes reported through photon correlation spectroscopy (PCS), and transmission electron microscopy (TEM) paired with image analysis. It was postulated that the light scattering technique used in PCS leads to an overestimated fiber lengths.

Work by Beck-Candanedo *et al.*, supports Dong's hypothesis about average particle size and distribution.[3] As reaction time and acid/pulp ratio were both increased, the average nanocrystal length decreased from 147 to 105 nm. More importantly, the standard deviation in the measured lengths of cellulose nanocrystals decreased from 65 to 36, an almost 50% decrease. In Beck-Candanedo's study, the samples were all ultrasonicated after purification in order to produce stable colloidal suspensions. The sonicator was used for 7 minutes at 60% power while the solution was cooled in an ice bath to prevent overheating. In our experiments the pulps were sonicated either at room temperature after the hydrolysis reaction or at 80°C and 100°C during the process.

The fact that cellulose nanocrystals have the innate capacity to form hydrogen bonds creates systems that may readily aggregate which can present serious characterization problems especially when examined under Scanning Electron Microscopy (SEM). Therefore, in accordance with previous work,[2] we confirmed that by applying ultrasonic energy after/during the acidic hydrolysis, the yields of the nanocrystals can dramatically be increased For instance, the ultrasonic treatment increased the hydrolysis yield (1.5M HBr, 100°C, 4 hr) from 39% to 50%. The produced cellulose nanocrystals were characterized with various techniques such as X-ray diffraction, atomic force microscopy, differential scanning calorimetry, thermogravimetric analysis, transmission electron microscopy. Furthermore, the molecular weight of cellulose nanocrystals was determined after making them organosoluble through derivatization reaction in ionic liquid.

3.3 Materials and Methods

Materials. Whatman #1 filter paper was used as a starting material for the cellulose nanocrystals. HBr and NaOH were received from Fisher. All other chemicals used in this research were purchased from Aldrich and used as received except otherwise stated.

3.3.1 Formation of Cellulose Nanocrystals. The cellulose nanocrystals were formed by acidic hydrolysis similar to the procedure used by Araki *et al.* as illustrated in Scheme 3.1.[4,5,6] A typical procedure was as follows. 2.0 g of cellulose pulp obtained from Whatman #1 filter paper (98% α-cellulose, 80% crystallinity) was blended by a 10 Speed Osterizer® Blender. Resulting pulp was hydrolyzed with 100 mL of 1.5, 2.5 or 4.0 M HBr at 100°C for 1, 2, 3 or 4 hours. The ultrasonication was applied either during (every 60 minutes) or after the reaction at the room temperature (Omni-Ruptor 250W ultrasonic homogenizer, 50% power, 5 min). The resulting mixture was diluted with de-ionized (D.I) water followed by five cycles of centrifugation at 1500g for 10 min. (IEC Centra-CL3 Series) to remove excess acid and water soluble fragments. The fine cellulose particles became dispersed in the aqueous solution approximately at pH 4. The turbid supernatant containing the polydisperse cellulose particles was then collected for further centrifugation at 15000 g for 45 min (Automatic Servall® Superspeed Centrifuge) to remove ultra-fine particles. Ultra-fine particles with small aspect ratio were removed from the upper layer, and the precipitation (after the high-speed centrifugation) was dried using a lyophilizing system (Labconco, Kansas City, MU).

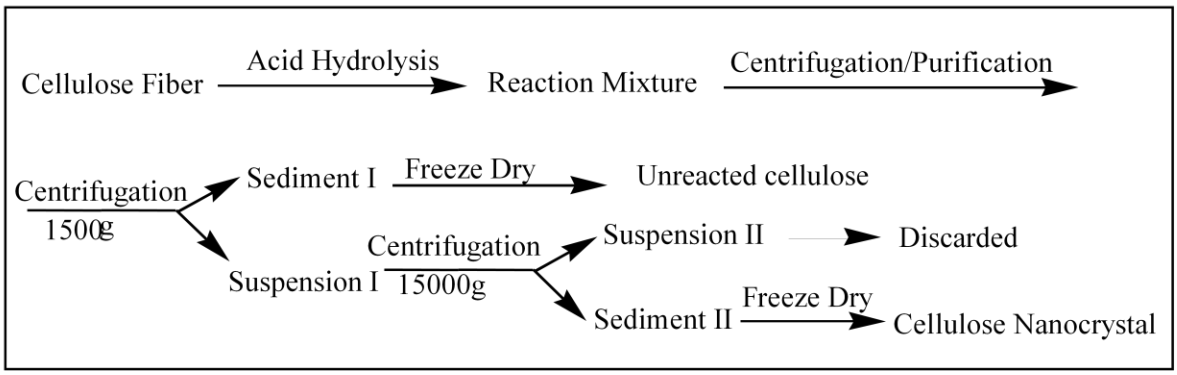

Scheme 3.1 Schematic of the cellulose nanocrystal formation & isolation procedure

3.3.2 Synthesis of 1-allyl-3-methylimidazolium chloride ([Amim]Cl). [Amim]Cl, the ionic liquid used initially, was synthesized by the reaction of allyl chloride with excess 1-methylimidazole to avoid the possible acid impurity. Freshly distilled allyl chloride (0.95 equivalents) was added dropwise to the solution of freshly distilled methyl imidazole (1 equivalent) in dry acetone and the mixture was slowly heated to 55°C (overnight) under nitrogen atmosphere. After cooling to room temperature, the acetone phase was separated and the excess methylimidazole was removed by extraction with acetone. The crude product was added dropwise to acetone and the mixture was stirred for 5 h at room temperature (in order to decrease the viscosity, the mixture was heated to 40°C) then the acetone phase was separated. This procedure was repeated five times. The ILs layer was separated and condensed by rotary evaporation to remove the organic solvent. The crude product was further purified using active carbon in boiling methanol. After filtration and condensation, the product was dried under vacuum at 40°C for 48 h before use. ^{1}H NMR (300 MHz, $CDCl_3$) δ 3.83 (3 H, s), 4.73 (2H, d, ^{3}J = 6.3 Hz), 5.10-5.20 (2H, m), 5.65–5.79 (1H, m), 7.30 (1H, s), 7.54 (1H, s), 10.10 (1H, s).

3.3.3 Benzoylation of Cellulose and Cellulose Nanocrystals. Whatman #1 filter paper was homogenized in a Wearing blender in prior to bezoylation. Ionic Liquid ([Amim]Cl, 950 mg) was added to cellulose sample (50 mg) in a 15 ml sample bottle, vortexed until all solid particles had dispersed and heated at 80^{o}C with magnetic stirring until the solution was transparent (2 hrs). Pyridine (330 µl, 3.7 mmol) was added and the solution was vortexed until visibly homogeneous and allowed to cool down to room temperature. Benzoyl chloride (380 µl, 3.3 mmol) was added in one portion and the resulting mixture was vortexed until the formation of homogeneous white paste. The sample was then heated at 55 °C for 3 hrs with magnetic stirring and then allowed to cool down to room temperature. The mixture of deionized water (2.5 ml) and EtOH (7.5ml) was added and the mixture vigorously shaken and vortexed for 5 min. The solid was filtered off through a sintered funnel (grade M), washed further with EtOH and purified with MeOH (stirred overnight without heating overnight). Finally, the resulting solid was filtered off to give white powders. The yields of benzoylated cellulose and cellulose nanocrystals were 100 mg and 84 mg, respectively. Cellulose benzoates were analyzed by ^{1}H-NMR and Gel Permeation Chromatography (GPC).

3.3.4 Thermal analysis. The glass transition temperatures (T_g) and the melting temperatures (T_m) of the samples were measured by differential scanning calorimetry using a TA Instrument DSCQ100. The instrument was calibrated with indium. Samples were first heated to 150°C, cooled rapidly to room temperature, and then scanned again at a rate of 20°C/min. The heat of evaporation for water [$\Delta H_{vap}(H_2O)$] values were determined by

using a heating rate of 10°C/min until 250°C and then integrating the endothermic water peak. The thermal decomposition temperature was determined using a TA Instrument TGAQ500 at a ramp of 10°C/min under N_2 purge. In prior to thermal analysis all the cellulose samples were conditioned at 69% relative humidity which achieved by placing a saturated KI solution at the bottom of a desiccator in which the samples were kept over a period of three days.

3.3.5 X-ray Diffraction. Wide-angle x-ray diffraction (WAXD) measurements were performed with a Siemens type-F X-ray diffractometer using a Ni-filtered CuK_α radiation source (k = 1.54 Å). The diffraction intensities were measured every 0.1° from 2θ = 5 to 30° at a rate of 2θ = 3°/min. The supplied voltage and current were 30 kV and 20 mA, respectively.

3.3.6 Transmission Electron Microscopy (TEM). A suspension (0.01% w/v in water) of cellulose nanocrystals was prepared. Drops of suspensions were deposited on carbon-coated electron microscope grids, negatively stained with uranyl acetate and allowed to dry. The grids were observed with a Philips 400T microscope operated at an accelerating voltage of 120 kV.

3.3.7 Gel Permeation Chromatography (GPC). Gel permeation chromatographic (GPC) measurements were carried out with a Waters GPC 510 pump equipped with UV and RI

detectors using THF as the eluent at a flow rate of 0.7 mL/min at room temperature. Two Ultrastyragel linear columns linked in series (Styragel HR 1 and Styragel HR 5E) were used for the measurements. Standard mono-disperse polystyrenes with molecular weight ranges from 0.82 to 1860 kg/mol were used for the calibration. The number- and weight-average molecular weights were calculated using the Millenium software of Waters.

3.3.8 ^{1}H NMR Spectroscopy. NMR measurements were acquired using on a Bruker 300 MHz spectrometer equipped with a Quad probe dedicated to ^{31}P, ^{13}C, ^{19}F, and ^{1}H acquisition.

3.3.9 Atomic Force Microscopy (AFM). The surface morphologies of cellulose nanocrystals were investigated by atomic force microscope (AFM, Q-Scope™ 250 from Quesant Instrument Corporation) with tapping mode under atmospheric conditions with a scanning speed set to 1 Hz .

3.4 Results and Discussion

A number of different factors affecting the acidic hydrolysis of cellulose were examined. A complete set of investigated parameters include: reaction time and temperature, the concentration of acid (HBr) and the effect of applied external energy (ultrasonic). The main focus was to optimize the conditions needed for the high yield production of cellulose nanocrystals while retaining the uniform dimensional appearance of produced crystals. In

our efforts to increase the yields of nanocrystals the ultrasonic energy will be applied on the course of the reaction or after the reaction to break down the aggregates and to further promote the efficiency of acid hydrolysis. While the application of ultrasonic energy after hydrolysis has been previously documented,[2] efforts to apply sonic energy during the acidic hydrolysis have never been undertaken. The ultrasonication device has a tip made of titanium which sets limitations for the type of acid used in the hydrolysis medium. Due to the corrosive nature of HCl toward the titanium tip of the sonic gun, our sonication hydrolysis experiments were carried out in HBr solutions (inert towards titanium).

Due to the cellulose's strong ability to form hydrogen bonds, the produced nanocrystals tended to agglomerate to form larger particles. Instead of being removed as part of the suspension after centrifugation, these aggregated particles precipitated at the bottom of the centrifugal tube and were discarded as sediment. This significantly decreased the yield of cellulose nanocrystals from the hydrolysis reaction. The aggregate formation manifested itself especially in the absence of surface charges when the repulsion forces between the individual nanocrystals were minimized. One solution for decreasing the aggregation issue is to introduce negative charges on the surface of cellulose nanocrystals. Sulfuric acid is known to introduce negative charges on the surface of the cellulose nanocrystals via an esterification reaction with the sulfate anions.[3,4,7] While such charges may be of some benefit in stabilizing nanocrystal suspensions in the study of their chiral nematic properties, such groups create labile centers and sites of potential side reactions during subsequent site-specific grafting. Therefore, to benefit our further aims to site-specifically modify the

produced cellulose nanocrystals we decided to use HBr for the acidic hydrolysis of cellulose in order to avoid the possible side reactions. Moreover, elemental analysis on well-washed nanocrystals prepared under HBr hydrolysis conditions showed the complete absence of bromine indicative of the lack of side reactions. It is also well known fact that HBr is a stronger acid than HCl or H_2SO_4 which can offer further savings in chemical use when a large scale manufacture of cellulose nanocrystals is considered.

3.4.1 The Effect of Acid Concentration, Reaction Temperature and Reaction Time to the Yield of Cellulose Nanocrystals

Reaction time, reaction temperature, and HBr concentration are the parameters that will affect on the efficiency of acid hydrolysis. It is expected that the reaction time and temperature will have a significant impact to the achieved yields as the heterogeneous diffusion of the acid to the amorphous regions of cellulose does not occur instantaneously. Furthermore, the relative rate of the hydrolysis will be faster in the beginning of the process when the easily accessible amorphous regions are being hydrolyzed and later slows down significantly as the acid attacks the reducing end and the surface of the residual crystalline regions. It is important to note here that the starting material is known to have 80% crystallinity (Whatman #1) thus containing 20% of more easily hydrolysable amorphous cellulose. Therefore, the maximum yield of highly crystalline cellulose nanocrystals is 80% from the starting weight of dry cellulose pulp. In practice, the yields are expected to be lower as small parts of the crystalline regions will be hydrolyzed as well. Nevertheless, the

hydrolysis conditions should be mild enough to avoid complete hydrolysis of cellulose to glucose or even carbonization.

Figures 3.1 and 3.2 demonstrate the effects of reaction time and temperature to the yield of cellulose nanocrystals during the hydrolysis with 2.5M HBr. It can be seen that in both selected hydrolysis temperatures, 80°C and 100°C, the yields are increasing along the hydrolysis time. The highest yield, 70% from the starting material, was achieved from the hydrolysis reaction of 3 hours at 100°C. It is worth to mention here that 70% yield is very close to theoretical maximum of 80% as mentioned above. At this point it can be stated that the 30% loss of material corresponds well with the amount of less ordered amorphous cellulose in starting material. Moreover, the results pointed out the positive effects of the applied ultrasonication which will be discussed later on this manuscript.

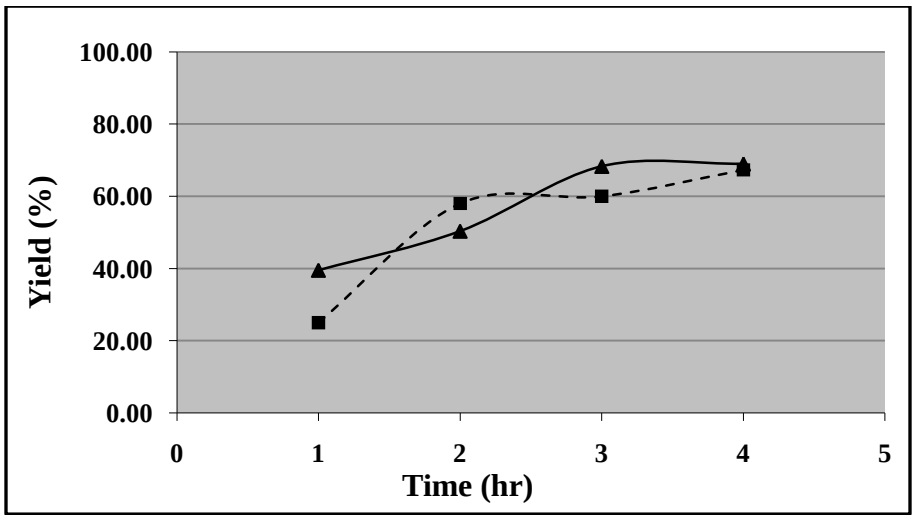

Figure 3.1 The effect of the reaction time and temperature to the yields of cellulose nanocrystals from the hydrolysis with 2.5M HBr (100°C solid line, 80°C dashed line; Ultrasonication during the hydrolysis reaction)

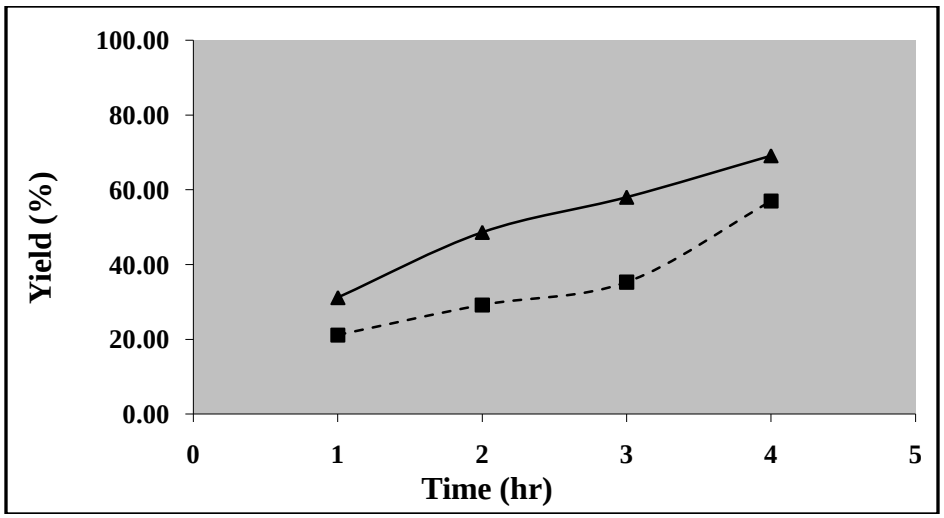

Figure 3.2 The effect of the reaction time and temperature to the yields of cellulose nanocrystals from the hydrolysis with 2.5M HBr (100°C solid line, 80°C dashed line; Ultrasonication after the hydrolysis reaction)

Figure 3.3 compares the yields of cellulose nanocrystals in relation to the acid concentration used in the hydrolysis reaction. It can clearly be seen that the yields are significantly higher when the HBr concentration is increased from 1.5M to 2.5M. However, further increase in concentration up to 4.0M did not improve the yields notably. It is also worth mentioning here that the cellulose nanocrystals collected after the 4.0M HBr treatment appeared darker in color than the ones from milder hydrolysis treatments. This can be indicative from the side reactions, such as dehydration, that are known to occur under harsh reaction conditions.

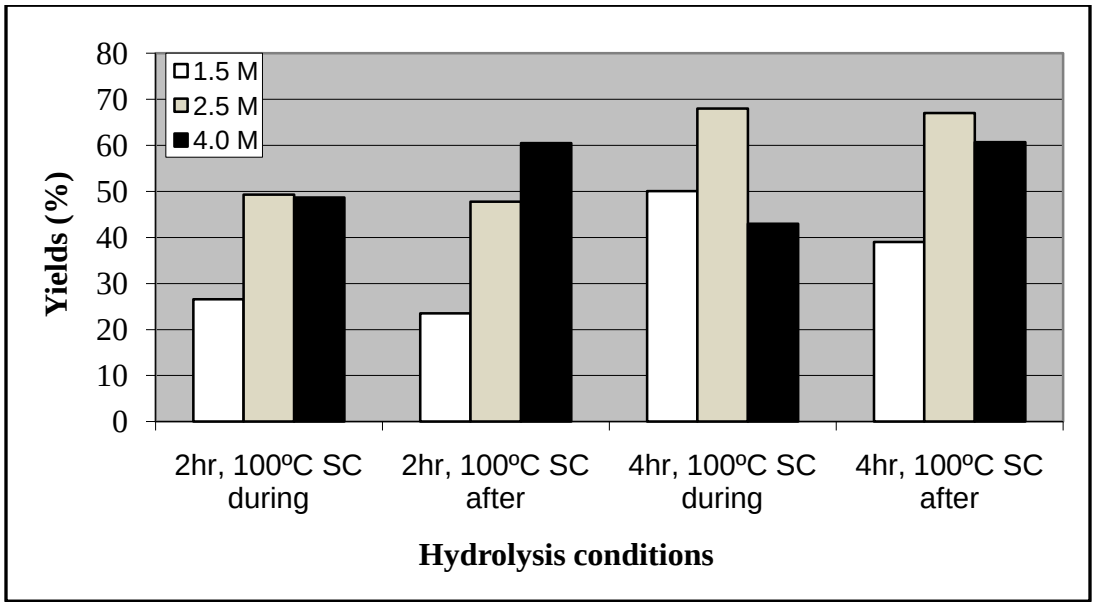

Figure 3.3 The yields of cellulose nanocrystals with different acid (HBr) concentrations

3.4.2 The Effect of Ultrasonication to the Yield of Cellulose Nanocrystals

We expect the sonic energy application to significantly affect the production of cellulose nanocrystals. Using sonic energy during hydrolysis will break up conglomerated particles when the pulp is still reacting with the HBr. This should affect the results by increasing the area of the pulp vulnerable to acid hydrolysis. The effect of ultrasonic irradiation on the property and yield of cellulose nanocrystals was examined by applying ultrasonication during or after the acidic hydrolysis. Typically, a 5 min 50% power (125W) ultrasound treatment was applied either after the hydrolysis reaction or in 5 min segments every 60 min during the hydrolysis reaction.

The nanocrystal yields shown in Table 3.1 indicate that the amount of cellulose nanocrystals (Sediment II, see Scheme 3.1) is increased at the expense of unreacted cellulose (Sediment I, see Scheme 3.1) due to the fact that the ultrasonic energy is able to disrupt possible nanocrystal aggregation more efficiently when it is applied during hydrolysis rather that after hydrolysis. It is also important to note that the total final yields were constant ranging from 83 to 85% for all conditions examined. These similar total yields imply that the ultrasonic energy applied during hydrolysis caused no irreversible chemical bond scission within the nanocrystals.

Table 3.1 Comparison of yields with/without ultrasonication applied during the hydrolysis of cellulose

Reaction time	2 hours	2 hours-U	4 hours	4 hours-U
Cellulose nanocrystals (Sediment II)	23.5%	26.6%	39.0%	50.1%
Unreacted cellulose (Sediment I)	61.8%	58.8%	45.1%	32.7%
Total	85.3%	85.4%	84.1%	82.8%

1. Hydrolysis in 1.5 M HBr at 100^{o}C 2 h or 4 h

2. U – 5 min. ultrasonication applied every 60 min during acid hydrolysis

3. For precise definition of these terms see Scheme 3.1

Furthermore, the effect of the applied ultrasonication after or during the hydrolysis reaction was compared. Figures 3.4 and 3.5 show the cellulose nanocrystal yields achieved from the hydrolysis conditions of 2.5M HBr at 80°C and 100°C as a function of hydrolysis time

comparing the moment of applied ultrasonication (during vs. after). It can be seen that at higher reaction temperature (100°C) the moment of ultrasonication has practically no effect on the yields of cellulose nanocrystals. However, at lower temperature (80°C) the effect is more pronounced i.e. ultrasonication during the hydrolysis reaction gave significantly higher cellulose nanocrystal yields especially at shorter reaction times (2 and 3 hours). The difference could be explained with the total amount of energy put in the hydrolysis system. At higher hydrolysis temperature the additional energy from the ultrasonication during the hydrolysis reaction does not benefit the formation of cellulose nanocrystals as much as at lower hydrolysis temperatures.

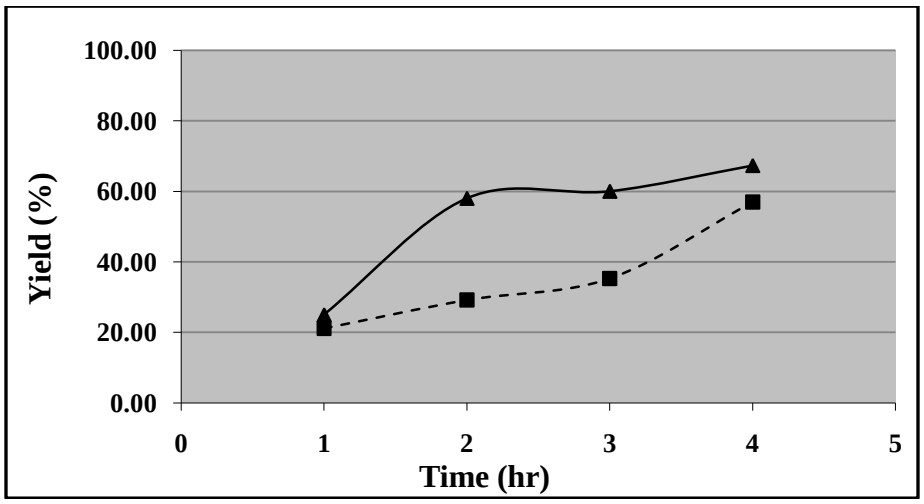

Figure 3.4 The effect of the applied ultrasonication to the yields of cellulose nanocrystals from the hydrolysis with 2.5M HBr at 80°C (solid line ultrasonication during the reaction, dashed ultrasonication after the reaction)

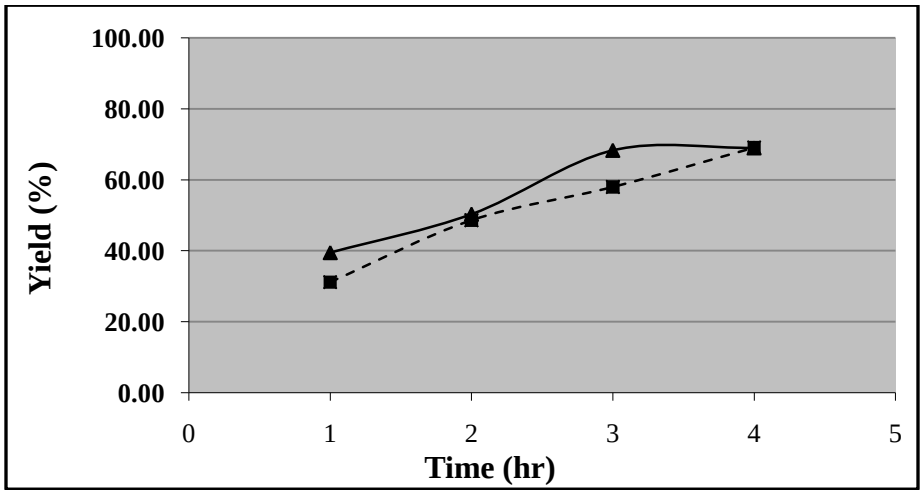

Figure 3.5 The effect of the applied ultrasonication to the yields of cellulose nanocrystals from the hydrolysis with 2.5M HBr at 100°C (solid line ultrasonication during the reaction, dashed line ultrasonication after the reaction)

3.4.3 Thermal Analysis of Cellulose Nanocrystals

In an effort to further understand the nature of our samples and attempt to correlate their macromolecular characteristics to the hydrolysis conditions we turned our attention to the use of thermal analysis. Thermogravimetric analyses showed that the obtained cellulose nanocrystals degraded in an identical fashion to that of a 40 mesh cellulose powder ground from the original filter paper (Figure 3.6) starting to decompose around 320°C. Since the thermal stability data of the original powdered cellulose and any of the nanocrystals was practically identical, it is logical to assume that the hydrolysis conditions did not introduce any sites within the nanocrystals that would make them more thermally labile.

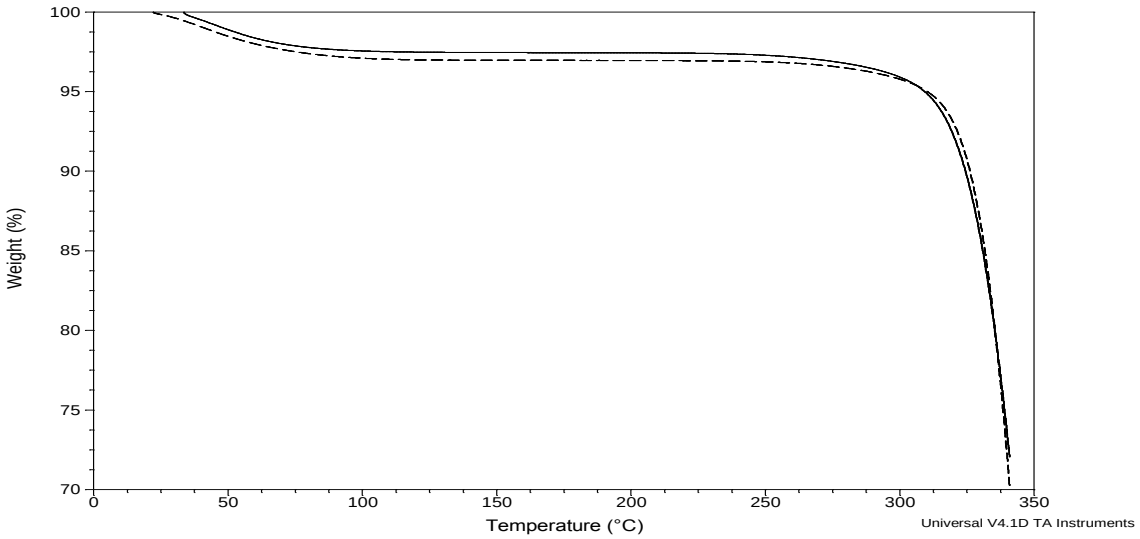

Figure 3.6 Thermal decomposition of cellulose (dashed line) and cellulose nanocrystals (solid line) measured by TGA.

Alternatively, Differential Scanning Calorimetry (DSC) was found to be a lot more revealing. The glass transition temperature (Tg) of the cellulose powder and the sediments was determined to be about 250^{o}C (dashed vertical line) as shown in Figure 3.7, which was consistent with the Tg values reported by Back *et al.* for semicrystalline wood cellulose.[8] The result that the Tg was not detected for cellulose nanocrystals further indicated the high crystallinity of the cellulose nanocrystals obtained.

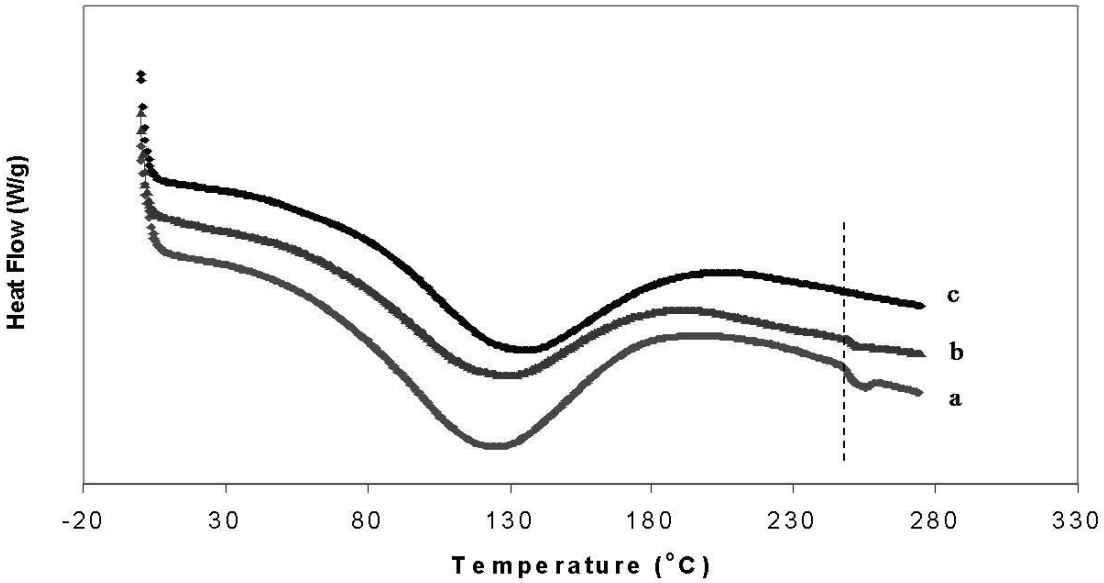

Figure 3.7 DSC thermograms of cellulose powder (a), cellulose sediments (b) and cellulose nanocrystals (c)

A typical differential scanning calorimeter curve for our cellulose samples shows an endotherm at around 100-180^{o}C, which is assumed due to dehydration, that is, loss of absorbed water (Figure 3.7). Integration of the endothermic water evaporation peaks allowed for the heat of evaporation values for water [$\Delta H_{vap}(H_2O)$] to be determined for cellulose powder (Whatman #1), cellulose sediments, and cellulose nanocrystals (Table 3.2). If a sample was cooled to room temperature after a DSC scan over the range 50-250°C and immediately rescanned over the same range, the endothermic peak almost disappeared. The cellulose samples possessing the smaller particle size were found to show smaller $\Delta H_{vap}(H_2O)$ values. This was due, most likely, to the fact that the nanocrystals and the sediment samples had lost all or part of their amorphous cellulose regions during the acid

hydrolysis. It is well known that the water sorption occurs almost totally in the amorphous regions of cellulose. Therefore, the area of endothermic peak due to the loss absorbed water is directly related to the amorphous fraction of cellulose which in turn correlates with the crystallinity of sample.

Table 3.2 Dependency of heat of evaporation of the adsorbed moisture on cellulose particle sizes

Sample	Dimension (μm)	$[\Delta H_{vap}(H_2O)]$ (kJ/g)
Cellulose powder (Whatman #1)	400	4.2
Cellulose sediment (Sediment I)	10 x 1	3.7
Cellulose nanocrystals (Sediment II)	0.1-0.3 x 0.02-0.03	2.9

For precise definitions of these terms see Scheme 3.1

3.4.3.1 The Correlation of $\Delta H_{vap}(H_2O)$ Values to the Crystallinity of the Cellulose Nanocrystals

Bertran et al. studied the correlation between the cellulose crystallinity and enthalpy of evaporation of absorbed water by using the DSC.[9] They found out that the higher is the crystallinity of the particles, the lower is the energy needed for water removal (Figure 3.8). It was postulated that most of the bulk water is absorbed in the amorphous regions of cellulose, i.e., the higher is the crystallinity of the cellulose sample the lower is the heat of evaporation for water $[\Delta H_{vap}(H_2O)]$. Their results were in good agreement with X-ray diffraction measurements.

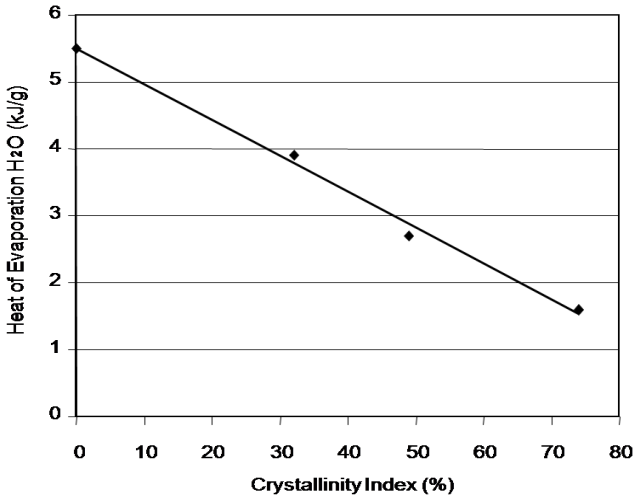

Figure 3.8 Heat of evaporation of H_2O for cotton linters vs. crystallinity index (Bertran *et al.* 1986)

We plotted the [$\Delta H_{vap}(H_2O)$] values against the hydrolysis reaction time and arrived at a similar conclusion (Figure 3.9)

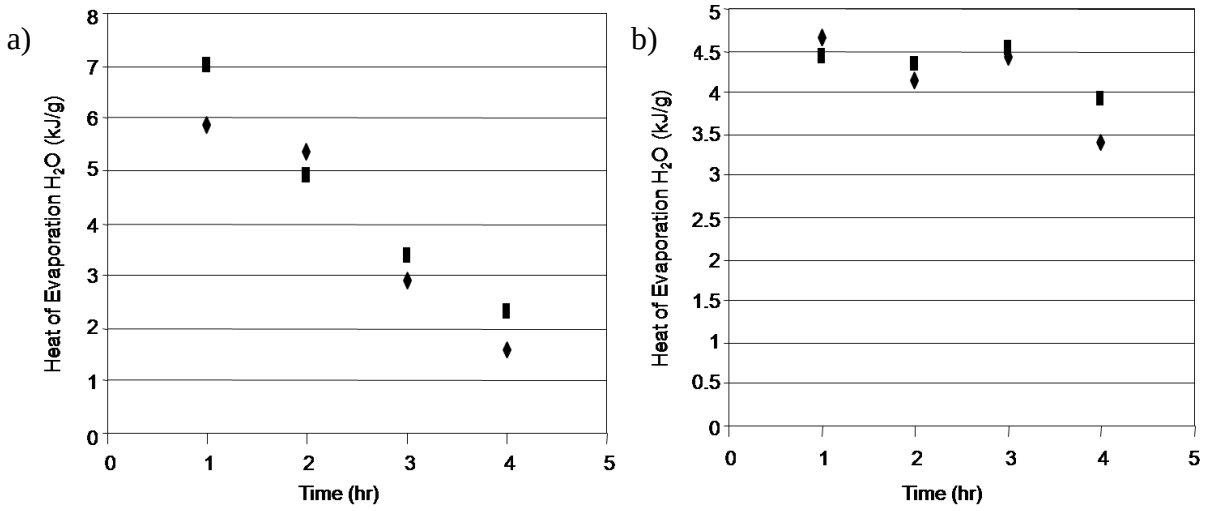

Figure 3.9 Heat of evaporation of H_2O for cellulose nanocrystals (a) and sediment I (unreacted cellulose, See Scheme 3.1) (b)

It was found out that the crystallinity of dispersed nanoparticles seems to increase during the hydrolysis as the [$\Delta H_{vap}(H_2O)$] values decrease along the increased reaction time. Moreover, the [$\Delta H_{vap}(H_2O)$] values for the sediments (Sediment I, Scheme 3.1) remained rather constant most likely due to the remaining regions of amorphous cellulose in them.

3.4.4 X-ray Diffraction Experiments

As anticipated, the cellulose nanocrystals obtained after acid hydrolysis were highly crystalline structures as shown by the X-ray diffraction data in Figure 3.10.

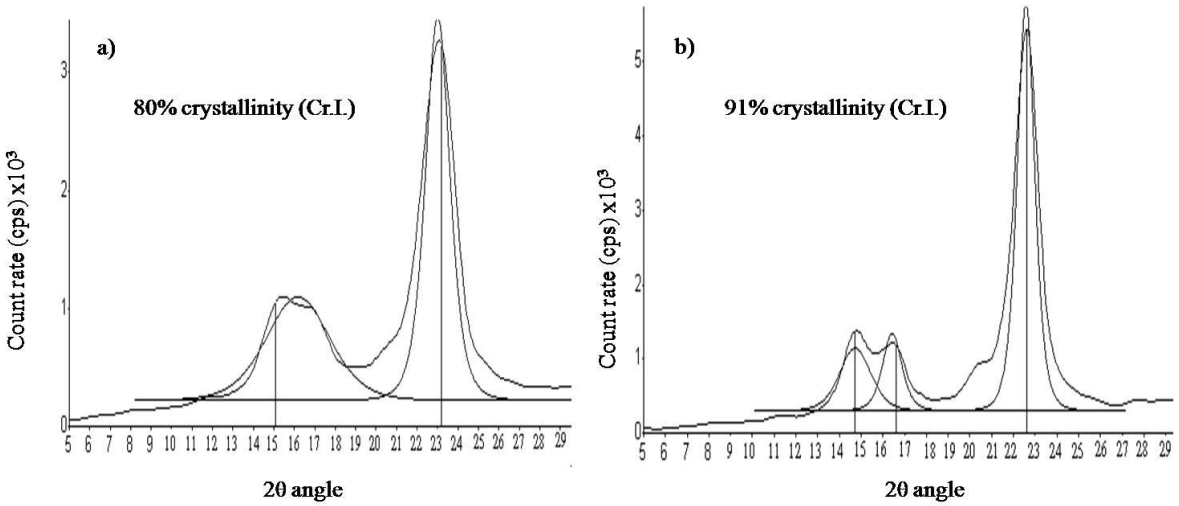

Figure 3.10 X-ray diffraction of cellulose powder (Whatman #1) (a) and cellulose nanocrystals (b)

Proper control of the hydrolysis conditions resulted in the selective degradation and preferential removal of the amorphous cellulosic fraction. The crystallinities were

calculated according to Segal *et al* (equation 1).[10] It was found out that crystallinity index increased from 80% to 91% during the acidic hydrolysis process.

$$Cr.I.\ (\%) = ((I_{002} - I_{am}) / I_{002}) \times 100 \qquad \text{(equation 1)}$$

where I_{002} is the maximum intensity from (002) plane at $2\theta = 22.8°$ and I_{am} is the intensity of the background scatter measured at $2\theta = 18°$

3.4.5 Atomic Force Microscopy (AFM)

The size distribution and shape of the nanocrystals are shown in the AFM photomicrographs displayed in Figure 3.11. It can be estimated from the AFM images that rod-like cellulose nanocrystals has an approximate length of 100-300 nm and a diameter of 20-30 nm.

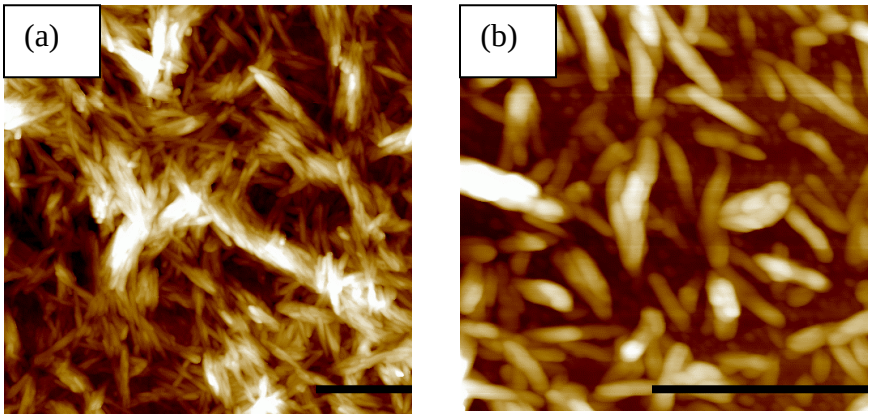

Figure 3.11 Atomic force photomicrographs of cellulose nanocrystals obtained (a) 1.5 M HBr, 100°C, 2 hr; (b) 2.5 M HBr, 100°C, 2 hr; scale bar = 500 nm.

3.4.6 Transmission Electron Microscopy (TEM)

The length distribution of cellulose nanocrystals were estimated from TEM images. TEM data demonstrates that at this point in our work we are able to develop rod-like nanocrystals of approximately 100-400 nm (Figure 3.12). However, the aggregation of cellulose whiskers hindered the determination of transverse dimensions.

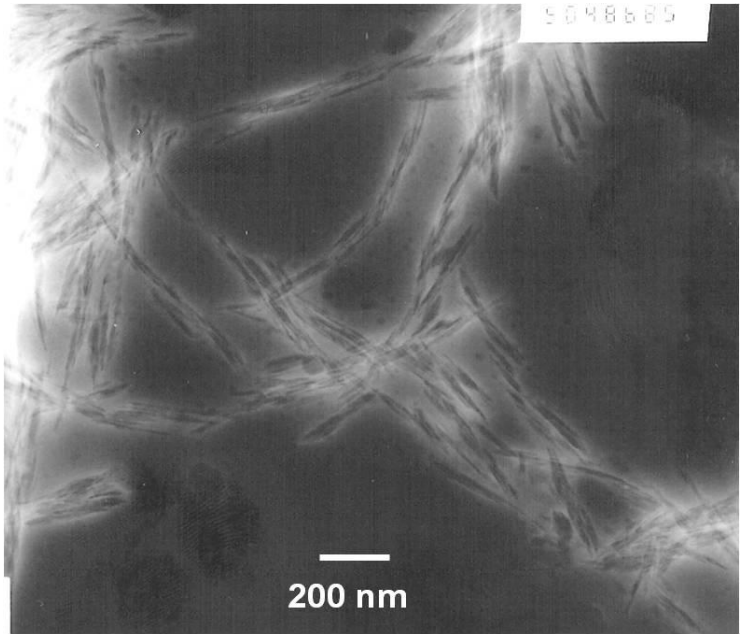

Figure 3.12 TEM image of cellulose nanocrystals (100°C, 3hr, ultrasonication during the hydrolysis reaction)

However, the average crystallite sizes can be obtained from the X-ray diffraction data by using the Debye-Scherrer formula (equation 2).[11] The results from X-ray diffraction and TEM are summarized in Table 3.3. The aggregation issue can also be overcome by

introducing negative charges on the surface of cellulose nanocrystals, either by oxidation or postsulfation.[4,6,12,13]

$$D = k \lambda Cu/\beta \cos\theta \qquad \text{(equation 2)}$$

here k = 0.9, λCu = 0.154056 nm, β = FWHM (full width at half maximum, or half-width) in radians, θ = the position of the maximum of diffraction.

Table 3.3 Crystallinity and average sizes of cellulose nanocrystals determined by XRD and TEM

Sample	Crystallinity index (Cr.I.)	Transverse 1 (nm)	Transverse 2 (nm)	Length (nm)
100°C, 1hr-U	88	7.0	7.6	100-400
100°C, 2hr-U	89	7.6	7.7	100-400
100°C, 3hr-U	91	8.6	7.7	100-400

U – 5 min. ultrasonication applied every 60 min during acid hydrolysis.

3.4.7 Molecular Weight Distribution of Cellulose Nanocrystals

The determination of molecular weight of cellulose is a challenging task because of its insolubility in most common solvents. Typically, the gel permeation chromatography analyses are carried out using tetrahydrofuran (THF) or chloroform ($CHCl_3$) as a mobile phase. In order to solubilize cellulose in these organic solvents its hydroxyl groups need to be derivatized so that the strong hydrogen bonding network will be disrupted. This can be achieved in several ways but the most common approaches are different esterification reactions such as acylation and benzoylation. However, derivatization with high degree of

substitution has been difficult to achieve because of the incomplete solubility of cellulose in common solvents. Recently, a novel class of solvents, ionic liquids, was discovered as excellent solvents for cellulosic materials. Since then, significant amount of the traditional synthetic cellulose chemistry has been conducted using ionic liquids as solvents producing highly substituted cellulose products.

The benzoylation reactions were carried out in 1-allyl-3-methylimidazolium chloride [Amim(Cl)], perhaps the most widely employed ionic liquid in chemical modifications of the cellulosic materials[14],[15],[16],[17] The cellulose benzoates were characterized by ^{1}H-NMR spectroscopy (Fig. 3.13). Cellulose benzoates have characteristic signals at δ = 6.8–8.2 for the phenyl protons, and at δ = 2.8–5.9 for the protons of cellulose backbone.[18]

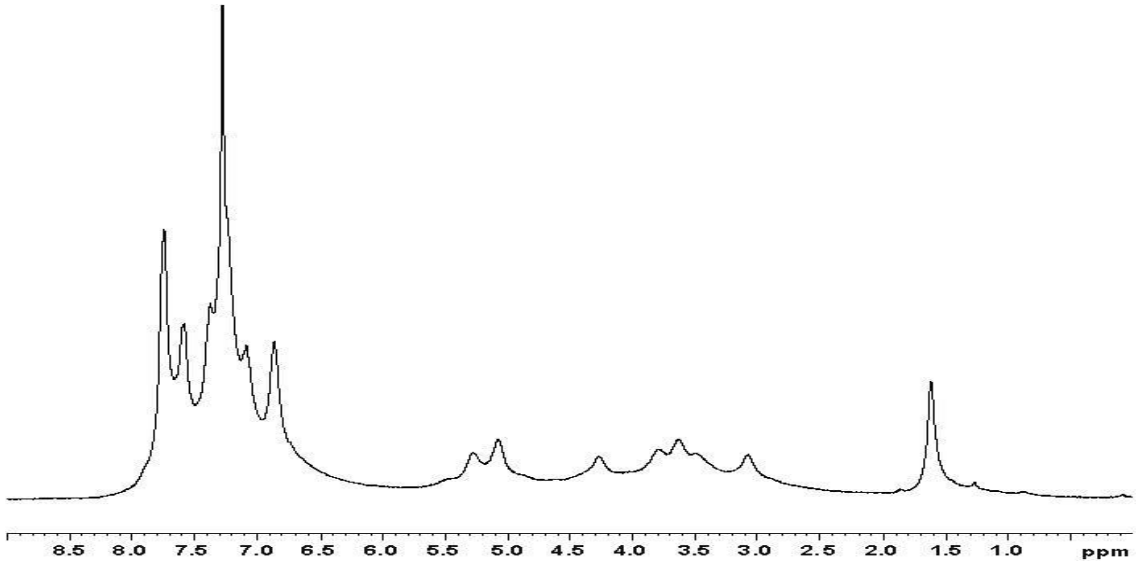

Figure 3.13 ^{1}H NMR spectrum of benzoylated cellulose nanocrystals dissolved in $CDCl_3$

By the virtue of the hydrophobic benzoyl groups introduced during the successful benzoylation reactions cellulose samples became soluble in THF which in turn made it possible to determine the molecular weight of cellulosic samples by using gel permeation chromatography. The GPC chromatograms for the starting material cellulose and cellulose nanocrystals are shown in Figure 3.14.

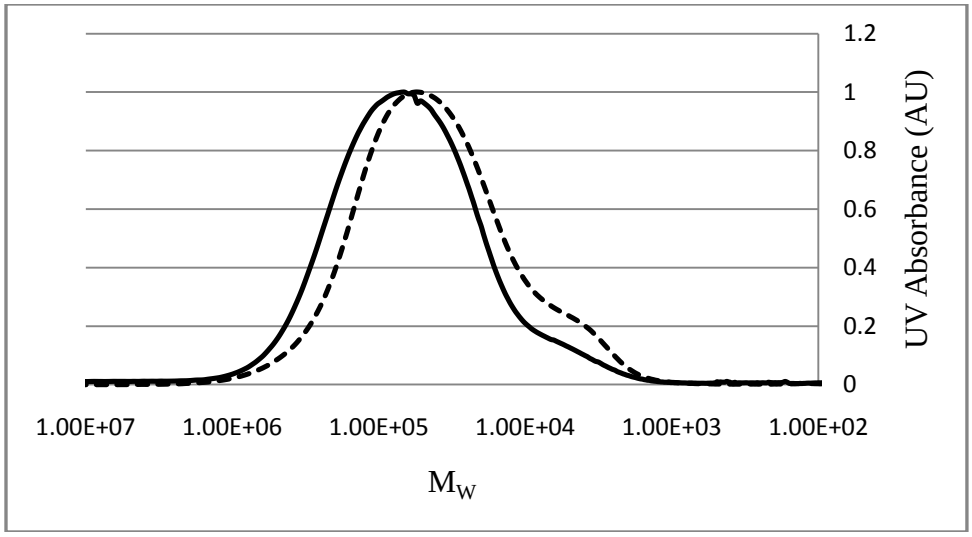

Figure 3.14 GPC chromatogram of benzoylated cellulose (Whatman#1, solid line) and benzoylated cellulose nanocrystal (dashed line)

It is obvious that the cellulose nanocrystals have lower molecular weight than the starting material cellulose due to the hydrolysis of the remaining amorphous regions of the starting cellulose. The molecular weight of cellulose dropped by 26 x 10^3 $gmol^{-1}$ during the acidic hydrolysis resulting in cellulose nanocrystals with a molecular weight of 69 x 10^3 $gmol^{-1}$ as can be seen from the Table 3.4.

Table 3.4 Molecular weight distributions of starting material cellulose (Whatman #1) and cellulose nanocrystals

Sample	Mw (1 x10^3 $gmol^{-1}$)	Polydispersity (PD)
Whatman #1	95	3.8
Cellulose nanocrystals	69	4.1

3.5 Conclusions

Hydrobromic acid (HBr) hydrolysis was used for the production of cellulose nanocrystals (CNCs) from the Whatman #1 filter paper. Different reaction parameters were studied and the optimum conditions for the hydrolysis reaction were found to be 2.5 M HBr, 3 hours at 100°C applying the ultrasonic energy in the course of the reaction. The produced CNCs were characterized with various methods and found to be highly crystalline and having transverse dimensions of 7-8 nm and being 100-400 nm length. Moreover, the methodology based on the dissolution of cellulose in the ionic liquid followed by the derivatization and the determination of the molecular weight was introduced.

3.6 References

1. Battista, O. A. (1950). "Hydrolysis and Crystallization of Cellulose," *Ind. Eng. Chem., 42*(3), 502-507.

2. Dong, X., Revol, J., and Gray, D. (1998). "Effect of microcrystallite preparation conditions on the formation of colloid crystals of cellulose," *Cellulose*, 5(1), 19-32.

3. Beck-Candanedo, S., Roman, M., and Gray, D. G. (2005). "Effect of Reaction Conditions on the Properties and Behavior of Wood Cellulose Nanocrystal Suspensions," *Biomacromolecules,* 6(2), 1048-1054.

4. Araki, J., Wada, M., Kuga, S., and Okano, T. (1999). "Influence of surface charge on viscosity behavior of cellulose microcrystal suspension," *J. Wood Sci.*, 45(3), 258-261.

5. Araki, J., Wada, M. and Kuga, S. (2001). "Steric stabilization of a cellulose microcrystal suspension by polyethylene glycol (PEG) grafting," *Langmuir*, 17(1), 21-27.

6. Araki, J., Wada, M., Kuga, S., and Okano, T. (1998). "Flow properties of microcrystalline cellulose suspension prepared by acid treatment of native cellulose," Colloids *and Surfaces A: Physicochemical and Engineering Aspects*, 142(1), 75–82.

7. Dong, X. M., Kimura, T., Revol, J., and Gray, D. G. (1996). "Effects of Ionic Strength on the Isotropic−Chiral Nematic Phase Transition of Suspensions of Cellulose Crystallites," *Langmuir*, 12(8), 2076-2082.

8. Back L. E. and Salmen N. L. (1982). "Glass transitions of wood components hold implications for molding and pulping processes," *Tappi*, 65(7), 107-110.

9. Bertran, M., S. and Dale, B., E. (1986). "Determination of Cellulose Accessibility by Differential Scanning Calorimetry,"*J. Appl. Pol. Sci.*, 32, 4241-53.

10. Segal, L., Creely, J. J., Martin Jr, A. E., and Conrad, C. M. (1959). "An empirical method for estimating the degree of crystallinity of native cellulose using X-ray diffractometer," *Textiles Research Journal*, 29(10)**,** 786–794.

11. Ahtee, M., Hattula, T., Mangs, J., and Paakkari, T. (1999). "An X-ray diffraction method for determination of crystallinity of wood pulp," *Paperi Ja Puu*, 8, 475–480.

12. Araki, J., Wada, M., Kuga, S., and Okano, T. (2000). "Birefringent glassy phase of a cellulose microcrystal suspension," *Langmuir*, 16(6), 2413-2415.

13. Orts, W. J., Godbout, L., Marchessault, R. H., and Revol, J.-F. (1998). "Enhanced Ordering of Liquid Crystalline Suspensions of Cellulose Microfibrils: A Small Angle Neutron Scattering Study," *Macromolecules*, 31(17), 5717-5725.

14. Granstrom, M., Kavakka, J., King, A., Majoinen, J., Makela, V., Helaja, J., Hietala, S., Virtanen, T., Maunu, S-L., Argyropoulos, D. S., and Kilpelainen, I. (2008). "Tosylation and acylation of cellulose in 1-allyl-3-methylimidazolium chloride," *Cellulose*, 15(3), 481–488.

15. Heinze, T., Schwikal, K., and Barthel, S. (2005). "Ionic Liquids as Reaction Medium in Cellulose Functionalization," *Macromolecular Bioscience* 5(6), 520-525.

16. Xie, H., King, A., Kilpelainen, I., Granstrom, M., and Argyropoulos, D. S. (2007). "Thorough chemical modification of wood-based lignocellulosic material in ionic liquids," *Biomacromolecules*, 8(12), 3740-3748.

17. Zhang, J., Wu, J., Cao, Y., Sang, S., Zhang, J., and He, J. (2009). "Synthesis of cellulose benzoates under homogeneous conditions in an ionic liquid," *Cellulose*, 16(2), 299-308.

18. Acemoglu, M., Kusters, E., Baumann, J., Hernandez, I., and Mak, C. P. (1998). "Synthesis of regioselectively substituted cellulose derivatives and applications in chiral chromatography," *Chirality*, 10, 294–306.

4. Determination of Cellulose Reactivity by Using Phosphitylation & Quantitative ^{31}P NMR Spectroscopy

4.1 Abstract

The phosphitylation of cellulose with 2-chloro-4,4,5,5-tetramethyl-1,3,2-dioxaphospholane [P(II)], is proposed as a means to determine its reactivity via an evaluation of its accessible hydroxyl groups. A variety of cellulose samples were subjected to this phosphitylation reaction and the consumption of phosphitylation reagent [P(II)], was followed by quantitative ^{31}P-NMR spectroscopy. This consumption was found to be directly proportional to the amount of reactive hydroxyl groups on the cellulosic material. To further evaluate the quantitative reliability of this methodology, cellulose samples were subjected to a series of mechanical beating treatments and the changes in the amount of accessible OH groups were evaluated. In addition, cellulose samples were equilibrated to various moisture contents and their accessible OH groups were determined using the developed methodology. Both variables examined were found to affect the amount of reactive OH groups present on the samples with variations in the moisture content having a greater effect. For example up to 6.5 mmol g^{-1}, of accessible OH groups were found to be created within the highly refined samples at the highest moisture content.

4.2 Introduction

Cellulose, the most abundant component of plant cell walls, exists as long fibers composed of aggregated cellulose chains called microfibrils[1]. These microfibrils consist of two distinctly different regions: highly ordered crystalline region and less ordered amorphous

regions. In nature, cellulose microfibrils are highly, albeit not completely, crystalline. As much as 70-80% of cellulose in cotton and about 60-70% of cellulose in wood is crystalline. The crystallinity of microfibrils is a combination of physicochemical factors such as linearity and structural uniformity of cellulose polymer that allows several individual cellulose chains to pack together and form a very ordered crystalline structure. Moreover, the cellulose polymer has a large number of hydroxyl groups capable of forming hydrogen bonds between (inter), and also within (intra) its polymeric chains. This extensive hydrogen bond network is known to greatly affect the accessibility of crystalline cellulose as it remains intact in the presence of most common solvents. Most aqueous reagents, however, can penetrate and swell the amorphous or non-crystalline regions of cellulose fibers. Thus, the concepts of crystallinity and accessibility of cellulose are closely related.

The accessibility of the hydroxyl groups within cellulose plays an important role in determining its reactivity toward the various chemical modifications of this material as far as its homogeneous chemical derivatization is concerned[2]. Furthermore, the accessibility of cellulose is one of the key parameters affecting the efficient production of bioethanol[3,4]. Early attempts to quantitatively determine the accessible hydroxyl groups in cellulose were carried out in 1930s[5,6]. These early experiments were focused on the hydrogen-deuterium exchange reaction of D_2O with the OH groups of cellulose. The measurements were based on the density changes of D_2O caused by the simultaneous liberation of H_2O. Since then, deuterium exchange has prevailed as one of the most common approaches to determine the amount of accessible OH groups in cellulosic materials.

Additional methods for quantifying the accessible hydroxyls in cellulosic materials also include acetylation and differential scanning calorimetric based methods (DSC)[7,8]. Among these, deuterium exchange and acetylation are typically used in combination of IR and/or NMR spectroscopic techniques[9,10]. For example, Phuong *et al*. studied the accessibility of heat-treated wood by using hydrogen-deuterium exchange and ^{2}H NMR.[9] The amount of accessible OH groups was found to be significantly lower after the heat treatment, most likely, due to the decreased hygroscopicity of the heat-treated wood. Bertran and co-workers, on the other hand, were able to correlate the cellulose crystallinity and accessibility values by using a DSC technique for determining the amount of the absorbed water. In addition to above methodologies, both X-ray diffraction and iodine sorption measurements have been used for the determination of the crystallinity and accessibility of cellulose. X-ray diffraction data offers a measure of the crystalline component of cellulose while iodine sorption data provides information on the amorphous part or the accessible hydroxyl groups[11,12]. Yet, the correlation of these methods with the reactivity under conditions of industrial relevance and production has not been established.

Dyes have also been used for the determination of cellulose accessibility[13,14]. However, these measurements do not reveal the exact amount of OH groups but can be used for resolving the specific surface area (SSA) of cellulose. The main advantage of using dyes derives from the possibility of determining the accessibility of wet swollen state samples. As a matter of fact, the surface area determinations for a dry nonswollen sample and for a

wet swollen cellulose sample have been reported to vary between 1.9 m^2 g^{-1} to 162 m^2 g^{-1}, respectively[15,16].

One widely used method, especially for determining the reactivity of dissolving pulps, was described by Fock in the late 1950s[17]. This method is a microscale process similar to the viscose process and it measures the amount of cellulose that is not soluble in sodium hydroxide when viscose is prepared. Recently, major efforts have been conducted with studies toward improving the reactivity of dissolved pulps by enzymatic treatment[18,19,20]. In these investigations, Fock's method has been proven particularly useful for determining the reactivity of the various cellulosic materials.

Derivatization of surface hydroxyl groups followed by different analytical techniques has been the chosen approach in several investigations[21,22,23,24]. Chemicals such as trifluoroacetic anhydride or N, N-diethylaziridinium chloride can be effectively utilized for the derivatization of cellulose. Trifluoroacetic anhydride is used in a vapor phase reaction and the derivatives are then characterized by various spectroscopic methods. More specifically, the analysis is carried out in the gaseous phase, thus offering some advantages over typical wet chemical methods. Another methodology, developed by Rowland, utilizes the mild reaction of N, N-diethylaziridinium chloride with the available hydroxyl groups to yield 2-diethylamino ethyl cellulose that can be further silylated and analyzed by gas liquid chromatography.

In this section of dissertation, a new approach, based on phosphitylation followed by quantitative ^{31}P NMR measurements, is proposed for measuring the amount of accessible OH groups in cellulosic materials. This protocol is comprised of phosphitylation of all OH groups present in cellulose using 2-chloro-4,4,5,5-tetramethyl-1,3,2-dioxaphospholane [P(II)] followed by quantitative ^{31}P NMR spectroscopy using guaiacol as the internal standard under carefully selected NMR acquisition conditions.

4.3 Materials and Methods

4.3.1 Sample Preparation and Refining of Cellulose. Samples from cellulose filter paper (Whatman #1, cotton, 80% crystallinity) were refined for specific number of revolutions (5000 and 30000) according to TAPPI method T 248 cm-85. After the refining treatments the samples were first air dried and then homogenized for ten seconds using a blender. The homogenized samples were used as they were for all air dry trials. Moreover, portions of samples were oven dried or conditioned at 69% relative humidity in order to examine the effect of moisture content. Drying was carried out in a heating chamber under reduced pressure (15 mmHg) for 24 hours. The 69% relative humidity was achieved by placing a saturated KI solution at the bottom of a desiccator in which the samples were conditioned over a period of three days prior to analyses. To better understand the effects of refining, control samples were always also examined. Control samples were prepared by first soaking the filter paper in water, then air dried and finally homogenized in a Wearing blender.

4.3.2 Moisture Content Measurements. An electronic moisture analyzer (Sartorius MA 30) was used for the determination of the moisture contents of all the cellulose samples (Table 4.1). The moisture contents for the oven dry samples, however, were not measured as they were readily transferred to the reaction flasks in order to avoid the absorption of ambient moisture.

4.3.3 Phosphitylation of Cellulose. Reactions were carried out in 50 mL pre-dried Schlenk flasks equipped with a magnetic stirrer, an Argon inlet and a septum for reagent addition via a stainless steel syringe. Cellulose sample (100 mg) was suspended in 15 mL of freshly distilled THF (distilled over the sodium lumps under argon atmosphere), 5 mL of dry pyridine containing 0.03 mmoles of 4-(dimethylamino) pyridine (DMAP) and 5 mL of dry chloroform containing 100 µL of guaiacol (0.9 mmol, internal standard). 600 µL of 2-chloro-4,4,5,5-tetramethyl-1,3,2-dioxaphospholane [P(II)] was then added slowly via the septum under slight agitation. The reaction kinetics was followed by taking aliquots (600 µL) from the reaction mixture and then determining the amount of remaining phosphitylation reagent using quantitative ^{31}P NMR spectroscopy. In order to ensure the sampling of clean and transparent samples for the NMR analysis it is essential to let the cellulose to settle on the bottom of the reaction flask prior to sampling. This was achieved by turning off the magnetic stirrer prior to withdrawing an aliquot. It is also worth to mention that in all experiments one flask containing all the chemicals but no cellulose was kept on the side as a blank. The use of this reference sample allowed taking into account the slow decomposition kinetics of the phosphitylation reagent that was observed to occur.

4.3.4 Quantitative ^{31}P NMR of Remaining P(II). Aliquots of 600 µL of the reaction mixture, prepared as described above, were transferred into a NMR tube containing 0.57 mg of chromium(III) acetylacetonate (relaxation agent) dissolved in 50 µL of deuterated chloroform. The quantitative ^{31}P NMR spectra were acquired immediately, using a Bruker 300 MHz spectrometer equipped with a Quad probe dedicated to ^{31}P, ^{13}C, ^{19}F and ^{1}H acquisition. A total of 128 scans were acquired for each sample with the relaxation delay time (d1) of 5.0 seconds[25,26]

4.3.5 Reactivity Calculations. The amount of reactive hydroxyls was calculated based on the theoretical value of 18.5 mmol of hydroxyl groups present per gram of anhydroglucose unit (AGU). The hydroxyl groups in positions 2, 3 and 5 were considered to be reactive.

4.4 Results and Discussion

4.4.1 Phosphitylation of Cellulose

Phosphitylation followed by quantitative ^{31}P NMR analysis have been previously used for the determination of various chemical functionalities of lignocellulosic materials.[25,26] The methodology is based on the phosphitylation reaction of hydroxyl groups in lignocellulosics which in turn improves the solubility of the material and makes the various OH groups NMR detectable (Figure 4.1).

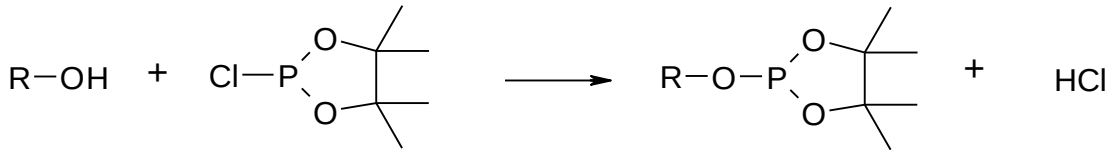

Figure 4.1 Reaction between 2-chloro-4,4,5,5-tetramethyl-1,3,2-dioxaphospholane [P(II)] and hydroxyl group of lignocellulosic material

The current approach, on the other hand, while it is based on the same reaction, it does not focus on the analysis of the dissolved material but instead the reaction is carried out in a heterogeneous non-swelling environment. The foundations of the methodology rest on the extreme reactivity of the cellulosic OH groups with the phosphitylating reagent, and the accurate detection of the unreacted (remaining) phosphitylating reagent. The latter value in turn provides information of the reactivity of the cellulosic material. Figure 4.2 shows a typical ^{31}P NMR spectrum of remaining phosphitylation reagent from a typical cellulosic reaction mixture.

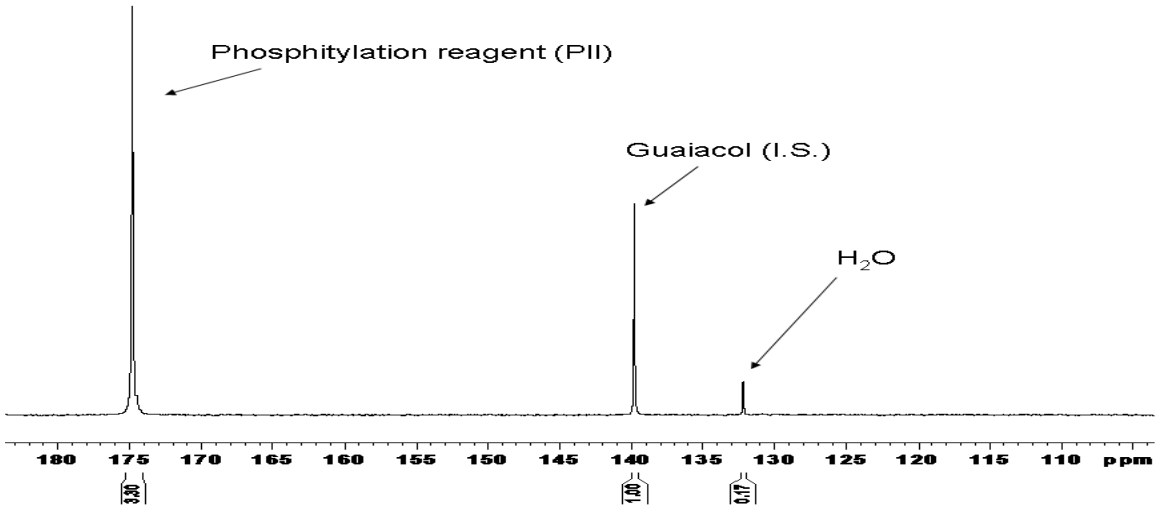

Figure 4.2 A typical quantitative ^{31}P NMR spectrum of remaining phosphitylation reagent. Signals: H_2O adduct of phosphitylation reagent (132.2 ppm), phosphitylated guaiacol (I.S., 139.9 ppm) and phosphitylation reagent (174.9 ppm)

Three signals are apparent, one derived from the H_2O adduct of the phosphitylation reagent (132.2 ppm), one from phosphitylated guaiacol (139.9 ppm) and one from remaining phosphitylation reagent (174.9 ppm), respectively.

4.4.2 Preliminary experiments with an air dry filter paper

In an effort to determine the reaction time required for complete phosphitylation, an air dried, Whatman #1 filter paper sample was subjected to the developed methodology as described in the experimental section. The consumption of phosphitylating reagent was seen to be complete after 30 minutes of reaction (Figure 4.3).

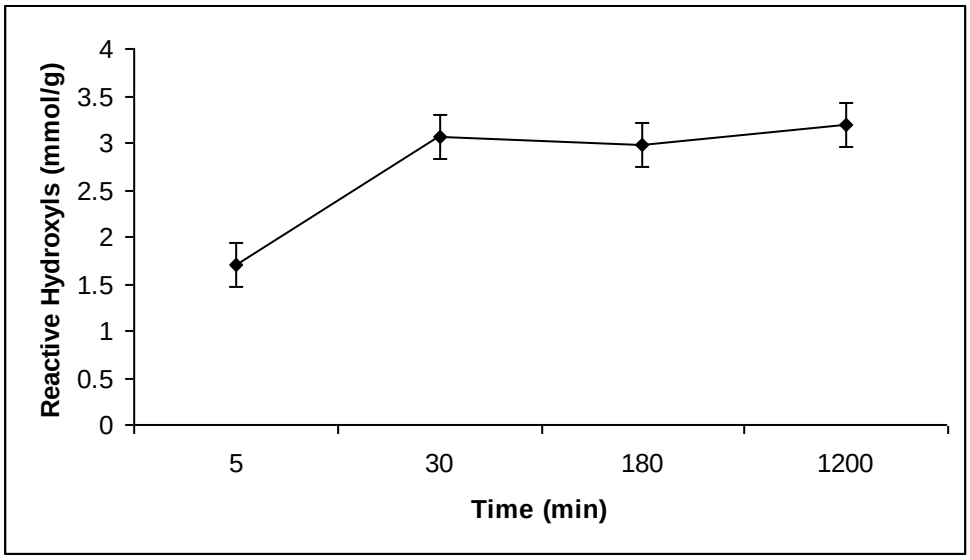

Figure 4.3 Preliminary phosphitylation experiments with an air dry sample. Reaction was seen to level off after 30 minutes

The amount of phosphitylating reagent was found to remain at constant level for up to 20 hours. Furthermore, in an effort to delineate any possible effects the sample size may have had on the determined reactivity, the amount of cellulose was increased to 300 mg. As shown in Figure 4.4, increased sample size did not affect the reactivity of cellulose. As a matter of fact, the reaction profiles were found to be very similar with an error of approximately 0.5 mmol g^{-1}.

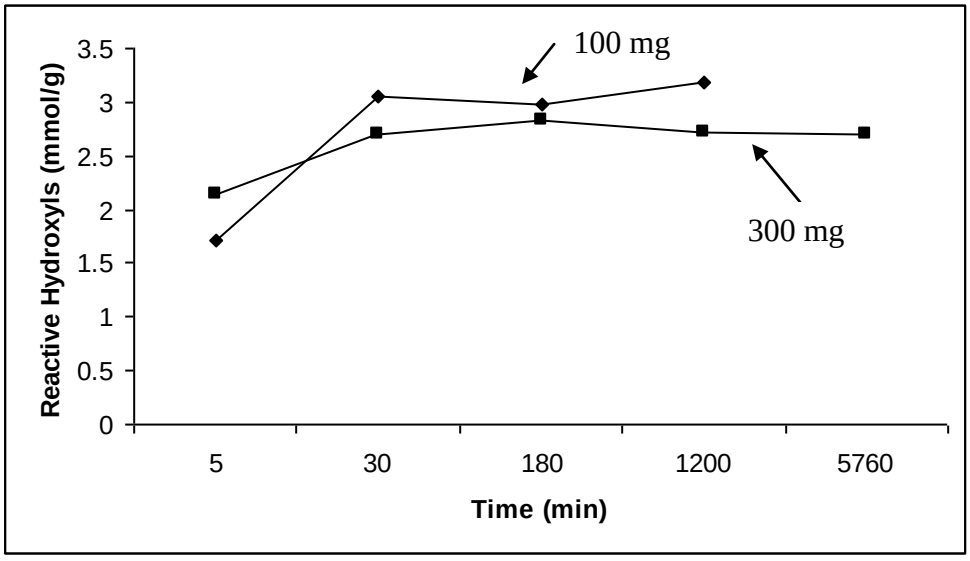

Figure 4.4 Scaling up experiments with air dry cellulose samples with two different sample sizes

4.4.3 Effect of Laboratory Beating

To further investigate the validity of the proposed methodology, cellulose samples from two different beating treatments were subjected to these analyses. The mechanical treatment of fibrous material results in several actions on the fiber: it can fibrillate the surface of the

fibers, it produces fines and also generates internal pores. All the aforementioned factors can be considered to increase the amount of available hydroxyl groups in cellulosic materials. This set of experiments clearly showed that intense (30000 rev.) refining increased the reactivity of the cellulose exposing more hydroxyl groups for reaction with the phosphitylating reagent. Alternatively, the difference between a control and slightly refined sample (5000 rev.) showed hardly any difference in the amount of available OH groups (Figures 4.5 and 4.6). However, at higher moisture contents, the slightly refined sample was seen to open up and the difference to the control became more distinguishable (Figure 4.7).

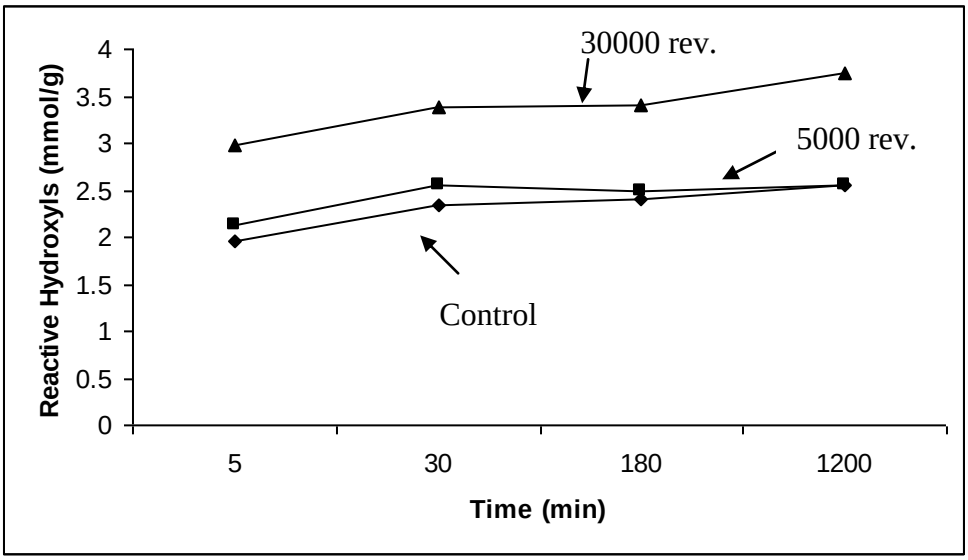

Figure 4.5 Reactivity of oven dry cellulose samples. Control refers to untreated sample; 5000 rev. refers to slightly refined sample and 30000 rev. refers to the most refined sample

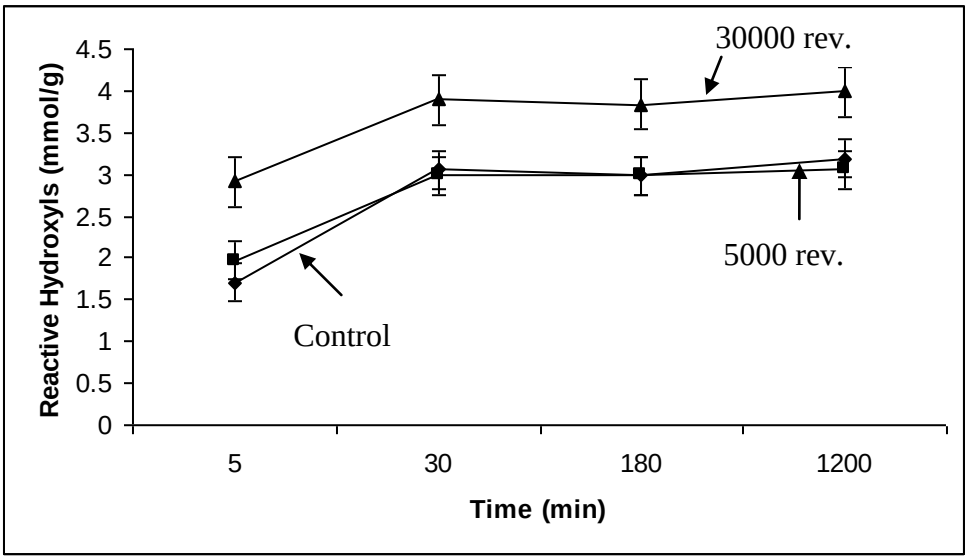

Figure 4.6 Reactivity of air dry cellulose samples. Control refers to untreated sample; 5000 rev. refers to slightly refined sample and 30000 rev. refers to the most refined sample

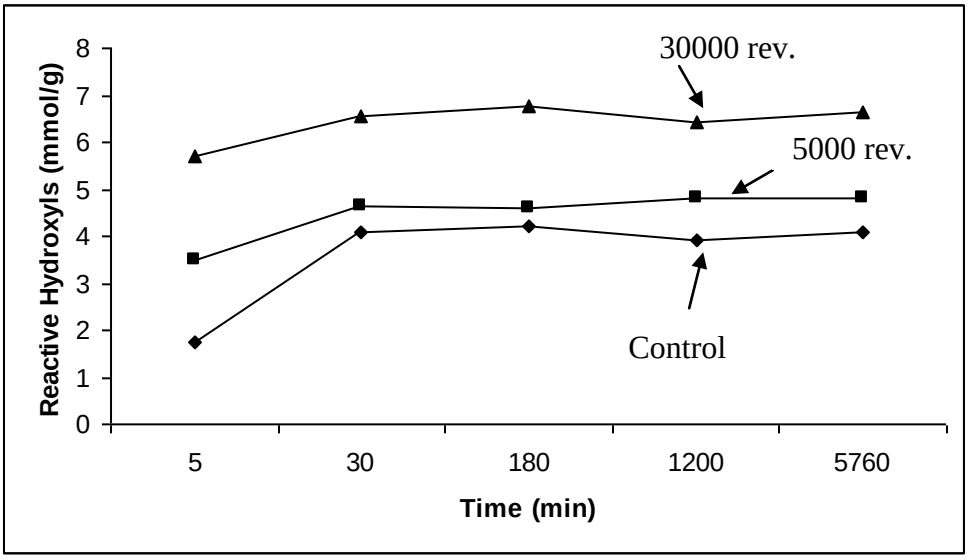

Figure 4.7 Reactivity of cellulose samples conditioned at 69% RH. Control refers to untreated sample; 5000 rev. refers to slightly refined sample and 30000 rev. refers to the most refined sample

It is worth to mention at this point that the starting filter paper sample had a crystallinity as high as 80%. Hence, in theory, 20% of its hydroxyl groups are to be located in the amorphous regions. This in turn implies that our method may determine up to t 20% of the stoichiometrically present OH groups in the starting untreated control samples. By using the previously described theoretical maximum value of 18.54 mmol g^{-1} for all accessible hydroxyl groups, our experimental data shows a maximum reactivity of 2.5 mmol g^{-1} (13%) for the oven dry sample, 3.2 mmol g^{-1} (17%) for the air dry sample and 4.1 mmol g^{-1} (22%) for the humidity conditioned control sample. These values all vary consistently and within range of the calculated theoretical value of 20% reactivity. It is worth mentioning here that Phuong *et al*. has reported a reactivity as high as 6.8 mmol g^{-1} for the hydroxyl groups in non-treated wood samples.[9] Although the value is considerably higher than the reactivity observed for our cellulose samples it is not totally surprising when the lower crystallinity and other reactive hydroxyl groups present in wood are taken into consideration.

The highest reactivity, approximately 6.5 mmol g^{-1}, was observed for the most refined (30000 rev.) sample with highest moisture content (Figure 4.7). Such reactivity is well above the amount of OH groups present within the amorphous region of the starting material and corresponds to 35% of the theoretically accessible maximum described above. One may assume that the mechanical treatment increased the reactivity of the sample by causing extensive fibrillation of the fibers and/or the production of fines, i.e., more surface area/unit sample weight.

At this point, it can be stated that the developed protocol was shown to be highly sensitive for probing the morphological changes in cellulose as experienced by mechanical refining. Moreover, the methodology, despite the fact that it is carried out in a nonswollen environment, it allows the monitoring of the effects of increased moisture content when in equilibrium with a cellulosic sample.

4.4.4 Effect of Moisture Content

Dry cellulose absorbs moisture from the air rather rapidly, to a given equilibrium moisture content. This absorption is particularly effective on the amorphous accessible regions of cellulose and it increases with the relative humidity (RH). Crystalline regions of cellulose, on the other hand, cannot be attacked by aqueous reagents, and therefore remain unchanged.[1] For the purposes of this work the data discussed is limited to a maximum moisture content of approximately 15% (Table 4.1). However, further investigations of extended moisture levels beyond the 15% level may also be examined either by increasing the amount of phosphitylation reagent or by decreasing the sample size.

Table 4.1 Moisture contents (%) of cellulose samples

Sample	Oven dry	Air dry	69% RH
Control	n.d.	7.8	11.0
5000 rev.	n.d.	7.9	10.9
30000 rev.	n.d.	9.7	14.2

n.d. = not determined
Oven dry samples were assumed to have near 0% moisture content
69% RH samples were conditioned in desiccator for 72h at 23°C

The effect of increased moisture content can clearly be seen from the data of Figures 4.5, 4.6 and 4.7. Initially, the amount of accessible hydroxyl groups is seen to increase in tandem with increased moisture content. For example, the OH reactivities were found to be elevated by approximately 1.5-3.0 mmol g^{-1} when comparing the values of the oven dry samples (Figure 4.5) to the ones that were conditioned at 69% RH (Figure 4.7). Secondly, the moisture content was found to have a greater effect to the accessibility of refined samples i.e. the difference between oven dry and moist samples is seen to be larger for the refined samples than for the control samples. Furthermore, the difference between the control and the slightly refined (5000 rev.) sample is more pronounced at the higher moisture content, most likely due to an increased swelling of fibers (Figure 4.7). The experimental data from the different moisture contents suggests that the structures subjected to the mechanical treatment are more susceptible to moisture changes because of the increased surface area produced by the mechanical treatment.

4.5 Conclusions

A newly developed sensitive methodology, based on a phosphitylation reaction of cellulose can be used for the determination of accessible hydroxyl groups in such materials. The sensitivity of the technique is such that allows for changes to be observed as they are induced on cellulose via mechanical refining as well as variable equilibrium moisture contents.

Error analyses and the reproducible and sensitive nature of the developed technique will be of further use in a multitude of applications that require the absolute and accurate measurement of cellulosic surface development, i.e., as a function of various industrially treatments (enzymatic, chemical, mechanical) as engaged in diverse applications of cellulose containing materials.

4.6 References

1. McGinnis, G. D. and Shafhadeh, F. (1980). *Pulp and Paper Chemistry and Chemical Technology*; Wiley-Interscience: New York.

2. Gandini, A. and Belgacem, M. N. (2005). "Modified cellulose fibers as reinforcing fillers for macromolecular matrices," *Macromolecular Symposia*., 221, 257.

3. Frederick, W. J., Lien, S. J., Courchene, C. E., DeMartini, N. A., Ragauskas, A. J., and Iisa, K. (2008). "Production of ethanol from carbohydrates from loblolly pine: A technical and economic assessment," *Bioresource Technology*, 99(11), 5051.

4. Galbe, M. and Zacchi, G. (2007). "Pretreatment of lignocellulosic materials for efficient bioethanol production," *Advances in Biochemical Engineering/Biotechnology*, 108, 41.

5. Bonhoeffer, K. F. (1934). "Reactions of heavy hydrogen,"*Z. Elektrochem*., 40, 469.

6. Champetier, G. and Viallard, R. (1938). "Exchange reaction of cellulose and heavy water. Hydration of cellulose," *Bull. Soc. Chim.*, 5, 1042.

7. Mann, J. and Marrinan, H. J. (1956). "The Reaction Between Cellulose and Heavy Water. Parts 1, 2 and 3," *Trans. Faraday Soc.*, 52, 481.

8. Bertran, M. S. and Dale, B. E. (1986). "Determination of Cellulose Accessibility by Differential Scanning Calorimetry," *Journal of Applied Polymer Science*, 32, 4241.

9. Phuong, L. X., Takayama, M., Shida, S., Matsumoto, Y., and Aoyagi, T. (2007). "Determination of the accessible hydroxyl groups in heat-treated *Styrax tonkinensis* (Pierre) Craib ex Hartwich wood by hydrogen-deuterium exchange and 2H NMR spectroscopy," *Holzforschung*, 61, 488.

10. Nishiyama, Y., Isogai, A., Okano, T., Müller, M., and Chanzy, H. (1999). "Intracrystalline Deuteration of Native Cellulose," *Macromolecules*, 32, 2078.

11. Hessler, L. E. and Power, R. E. (1954). "The use of iodine adsorption as a measure of cellulose fiber crystallinity," *Textile Res. J.*, 24, 822.

12. Racz, I., Borsa, J., and Bodor, B. (1996). "Crystallinity and accessibility of fibrous carboxymethyl cellulose by pad-roll technology," *J. Appl. Polym. Sci.*, 62(12), 2015.

13. Inglesby, M. K. and Zeronian, S. H. (1996). "The accessibility of cellulose as determined by dye adsorption," *Cellulose*, 3, 165.

14. Bairathi, A. (1993). "Dyeing sorption isotherms of three direct dyes and their mixtures on purified cotton," *Textile Chemist and Colorist*, 25(12), 41.
15. Warwicker, J. O., Jeffries, R., Colbran, R. L., and Robinson, R. N. (1966) A Review of the Literature on the Effect of Caustic Soda and Other Swelling Agents on the Fine Structure of Cotton. Shirley Institute Pamphlet No. 93, Manchester, U.K., The Cotton Silk and Man-Made Fibres Research Association.

16. Zeronian, S. H. (1985) In Cellulose Chemistry and its Applications (T. P. Nevell and S. H. Zeronian, eds.), Chichester, England: Ellis Horwood Ltd., pp. 138-158.

17. Fock, W. (1959). "A modified method for determining the reactivity of viscose-grade dissolving pulps," *Papier*, 13, 92.

18. Rahkamo, L., Siika-aho, M., Vehviläinen, M., Dolk, M., Viikari, L., Nousiainen, P., and Buchert, J. (1996). "Modification of hardwood dissolving pulp with purified *Trichodserma reesei* cellulases," *Cellulose*, 3, 153.

19. Henriksson, G., Christiernin, M., and Agnemo, R. "Monocomponent endoglucanase treatment increases the reactivity of softwood sulphite dissolving pulp," *J Ind Microbiol Biotechnol*., 32, 211.

20. Engström, A.-C., Ek, M., and Henriksson, G. (2006). "Improved accessibility and reactivity of dissolving pulp for the viscose process: pretreatment with monocomponent endoglucanase," *Biomacromolecules*, 7, 2027.

21. Östenson, M., Järund, H., Toriz, G., and Gatenholm, P. (2006). "Determination of surface functional groups in lignocellulosic materials by chemical derivatization and ESCA analysis," *Cellulose*, 13, 157.

22. Tasker, S. and Badyal, J. P. S. (1994). "Hydroxyl accessibility in celluloses," *Polymer*, 35, 4717.

23. Rowland, S. P., Roberts, E. J., and Wade, C. P. (1969). "Selective accessibilities of hydroxyl groups in the microstructure of cotton cellulose," *Textile Research Journal*, 39(6), 530.

24. Verlhac, C. and Dedier, J. (1990). "Availability of Surface Hydroxyl Groups in *Valonia* and Bacterial Cellulose," *Journal of Polymer Science: Part A: Polymer Chemistry*, 28, 1171.

25. Argyropoulos, D. S. (1994). "Quantitative phosphorus-31 NMR analysis of lignins, a new tool for the lignin chemist," *J. Wood Chem. Technol., 14*, 45.

26. Granata, A. and Argyropoulos, D. S. (1995). "2-Chloro-4,4,5,5-tetramethyl-1,3,2-dioxaphospholane, a Reagent for the Accurate Determination of the Uncondensed and Condensed Phenolic Moieties in Lignins," *J. Agric. Food Chem., 43*, 1538.

5. Grafting onto Reducing End Group of Cellulose Nanocrystals

5.1 Abstract

Synthetic strategies to create a new class of cellulose nanocrystal materials and exploit the applications of the novel materials have been investigated. More precisely, the chemistry of creating rod-like cellulose nanocrystals and selectively grafting of polymer chains at one end of the nanocrystals were examined. Cellulose nanocrystals were formed from natural cellulose resources by hydrobromic acid (HBr) hydrolysis. Polystyrene (PS) with terminal primary amine functional group was prepared via anionic living polymerization. Coupling reaction of the functional PS to the cellulose nanocrystals through the reducing end groups were demonstrated via reductive amination.

5.2. Introduction

Cellulose molecule is composed of D-glucose rings connected with ß-(1,4) glucosidic linkages. Each cellulose chain has an end glucose unit with its C1 carbon unlinked. The hemiacetal carbon (C1) at the end of the glucose ring converts into an aldehyde functional group when the chain end glucose unit equilibrates with its open-chain form. X-ray and neutron diffraction studies indicate that the molecules in native cellulose are arranged in a parallel fashion, that is, with their reducing ends always on the same side within the crystalline domains.[1,2,3,4] Therefore, all the reducing end groups should locate at one end of the cellulose nanocrystals due to the characteristic chain packing. Actually, Kuga et al observed that only one end of micro-crystals of native cellulose could be stained via

reductive silver labeling.[5,6] More recently, Koyama *et al.* and Kim *et al.* further confirmed the asymmetric location of the reducing end groups in the crystalline domains of native cellulose.[7,8] Therefore, the rod-like cellulose nanocrystals consist of reducing end groups (hemiacetal groups) at one ends, while the walls and the other ends are dominated by OH groups.

It is this asymmetric structural characteristic of cellulose nanocrystals that provides unique opportunities to selectively graft polymer chains to one end of these rigid rods, thus creating a novel class of nanomaterials. The validity of this paradigm has actually been demonstrated by Sipahi-Sağlam et al. who introduced a selective grafting strategy of various molecules at the end of cellulose micro-crystals.[9] This was then followed by further coupling with polydimethylsiloxanes. Evidently, the cellulose-polydimethylsiloxane block copolymers exhibited a pronounced tendency to form specific super-structures in slurries and films made from it. Bosker *et al.* and Loos *et al.* have demonstrated the grafting of polystyrene to amylose oligomers using reductive amination coupling at the reducing end groups.[10,11]

Polystyrene, as a hydrophobic polymer, was used as the grafting polymer in order to introduce nonpolar polymer chains to the polar cellulose nanoctystals. The modified cellulose nanocrystals thus shall have interesting asymmetric polar and nonpolar structure. Varity of the grafting factors, such as degree of grafting, molecular weight and molecular weight distribution, types of polymers, and so on, can be altered to tailor the properties of

the functional cellulose nanocrystals. In this communication the grafting of polystyrene onto the cellulose nanocrystals is demonstrated via a coupling reaction (reductive amination) between the primary amine of amine-terminated polystyrene (PS-NH_2) and the reducing end aldehyde groups of cellulose nanocrystals.

5.3. Materials and Methods

Materials. Whatman #1 filter paper was used as a starting material for the cellulose nanocrystals. All chemicals used in this research were purchased from Aldrich and used as received except otherwise stated. HBr, NaOH, hexane, and methanol were received from Fisher. Dry dichloromethane was obtained after washing it with concentrated H_2SO_4 followed by fractional distillation over CaH_2. Dry triethylamine was obtained from fractional distillation over CaH_2. THF free of proton labile impurities was obtained by refluxing over a freshly prepared deep purple colored sodium benzophenone complex. Styrene was purified by eluting it over an active basic Al_2O_3 column, refluxing over CaH_2 and finally collecting it by fractional distillation under reduced pressure prior to the polymerization reaction.

5.3.1 Formation of Cellulose Nanocrystals. The cellulose nanocrystals were formed by acidic hydrolysis similar to the procedure used by Araki *et al.*[12,13,14] A typical procedure was as follows. 2.0 g of cellulose pulp obtained from Whatman #1 filter paper (98% α-cellulose, 80% crystallinity) was blended by a 10 Speed Osterizer® Blender. Resulting pulp

was hydrolyzed with 100 mL of 2.5 M HBr at 100^{o}C for 3 hours. The ultrasonication was applied during (every 60 minutes) the reaction (Omni-Ruptor 250W ultrasonic homogenizer, 50% power, 5 min). The resulting mixture was diluted with de-ionized (D.I) water followed by five cycles of centrifugation at 1500g for 10 min. (IEC Centra-CL3 Series) to remove excess acid and water soluble fragments. The fine cellulose particles became dispersed in the aqueous solution approximately at pH 4. The turbid supernatant containing the polydisperse cellulose particles was then collected for further centrifugation at 15000 g for 45 min (Automatic Servall® Superspeed Centrifuge) to remove ultra-fine particles. Ultra-fine particles with small aspect ratio were removed from the upper layer, and the precipitation (after the high-speed centrifugation) was dried using a lyophilizing system (Labconco, Kansas City, MU).

5.3.2 Coupling of Benzylamine to Glucose via Reductive Amination. 3.6 g (20 mmol) α-D-glucose was added to 1.07 g (10 mmol) of benzylamine in 25 mL borate buffer (pH 8.5) at 55^{o}C for 4 days. 20 mg (0.32 mmol) of $NaCNBH_3$ was added as the reducing agent each day. Brown precipitates were collected by centrifugation and purified by repeated D.I. water washing and filtration. 2.65 g (yield 99%) product was obtained after drying at 50^{o}C for 2 days under vacuum. ^{1}H NMR (300 MHz; DMSO; δ/ppm): 3.5 – 4.1(w, H of glucose), 6.5 –7.3 (w, H of aromatic) (sample not completely dissolved).

5.3.3 Coupling of Benzylamine to Cellulose Nanocrystals via Reductive Amination. 500 mg of cellulose nanocrystals (no need) were mixed with 16 mg (0.15 mmol) of benzylamine and 5 mg (0.08 mmol) of $NaCNBH_3$ in 15 mL of borate buffer (pH 8.5) at 60^{o}C for 5 days. 2 mg (0.03 mmol) of $NaCNBH_3$ were added each day. The product was repeatedly washed with D.I. water and centrifuged. 495 mg of the final product was collected and dried under vacuum. ^{1}H NMR (300 MHz; DMSO (emulsion sample); δ/ppm): 3.5 – 4.1 (w, H of glucose), 6.5 –7.3 (w, H of aromatic).

5.3.4 Synthesis of the Functional Termination Compound, 2,2,5,5-Tetramethyl-1-(3-chloropropyl)-1-aza-2,5-disilacyclopentane. The method of Hirao et al.[15] was followed with minor modifications as shown in Scheme 5.1. A solution of 10 g (47 mmol) of 1,1,4,4-tetramethyl-1,4-dichloro-1,4-disilabutane in 25 mL of dry dichloromethane was added dropwise to a solution of 6.1 g (65 mmol) of 3-chloropropylamine hydrochloride in 20 mL of dry triethylamine, and 25 mL of dry dichloromethane in a 100 mL Schlenk flask under an argon atmosphere. The solution was allowed to react under constant agitation for 2 h at room temperature and then the solvent was evaporated and the residue dissolved in hexane. The undissolved residues were removed by filtration and the hexane phase was washed three times with a 5% NaOH solution and once with D.I. water. Subsequently the solution was dried over solid $CaCl_2$, filtered, and the hexane was evaporated. 5.0 mL (50% yield) of a clear colorless liquid product was obtained after fractional distillation at 75 °C and a pressure of 7.6 mmHg. ^{1}H-NMR (300 MHz; $CDCl_3$; δ/ppm): 3.51 (t, 2H, $ClCH_2$), 2.91 (t,

2H, NCH_2), 1.86 (m, 2H, CH_2), 0.37 (s, 4H, $SiCH_2$), 0.0 (s, 12H, $SiCH_3$); ^{13}C-NMR: 43.0, 39.5, 36.9, 9.9, 0.0. (Figure 5.1)

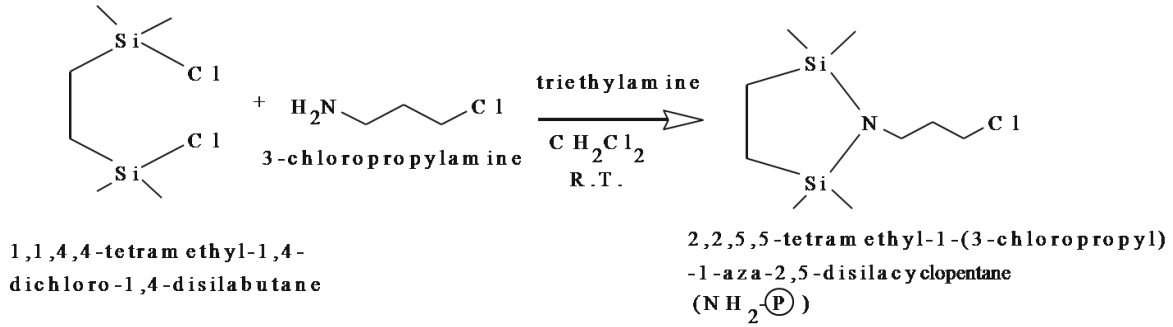

1,1,4,4-tetramethyl-1,4-dichloro-1,4-disilabutane

2,2,5,5-tetramethyl-1-(3-chloropropyl)-1-aza-2,5-disilacyclopentane (NH_2-P)

Scheme 5.1 Synthesis of the functional termination compound (2,2,5,5-tetramethyl-1-(3-chloropropyl)-1-aza-2,5-disilacyclopentane)

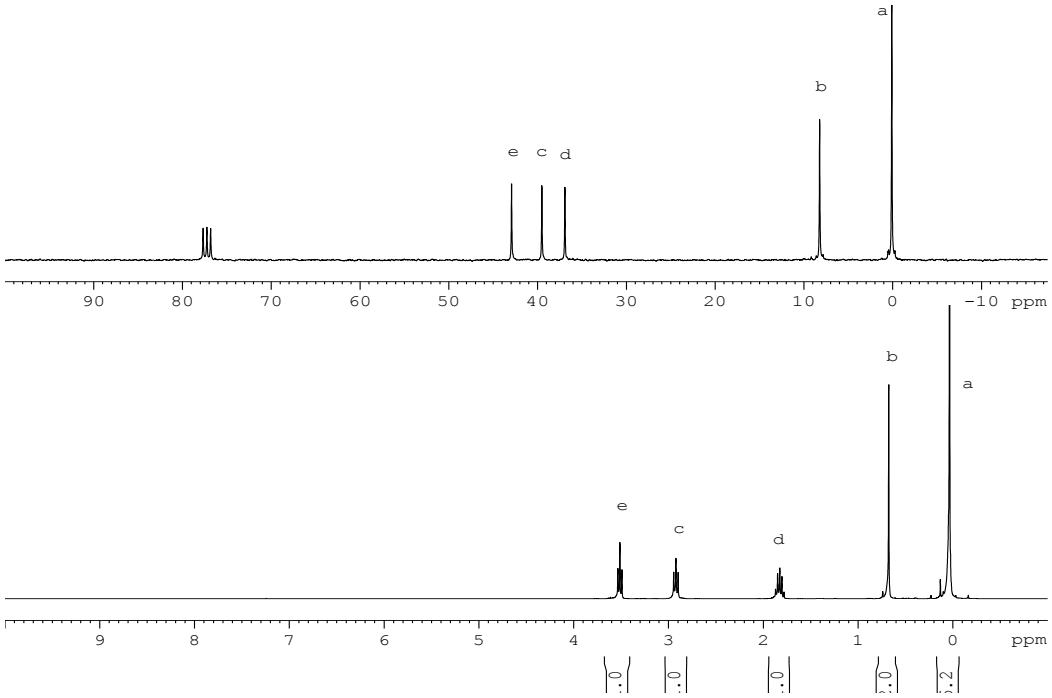

Figure 5.1 ^{13}C NMR and ^{1}H NMR spectra of the functional termination compound (2,2,5,5-tetramethyl-1-(3-chloropropyl)-1-aza-2,5-disilacyclopentane)

5.3.5 Synthesis of Amine Terminated Polystyrene. Amine terminated polystyrene (PS-NH_2) was synthesized using anionic living polymerization according to the procedure developed by Hirao *et al.* with minor modifications (see Scheme 5.2).[15] Polymerizations were carried out under an argon atmosphere in a previously flamed Schlenk flask. A typical example of the polymerization is described was as follows: 50 mL of freshly distilled THF were introduced into a 100 mL Schlenk flask equipped with a magnetic bar and cooled to –78^{o}C. 0.5 mL 1.4 M (0.7 mmol) of *sec*-buthyllithium was transferred into the reactor using an airtight syringe. The initiator solution should retain yellow color prior to the addition of the monomer. 5 g (48 mmol) of pure styrene was injected slowly via an Argon purged syringe. The reaction turned into red orange color and stirred for 60 min. The color gradually disappeared within 30 min after the addition of 0.33 g (1.4 mmol) of the termination compound, 2,2,5,5-tetramethyl-1-(3-chloropropyl)-1-aza-2,5-disilacyclopentane. The reaction solution was allowed to reach room temperature slowly. The polymer was precipitated into 500 mL stirred methanol. 2 mL 1N HCl was also added in the precipitation mixture to ensure the conversion of the termination compound to the primary amine. The polymer was collected via filtration and it was repeatedly washed with methanol and D.I. water. The amine terminated PS (PS-NH_2) was then dried under vacuum at 50^{o}C for 48 h with a yield of 4.5 g (92% yield); (M_n = 7,200 gmol^{-1}, M_w = 7,900 gmol^{-1}, PD =1.1, determined by gel permeation chromatography); ^{1}H-NMR (300 MHz, $CDCl_3$, δ/ppm): 7.1 (b, 3H, benzene ring CH), 6.6 (b, 2H, benzene ring CH). The nitrogen content of PS-NH_2 was determined by elemental analysis and it was found to be 0.18%. The molecular weight can now be calculated assuming each polystyrene chain contains one

terminal amine group (M_n = 14 / 0.0018 = 7,800 $gmol^{-1}$). This value is in good agreement with the results achieved by gel permeation chromatography.

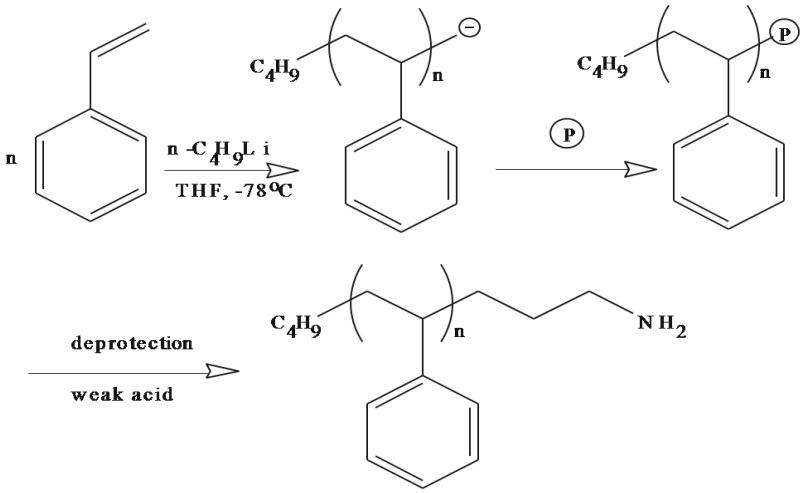

Scheme 5.2 Synthesis of amine terminated polystyrene (PS-NH_2)

5.3.6 Coupling of PS-NH_2 to Cellulose Nanocrystals via Reductive Amination. Polystyrene with primary amine end groups was grafted to cellulose nanocrystals via reductive amination. 50 mg of cellulose nanocrystals (0.31mmol of equivalent anhydroglucose unit) and 3.0 g of PS-NH_2 (M_n=7,200 $gmol^{-1}$, PDI=1.1, 0.42mmol), and 15.0 mL of dry THF were mixed in a flask. Stirring was continued at room temperature for 5 days with the addition of 1 mg (0.02 mmol) $NaCNBH_3$ each day. The reaction mixture was centrifuged to collect the cellulose nanocrystals. The collected nanocrystals were re-dispersed in THF and the un-reacted PS-NH_2 was removed after four cycles of centrifugation until no PS signals were detected by UV spectrometry. The product was

further washed repeatedly with D.I water and THF in filtration, and finally it was dried under vacuum at a yield of 46 mg.

5.3.7 ^{1}H NMR Spectroscopy. NMR measurements were acquired using on a Bruker 300 MHz spectrometer equipped with a Quad probe dedicated to ^{31}P, ^{13}C, ^{19}F, and ^{1}H acquisition.

5.3.8 Elemental Analysis. The elemental analysis was carried on a Perkin Elmer Series II CHNS/O Analyzer 2400.

5.3.9 UV Spectroscopy. UV measurements were carried out on a HP 8453E UV-Visible Spectroscopic System.

5.3.10 Gel Permeation Chromatography. Gel permeation chromatographic (GPC) measurements were carried out with a Waters GPC 510 pump equipped with UV and RI detectors using THF as the eluent at a flow rate of 0.7 mL/min at room temperature. Two Ultrastyragel linear columns linked in series (Styragel HR 1 and Styragel HR 5E) were used for the measurements. Standard mono-disperse polystyrenes with molecular weight ranges from 0.82 to 1860 kg/mol were used for the calibration. The number- and weight-average molecular weights were calculated using the Millenium software of Waters.

5.4. Results and Discussion

5.4.1 Reactions with a Small Model Compound (Reductive Amination)

In prior to actually grafting polystyrene to cellulose nanocrystals (CNCs), model reactions were performed to study the feasibility of the reaction in heterogeneous media. Benzylamine and glucose were used as the model compounds of PS-NH_2 and cellulose nanocrystals. When glucose is dissolved in water an equilibrium between its ring and open-chain form is established (Scheme 5.3). Therefore, the primary amine of benzylamine and the aldehyde group at C-1 of glucose can be coupled via reductive amination in the presence of $NaCNBH_3$.

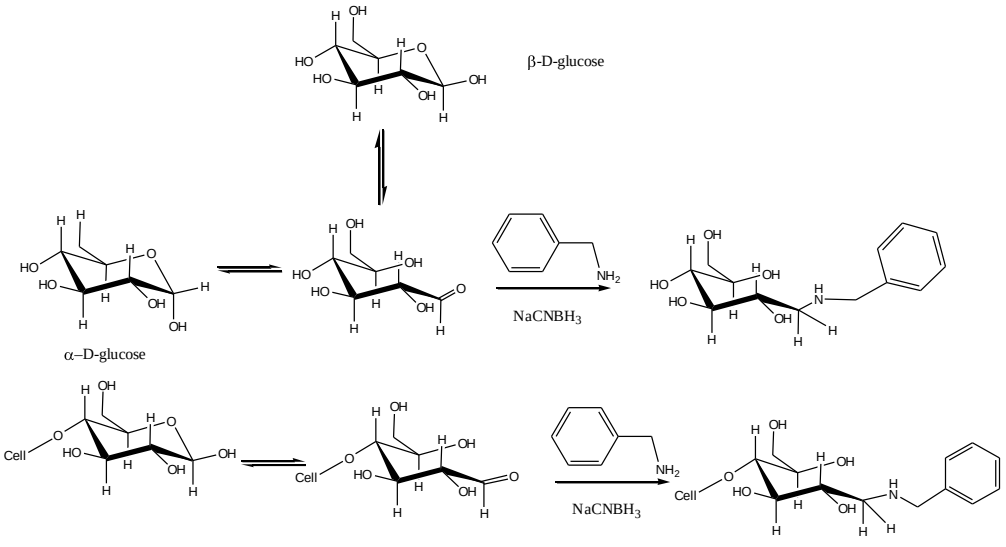

Scheme 5.3 The synthetic strategy for the coupling reaction of α-D-glucose and benzylamine

^{1}H NMR spectra of the grafted glucose revealed the signals in aromatic region of the NMR spectra (Figure 5.2). Due to the poor solubility of the sample in NMR solvents the signals corresponding to the glucose structure are not visible. However, the appearance of the aromatic signals at 7.5-7.0 ppm indicates of the successful coupling reaction.

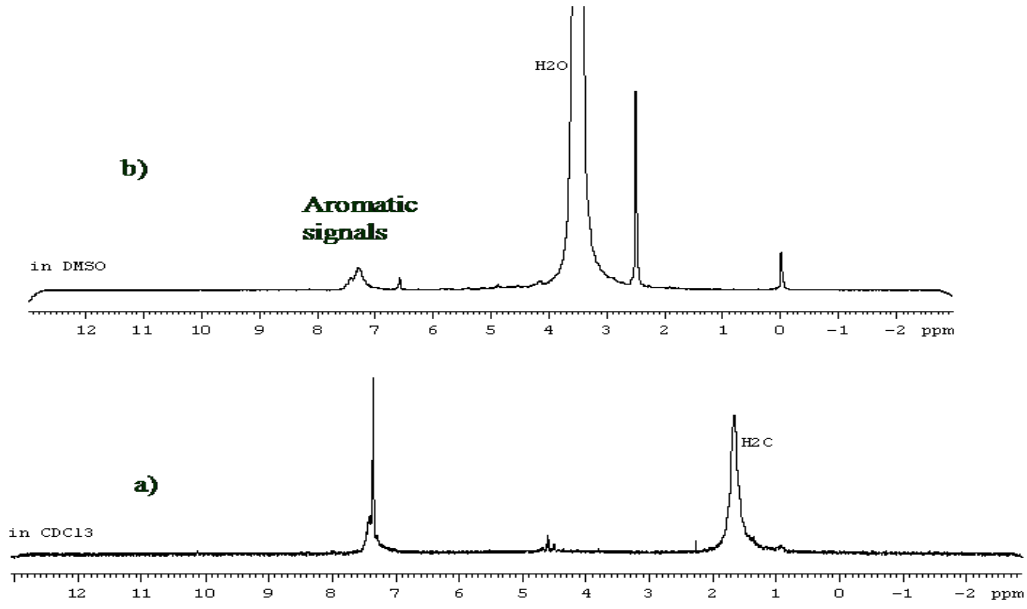

Figure 5.2 1H NMR spectra of benzylamine grafted α-D-glucose dispersed in CDCl3 (a) and in DMSO-d6 (b)

To further demonstrate the potential of the coupling reaction between amine-terminated polystyrene and cellulose nanocrystal, the reductive amination of CNCs was conducted with benzylamine in heterogeneous conditions. Again, the aromatic signals are apparent at 7.5-7.0 ppm suggesting successful grafting reaction (Figure 5.3).

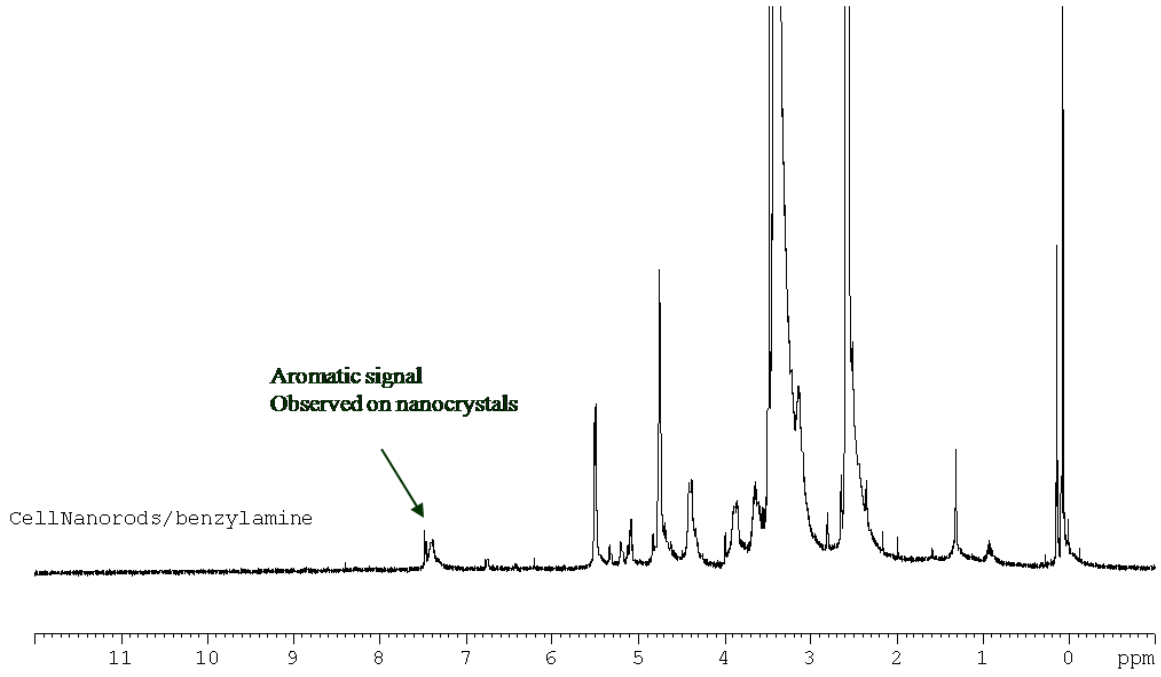

Figure 5.3 ^{1}H NMR spectrum of benzylamine grafted cellulose nanocrystals dispersed in DMSO-d_6

5.4.2 Reactions with Amine-terminated Polystyrene (PS-NH_2)

As a result of the parallel chain conformation of native cellulose (cellulose I), the potential aldehyde groups are concentrated at one end of the cellulose nanocrystals as illustrated in the Scheme 5.4. Therefore, the grafting can be targeted at one end of the cellulose nanocrystals. The terminal primary amine on PS-NH_2 can be reacted with the reducing end aldehyde in mild conditions to form an imine (Schiff base). Subsequently, the reduction of imine will covalently link polystyrene to the one end of cellulose nanocrystals.

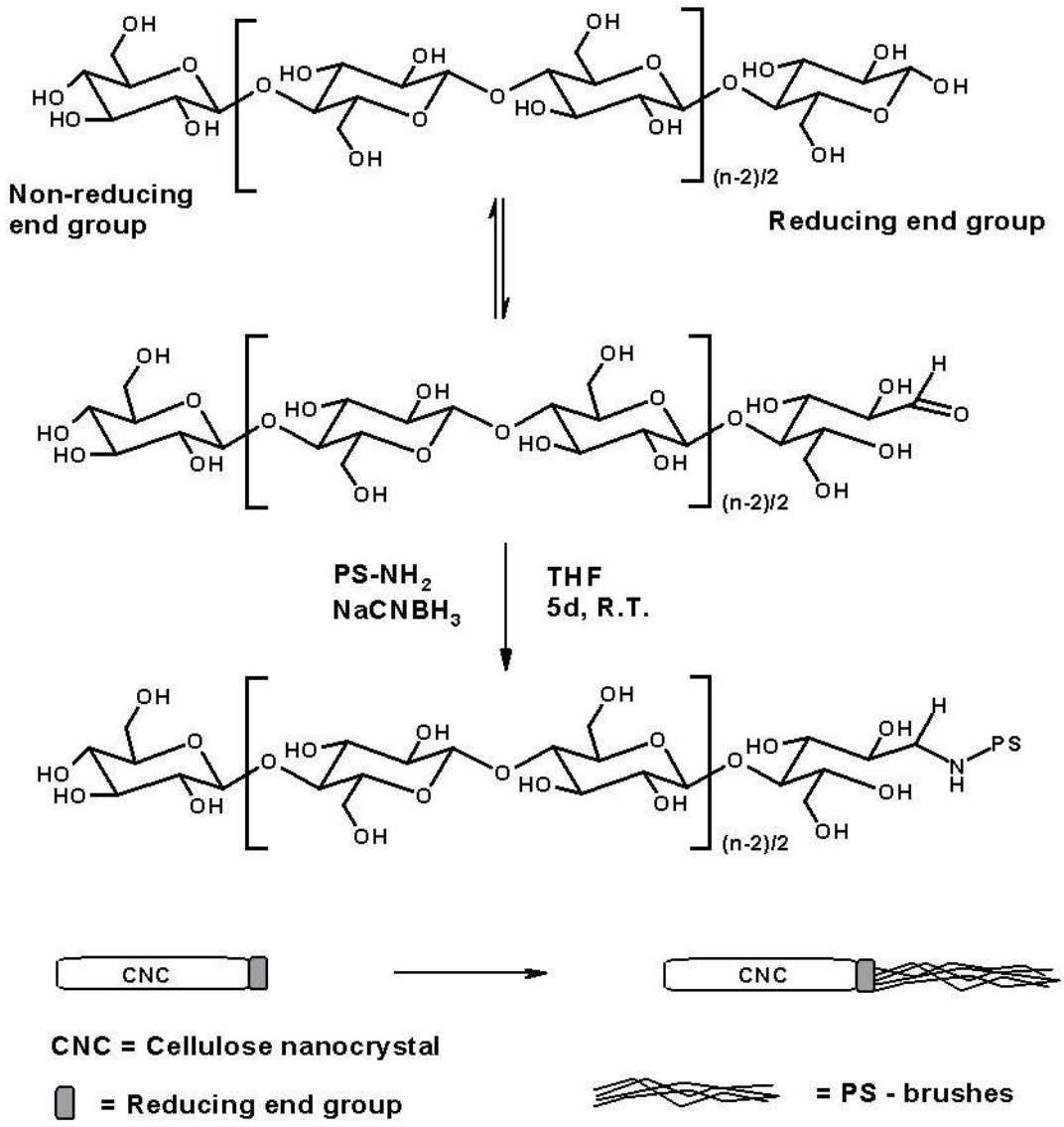

Scheme 5.4 Molecular structure of cellulose and the equilibrium of its open-chain form

PS graft on cellulose nanocrystals was carried via a reductive amination coupling reaction between the primary amine of PS-NH_2 and the aldehyde group of cellulose. Bosker *et al.* and Loos *et al.* had demonstrated the grafting of polystyrene to amylose oligomers using

reductive amination coupling at the reducing end groups.[10,11] Due to the solubility limitations of cellulose nanocrystals the coupling reaction had to be conducted in two phase reaction environment i.e. cellulose nanocrystals were suspended in THF in which the amine-terminated polystyrene is soluble.

It is worth mentioning here that the nitrogen content of the PS-NH_2 grafted cellulose was found to be 0.08%. If one now considers the molecular weights of cellulose nanocrystals (69,000 $gmol^{-1}$) and PS-NH_2 (7,800 $gmol^{-1}$) the grafting density can be approximately calculated as follows: (69,000 + 7,800) / (14 /0.0008) = 4.39 which means that approximately every 4.4 of the cellulose chains within the cellulose nanocrystal have been grafted with the polystyrene.

In an effort to ensure that the observed PS was bonded covalently on the nanocrystals, a controlled coupling experiment was performed with unmodified PS i.e. polystyrene without the terminal amine functionality. The grafted cellulose nanocrystal was evaluated by ^1H NMR measurements (Figure 5.4). Although, the ^1H NMR measurements gave fairly weak signals due to the incomplete solubility of the grafted cellulose nanocrystals in DMSO, the aromatic peaks (7.2-6.5 ppm) appeared on the spectrum of the grafted cellulose nanocrystals while the control sample had none. This indicates that the PS was grafted on the reducing end groups of cellulose nanocrystals. However, the grafting density of PS-NH_2 on the reducing end groups of CNCs seemed to be rather low probably due to the steric reasons. To overcome the steric limitations the use of grafting from approach, such as atom

transfer radical polymerization (ATRP), would be of importance to achieve more complete grafting of polystyrene.

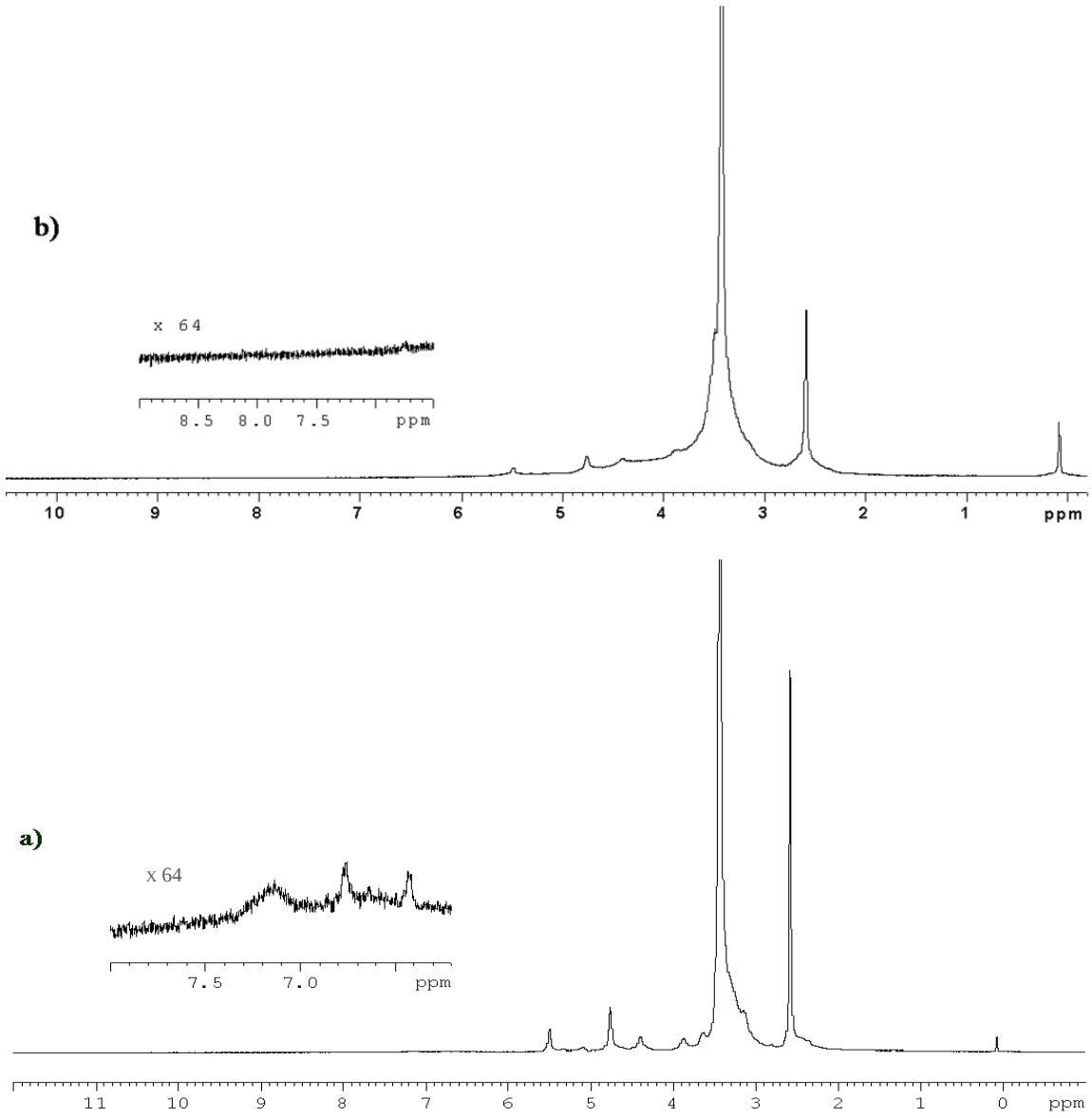

Figure 5.4 ^{1}H NMR spectra of PS-NH_2 grafted cellulose nanocrystals (a) and cellulose nanocrystals from the control experiment with unmodified polystyrene (PS) (b) dispersed in DMSO-d_6

5.5 Conclusions

The study shows that cellulose nanocrystals may be grafted directly and selectively at their front end surfaces by employing the reducing end aldehyde groups located there. The feasibility of the grafting on approach by using reductive amination was demonstrated with α-D-glucose and small model compound benzylamine. Furthermore, the reducing end groups of cellulose nanocrystals were successfully grafted with benzylamine. However, incomplete grafting of amine-terminated polystyrene suggested that the grafting from approach, such as atom transfer radical polymerization (ATRP), would be more feasible for such derivatization reactions.

5.6 References

1. Sarko, A. and Muggli, R. (1974). "Packing Analysis of Carbohydrates and Polysaccharides. III. Valonia Cellulose and Cellulose II," *Macromolecules*, 7(4), 486-494.

2. Gardner, K. H. & Blackwell, J. (1974). "The structure of native cellulose," *Biopolymers*, 13(10), 1975-2001.

3. Nishiyama, Y., Langan, P., and Chanzy, H. (2002). "Crystal structure and hydrogen-bonding system in cellulose I_β from synchrotron X-ray and neutron fiber diffraction," *J. Am. Chem. Soc*., 124(31), 9074-9082.

4. Nishiyama, Y., Sugiyama, J., Langan, P., Chanzy, H., and Langan, P. (2003). "Crystal structure and hydrogen bonding system in cellulose I_α from synchrotron X-ray and neutron fiber diffraction," *J. Am. Chem. Soc*., 125(47), 14300-14306.

5. Hieta, K., Kuga, S., and Usuda, M. (1984). "Electron staining of reducing ends evidences a parallel-chain structure in *Valonia* cellulose," *Biopolymers*, 23(10), 1807-1810.

6. Kuga, S. and Brown, R. M. Jr. (1988). “Silver labeling of the reducing ends of bacterial cellulose,” *Carbohydrate Research*, 180(2), 345-350.

7. Koyama, M., Sugiyama, J., and Itoh, T. (1997). “Systematic survey on crystalline features of algal celluloses,” *Cellulose*, 4(2), 147–160.

8. Kim, N. H., Imai, T., Wada, M., and Sugiyama, J. (2006). “Molecular Directionality in Cellulose Polymorphs,” *Biomacromolecules*, 7(1), 274-280.

9. Sipahi-Sağlam, E., Gelbrich, M., and Gruber, E. (2003). “Topochemically modified cellulose,” *Cellulose*, 10(3), 237-250.

10. Bosker, W. T. E., Ägoston, K., Stuart, M. A. C., Norde, W., Timmermans, J. W. and Slaghek, T. M. (2003). “Synthesis and Interfacial Behavior of Polystyrene−Polysaccharide Diblock Copolymers,” *Macromolecules*, 32(6), 1982-1987.

11. Loos, K. and Muller, A. H. E. (2002). “New Routes to the Synthesis of Amylose-*block*-polystyrene Rod−Coil Block Copolymers,” *Biomacromolecules*, 3(2), 368-373.

12. Araki, J., Wada, M., Kuga, S., and Okano, T. (1999). “Influence of surface charge on viscosity behavior of cellulose microcrystal suspension,” *J. Wood Sci.*, 45(3), 258-261.

13. Araki, J., Wada, M. and Kuga, S. (2001). “Steric stabilization of a cellulose microcrystal suspension by polyethylene glycol (PEG) grafting,” *Langmuir*, 17(1), 21-27.

14. Araki, J., Wada, M., Kuga, S., and Okano, T. (1998). “Flow properties of microcrystalline cellulose suspension prepared by acid treatment of native cellulose,” Colloids *and Surfaces A: Physicochemical and Engineering Aspects*, 142(1), 75–82.

15. Ueda, K., Hirao, A. and Nakahama, S. (1990). “Synthesis of polymers with amino end groups. 3. Reactions of anionic living polymers with α-halo-ι-aminoalkanes with a protected amino functionality,” *Macromolecules*, 23(4), 939-945.

6. Grafting of TEMPO-oxidized Cellulose Nanocrystals

6.1 Abstract

Surface carboxylated cellulose nanocrystals were prepared by 2,2,6,6-tetramethyl-1-piperidinyloxy (TEMPO)-mediated oxidation of cotton cellulose (Whatman #1 filter paper). The oxidized cellulose nanocrystals were characterized by Fourier Transfer Infrared Spectroscopy (FTIR), acid-base titration and a novel ^{31}P NMR spectroscopic method. It is known that TEMPO oxidation selectively converts surface primary hydroxyl groups into carboxylic groups. This creates potential reaction sites for the site-specific grafting of cellulose nanocrystals as the produced surface carboxyl groups can be reacted with the compounds bearing amine functionality. The coupling reaction was validated by using a simple model, octadecylamine and the same approach was used for the grafting of amine terminated polystyrene on the surface of TEMPO-oxidized cellulose nanocrystals.

6.2 Introduction

It has been known for a number of years that the hydrolysis of cellulose with strong hydrochloric or sulfuric acid under controlled conditions produces cellulose nanocrystals (CNCs) sometimes called cellulose whiskers.[1,2] The shape and size of CNCs depends from their origin: different samples such as tunicin, cotton, wood fibers, bacterial cellulose, parenchyma cell cellulose, etc. will produce different sizes of nanocrystals even under similar hydrolysis conditions. Typical figures for crystallites derived from different species

vary: 20×(100-2000) nm for *Valonia*, (3-5)×180±75 nm for bleached softwood kraft pulp, and 7×(100-300) nm for cotton.[3,4,5]

CNCs can form stable colloidal suspensions having properties of which depend on the cellulose source and the preparation conditions, such as the nature of the acid, the reaction temperature and the reaction time.[6] The cellulose whiskers prepared by hydrolysis in hydrochloric acid have minimal surface charges and their dispersibility is limited and their aqueous suspensions are known to flocculate.[4,7] Alternatively, the CNCs resulting from sulfuric acid hydrolysis have charged sulfate esters groups in their surface which in turn promotes an electrostatic repulsion and the dispersion of these whiskers in water.[8,9] When these homogeneous suspension are concentrated and their concentration exceed a critical value, the suspensions form chiral nematic ordered phases.[2,6,8] However, it has been reported that stable colloidal aqueous suspension of HCl-hydrolyzed CNCs can also be prepared by postsulfation method.[4,7,10]

In 1994, De Nooy *et al.* reported that the primary alcohol groups of carbohydrates can be selectively oxidized in aqueous media by using the 2,2,6,6-tetramethyl-1-piperidinyloxy (TEMPO) radical.[11] Since then the technique has been applied with success to various cellulose samples.[12,13,14,15,16] During the course of these investigations it was found that regenerated cellulose could be completely converted into water-soluble polyglucuronic acid whereas in the case of native cellulose fibers, the oxidation proceeded throughout the fibers but occurred only at the surface of the microfibrils, which therefore became negatively

charged. As such, the TEMPO-mediated oxidation is an alternate way to form stable colloidal suspensions of CNCs without having the lability of the sulfate ester groups.

In 2001, Araki and coworkers demonstrated a method for grafting amine-terminated poly(ethylene glycol) to surface-modified CNCs, thus improving the stability of the microcrystal suspensions through steric stabilization.[17] In this work, the technique has been extended to grafting of amine-terminated polystyrene to TEMPO-oxidized CNCs. The oxidized CNCs could be dispersed in THF, allowing the dissolution of a range of hydrophobic amine-functionalized polymers and their subsequent coupling *via* carbodiimide / N-hydroxy succinimide-mediated amidation.

6.3 Materials and Methods

Materials. Whatman #1 filter paper was used as a starting material for the cellulose nanocrystals. 1-octadecylamine (98%) was purchased from Alfa Aesar. All other chemicals were purchased from Aldrich or Fisher and used as received unless otherwise stated.

6.3.1 TEMPO Oxidation of Surface Primary Hydroxyl on Cellulose Nanocrystals. In a typical experiment 648 mg (4 mmol of glucosyl units) of cellulose nanocrystals were suspended in water (50 mL) containing 10 mg of 2,2,6,6-tetramethyl-1-piperidinyloxy-radical (TEMPO, 0.065 mmol) and 200 mg of sodium bromide (1.9 mmol) at room temperature for 30 min. The TEMPO-mediated oxidation of the cellulose nanocrystals was

initiated by slowly adding 4.90 mL of 13% NaClO (8.6 mmol) over 20 min at room temperature under gentle agitation. The reaction pH was monitored using a pH meter and maintained at 10 by incrementally adding 0.5 M NaOH. When no more decrease in pH was observed, the reaction was considered complete. About 5 mL of methanol was then added to react and quench with the extra oxidant. After adjusting the pH to 7 by adding 0.5 M HCl, the TEMPO-oxidized product was washed with D.I. water by centrifugation and further purified by dialysis against D.I. water for two days. 550 mg of solid was recovered after freeze-drying. FTIR measurements showed a carboxylic acid peak at 1730 cm^{-1}. The carboxylic content in the oxidized cellulose nanocrystals was determined by acid-base titration, FTIR and novel ^{31}P NMR methodology.

6.3.2 Synthesis of Amine Terminated Polystyrene. Amine terminated polystyrene (PS-NH_2) was synthesized using anionic living polymerization according to the procedure developed by Hirao *et al.* with minor modifications (see Scheme 2).[18] Polymerizations were carried out under an argon atmosphere in a previously flamed Schlenk flask. A typical example of the polymerization is described was as follows: 50 mL of freshly distilled THF were introduced into a 100 mL Schlenk flask equipped with a magnetic bar and cooled to –78^{o}C. 0.5 mL 1.4 M (0.7 mmol) of *sec*-buthyllithium was transferred into the reactor using an airtight syringe. The initiator solution should retain yellow color prior to the addition of the monomer. 5 g (48 mmol) of pure styrene was injected slowly via an Argon purged syringe. The reaction turned into red orange color and stirred for 60 min. The color gradually disappeared within 30 min after the addition of 0.33 g (1.4 mmol) of the

termination compound, 2,2,5,5-tetramethyl-1-(3-chloropropyl)-1-aza-2,5-disilacyclopentane. The reaction solution was allowed to reach room temperature slowly. The polymer was precipitated into 500 mL stirred methanol. 2 mL 1N HCl was also added in the precipitation mixture to ensure the conversion of the termination compound to the primary amine. The polymer was collected via filtration and it was repeatedly washed with methanol and D.I. water. The amine terminated PS (PS-NH_2) was then dried under vacuum at 50^{o}C for 48 h with a yield of 4.5 g (92% yield); (M_n = 7,200 gmol^{-1}, M_w = 7,900 gmol^{-1}, PD =1.1, determined by gel permeation chromatography); ^{1}H-NMR (300 MHz, $CDCl_3$, δ/ppm): 7.1 (b, 3H, benzene ring CH), 6.6 (b, 2H, benzene ring CH).

6.3.3 Grafting of Octadecylamine onto TEMPO-oxidized Cellulose Nanocrystals. TEMPO-oxidized cellulose nanocrystals (50mg, 0.31mmol of equivalent anhydroglucose unit) were dispersed in dry tetrahydrofuran (THF, 10ml) by mixing with magnetic stirrer at room temperature. In typical synthesis, EDC·HCl (*N*-(3-dimethylaminopropyl)-*N'*-ethylcarbodiimide hydrochloride, 13.0mg, 68mmol), NHS (*N*-hydroxysuccinimide, 8.0mg, 68 mmol), and octadecylamine (18.3mg, 68mmol), respectively, were added to the cellulose nanocrystal suspension. The reaction was performed at room temperature under stirring for 24 h. The resulting mixture was filtered with sintered funnel (Grade M). The solid residue was extensively washed with THF in order to remove the excess and unbound octadecylamine. The resulting white powder was collected and dried under vacuum overnight at 40°C with the yield of 45 mg.

6.3.4 Grafting of Amine Terminated Polystyrene (PS-NH_2) onto TEMPO-oxidized Cellulose Nanocrystals. TEMPO-oxidized cellulose nanocrystals (50mg, 0.31mmol of equivalent anhydroglucose unit) were dispersed in dry tetrahydrofuran (THF, 30ml) by mixing with magnetic stirrer at room temperature. In typical synthesis, EDC·HCl (*N*-(3-dimethylaminopropyl)-*N'*-ethylcarbodiimide hydrochloride, 13.0mg, 68mmol), NHS (*N*-hydroxysuccinimide, 8.0mg, 68mmol), and previously prepared amine terminated polystyrene (PS-NH_2, 3.0g, M_n=7200 $gmol^{-1}$, PDI=1.1, 0.42mmol), respectively, were added to the cellulose nanocrystal suspension. The reaction was performed at room temperature under stirring for 24 h. The resulting mixture was filtered with sintered funnel (Grade M). The collected nanocrystals were re-dispersed in THF and the un-reacted PS-NH_2 was removed after four cycles of centrifugation until no PS signals were detected by UV spectrometry. The resulting white powder was collected and dried under vacuum overnight at 40°C with the yield of 60 mg.

6.3.5 Acid-base Titration. The carboxylic acid content of the oxidized CNCs was determined by acid-base titration following the procedure developed for the conductometric titrations of such materials.[19] In this procedure TEMPO-oxidized CNC samples (50mg) were suspended into 0.01 M hydrochloric acid (HCl) solutions (15 ml) with stirring. The resulting suspensions were then titrated with 0.01 M sodium hydroxide (NaOH) solution. Typical titration curve is shown in Figure 6.2. The degree of oxidation (DO) values were calculated as already published and very reproducible results were obtained.[19] The carboxyl groups content or degree of oxidation (DO) is given by the following equation:

$$DO = 162 \times (V2 - V1) \times C \times [w - 36 \times (V2 - V1) \times C]^{-1} \qquad \text{(equation 1)}$$

where V1 and V2 are the amount of NaOH (in L), c is the NaOH concentration (mol/L), w is the weight of oven-dried sample (g), value 36 is the difference between the molecular weight of an anhydroglucose unit (AGU) and that of the sodium salt of a glucuronic acid.

6.3.6 Infrared Spectroscopy. FTIR spectra were measured on a Thermo Nicolet NEXUS 670 FT-IR infrared spectrophotometer. Spectra in the range of 4000 – 650 cm^{-1} were obtained with a resolution of 4 cm^{-1} by cumulating 64 scans. Degree of oxidation (DO) measurements were carried out by comparing the intensities of absorption band near 1730 cm^{-1} (carbonyl stretching frequency) to that of 1050 cm^{-1} (cellulose backbone)[20]

6.3.7 Thermal Analysis. Thermal decomposition temperatures were determined using a TA Instrument TGAQ500 at a ramp of $10^{o}C$/min under N_2 purge.

6.3.8 UV Spectroscopy. UV measurements were carried out on a HP 8453E UV-Visible Spectroscopic System.

6.3.9 Gel Permeation Chromatography. Gel permeation chromatographic (GPC) measurements were carried out with a Waters GPC 510 pump equipped with UV and RI detectors using THF as the eluent at a flow rate of 0.7 mL/min at room temperature. Two

Ultrastyragel linear columns linked in series (Styragel HR 1 and Styragel HR 5E) were used for the measurements. Standard mono-disperse polystyrenes with molecular weight ranges from 0.82 to 1860 kg/mol were used for the calibration. The number- and weight-average molecular weights were calculated using the Millenium software of Waters.

6.3.10 ^{31}P NMR Spectroscopy. The quantitative ^{31}P NMR spectra were acquired immediately, using a Bruker 300 MHz spectrometer equipped with a Quad probe dedicated to ^{31}P, ^{13}C, ^{19}F and ^{1}H acquisition. A total of 512 scans were acquired for each sample with the relaxation delay time (d1) of 8.0 seconds.

6.3.11 ^{1}H NMR Spectroscopy. NMR measurements were acquired using on a Bruker 300 MHz spectrometer equipped with a Quad probe dedicated to ^{31}P, ^{13}C, ^{19}F, and ^{1}H acquisition.

6.3.12 Phosphitylation of Tempo-oxidized Cellulose Nanocrystals Followed by Quantitative ^{31}P NMR Spectroscopy. TEMPO-oxidized cellulose nanocrystals (15.7 mg) were stirred in 1-allyl-3-methylimidazolium chloride ([amim]Cl) (~0.4 ml, 475 mg) for 18 hours at 80 °C in a 15 ml screw-top glass sample bottle. Pyridine (150 µl) was added in one portion and the sample vortexed, at 1200 rpm using a vortexer, until visibly homogeneous (~20 s). The sample was allowed to cool to RT, whereby 2-chloro-4,4,5,5-tetramethyl-1,3,2-dioxaphospholane (200 µl, 1.26 mmol) was added in one portion and vortexed until visibly homogeneous (~30 s) as a cream paste. A pre-prepared stock solution of

chromium(III)acetylacetonate Cr(acac)3/CDCl3 (1 mg/ml, 500 µl) was added in 4 x 125 µl portions with vortexing (~30 s) between each additions. Finally, internal standard i.e. endo-N-hydroxy-5-norbornene-2,3-dicarboximide (e-HNDI) solution (121.5 mM in 3/2:Pyridine/CDCl3, 125 µl) was added in one portion and the solution vortexed (~30 s). The sample was further diluted with Cr(acac)3/CDCl3 solution additions to total volume of 3000 µl. ^{31}P NMR spectra were recorded with 700 µl samples in a 5 mm o.d. NMR tube.

6.4 Results and Discussion

6.4.1 TEMPO-mediated Oxidation of Cellulose Nanocrystals

TEMPO-oxidation selectively oxidizes the primary hydroxyl groups while leaving unaffected the secondary hydroxyl groups (Scheme 6.1).[13,19] With proper reaction conditions, TEMPO-oxidation can be controlled only occurring on the surface of native cellulose crystalline.[14,21] Due to the cellulose molecule's packing fashion, one-half of the primary hydroxyl (hydroxymethyl) groups on the surface cellulose chains point toward the core of the crystalline domain, and are thus inaccessible to the oxidation. Therefore, carboxyl groups can be introduced on the surface of the cellulose nanocrystals with a regular pattern without destroying the crystallinity. Based on the arrangement of the cellulose molecule in the crystalline unit cell,[22] the carboxylic groups created on the nanocrystal surface should be 1.0 nm apart in the longitudinal direction and 0.8 nm apart in the width direction thus allowing a great potential to build devices in nanoscale.

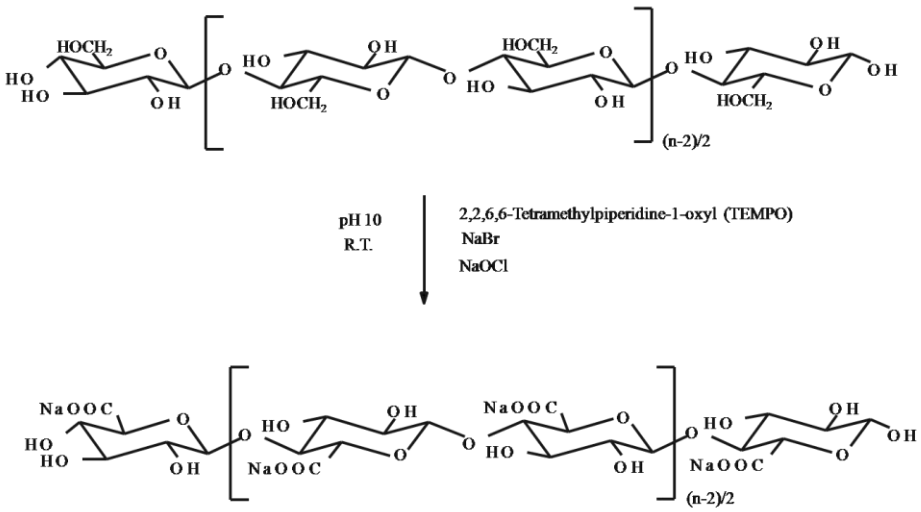

Scheme 6.1 TEMPO-mediated oxidation of cellulose nanocrystals

6.4.2 Chemical Characterization of Oxidized Cellulose Nanocrystals

The cotton crystals have rectangular shape with average dimensions of 40 ± 18 Å.[23] Thus, the amount of individual cellulose chains within a cotton crystallite can be calculated using the two lattice parameters of cellulose I_β unit cell, a = 0.801 nm and b = 0.817 nm, respectively. This model corresponds minimum of 4 x 4 and maximum of 8 x 8 packing (using 40 ± 18 Å as dimensions) of cellulose chains within a crystallite. Therefore, either 12 of the 16 chains or 28 of the 64 chains constitute on the surfaces of the crystallite and are thus susceptible to be oxidized. Consequently, the ratio of surface chains to the total number of chains within the crystals is 0.75 or 0.44 i.e. 75% or 44% of the cellulose chains can be oxidized, respectively. However, due to the two fold screw axis of the cellulose chain only half of the hydroxymethyl groups are accessible for the oxidation, the other half pointing toward the core of the crystalline domain. Therefore, the corresponding degrees of

oxidation (DO) that can be achieved for the cotton nanocrystals are 0.75/2 = 0.375 or 0.44 /2 = 0.22. However, using the average dimension of 40 Å for a cotton crystallite leads to the DO value of 0.28.

The carboxyl content of oxidized cellulose samples was determined by acid-base titrations as described in the experimental section. The titration curves showed the presence of strong acid, corresponding with the excess of HCl and weak acid corresponding to the carboxyl content, as shown in Figure 6.1.

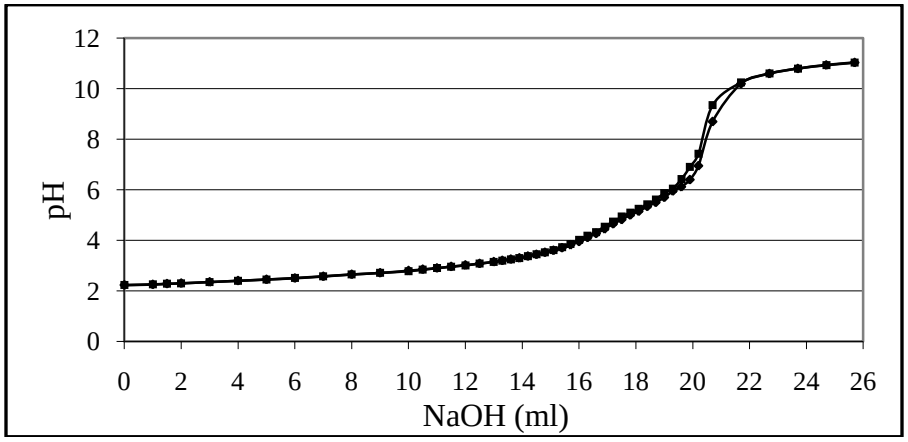

Figure 6.1 Titration curves of the oxidized (TEMPO) cellulose nanocrystals

In the first step of titration, NaOH neutralizes the added hydrochloric acid (strong acid) which is then followed by the neutralization of the carboxylic acid groups (weak acid). The amount of NaOH needed for the neutralization of the carboxylic acid groups was determined as the difference between the known amount (15 mL) of NaOH consumed for the neutralization of HCl and the equivalence point of the weak acid titration of carboxylic

acid groups. As can been seen from the Figure 6.1 the equivalence point appears at pH 8.0 subsequent to the overall NaOH consumption of 20.5 mL. Thus, the neutralization of the carboxylic acid groups consumes 5.5 mL of NaOH (20.5-15.0 mL) corresponding to the DO value of 0.19 (equation 1).

FTIR spectra of TEMPO-oxidized cellulose nanocrystals contains new band around 1730 cm^{-1} when compared to the starting cellulose nanocrystals (Figure 6.2).

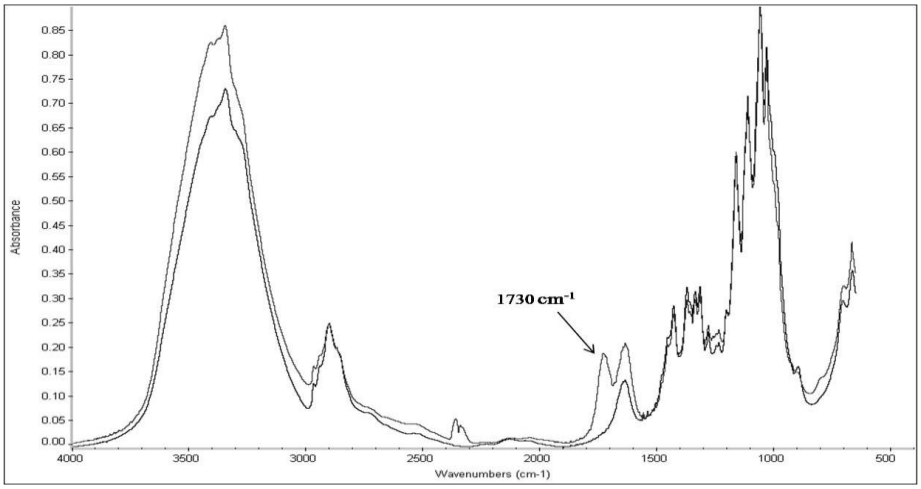

Figure 6.2 FTIR spectrum of cellulose nanocrystals (lower) and TEMPO-oxidized cellulose nanocrystals (upper)

The new band corresponds to the C=O stretching frequency of carboxyl groups in their acidic forms. The degree of oxidation (DO) values can be roughly estimated by comparing the intensity of the new band at 1730 cm^{-1} to that near 1050 cm^{-1} which derives from the cellulose backbone.[20] For example, the corresponding band intensities in Figure 6.2 are 0.2

and 0.95 leading to a DO value of 0.21 (0.2/0.95). At this point it can be concluded that the DO values achieved from acid-base titration and FTIR are in good agreement.

6.4.3 Determination of the Degree of Oxidation (DO) for Cellulosic Samples by Using Novel ^{31}P NMR Technique

The quantitative ^{31}P NMR technique for the analysis of variety of lignin samples was first introduced by Argyropoulos *et al.*[24,25] Since then the methodology has been successfully used in several investigations focusing on the assignment and quantification of individual hydroxylic and carboxylic functionalities in lignins.[26,27,28] The foundation of the technique is the complete phosphitylation of hydroxyl groups in lignin with 2-chloro-4,4,5,5-tetramethyl-1,3,2-dioxaphospholane in the presence of organic base pyridine (Scheme 6.2). Purified lignin samples, in the absence of cellulose, can be completely dissolved in traditional organic solvents.

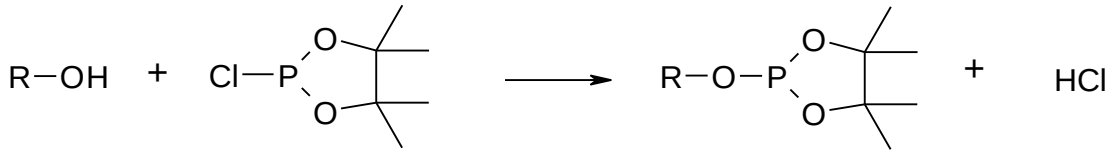

Scheme 6.2 Reaction between 2-chloro-4,4,5,5-tetramethyl-1,3,2-dioxaphospholane and hydroxyl group of lignocellulosic material

Due to the complete solubility of lignin, homogeneous phosphitylation can be carried out to introduce the ^{31}P label necessary for the solution phase NMR analysis. The phosphitylated hydroxyls in lignin can then be quantitatively determined against an internal standard such as *endo*-*N*-hydroxy-5-norbornene-2,3-dicarboximide (*e*-HNDI).

However, due to the insolubility of wood polysaccharides under standard molecular solvent conditions the quantitative ^{31}P NMR technique has been applicable only for the analysis of rather purified lignin preparations. Recently, the quantitative ^{31}P NMR technique was extended for the quantitative analysis of the hydroxyl groups in cellulose polymer.[29] This was achieved by combining the ^{31}P-labeling and NMR analysis technique with the cellulose dissolving ionic liquid media. Ionic liquid, 1-allyl-3-methylimidazolium chloride ([amim]Cl), is now a common solvent for cellulose and it has been used for various functionalization reactions of cellulose.[30,31,32,33]

The recently developed ionic liquid based quantitative ^{31}P NMR methodology was used for the determination of the carboxylic acid moieties in the TEMPO-oxidized cellulose nanocrystals. In the first step the method was validated by using a commercial sample of partially acetylated cellulose [Aldrich, acetyl content 39.8 weight%, degree of substitution (DS) = 2.67]. Figure 6.3 shows a typical spectrum of the phosphitylated cellulose sample. The amount of free hydroxyl groups was determined by integrating the spectral region of aliphatic hydroxyls (145.3-150.4 ppm) against the internal standard (151.8-153.2 ppm). It is worth to mention here that the maximum value for total hydroxyls in cellulose is 18.52 $mmolg^{-1}$ (3/162). The amount of free hydroxyl groups on partially acetylated cellulose sample was found to be 2.25 $mmolg^{-1}$ which corresponds to 12% of total amount of hydroxyl groups on cellulose (2.25/18.52) i.e. the DS = 2.64. Therefore, an excellent correlation between the experimental (2.64) and the DS value given by the manufacturer (2.67) was established.

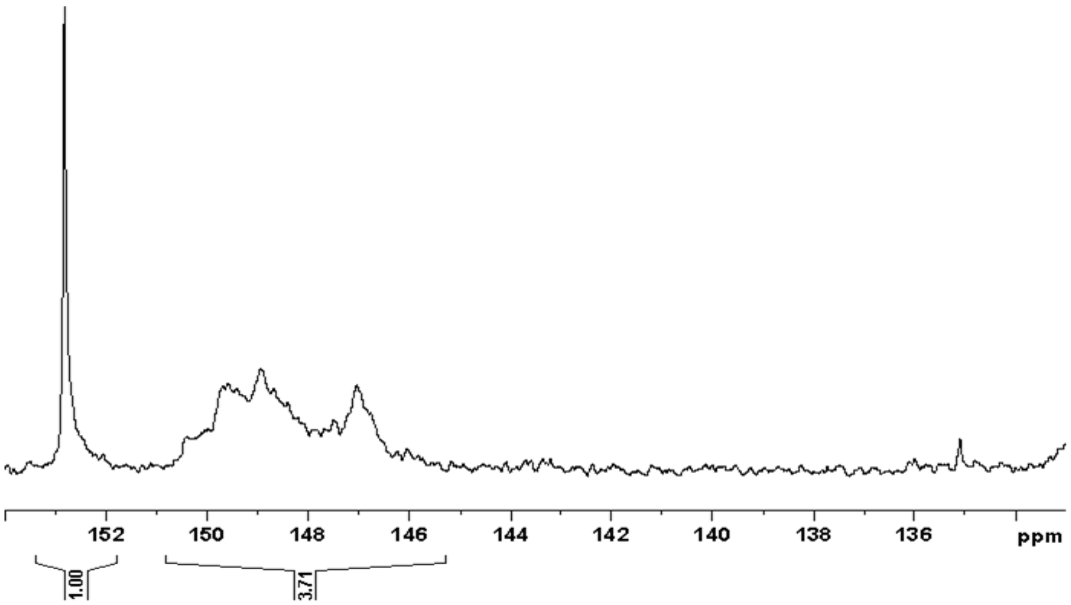

Figure 6.3 ^{31}P NMR spectra of phosphitylated partially acetylated cellulose

After successful validation of the ^{31}P NMR technique the same methodology was applied for the cellulose nanocrystals (CNCs) and TEMPO-oxidized CNCs. Figure 6.4 shows the spectra of phosphitylated TEMPO-oxidized CNCs (6.4a) and phosphitylated CNCs (6.4b). The appearance of new signals in the carboxylic acid region (134.2-136.8 ppm) is evident for the TEMPO-oxidized CNCs (6.4a). The amount of free hydroxyl groups on CNCs was found to be 18.9 mmolg^{-1} which is in good agreement with the maximum theoretical value of 18.52 mmolg^{-1}. This result further confirms the validity of current methodology. Moreover, the amount of carboxylic acid groups in TEMPO-oxidized CNCs was determined to be 0.57 mmolg^{-1}.

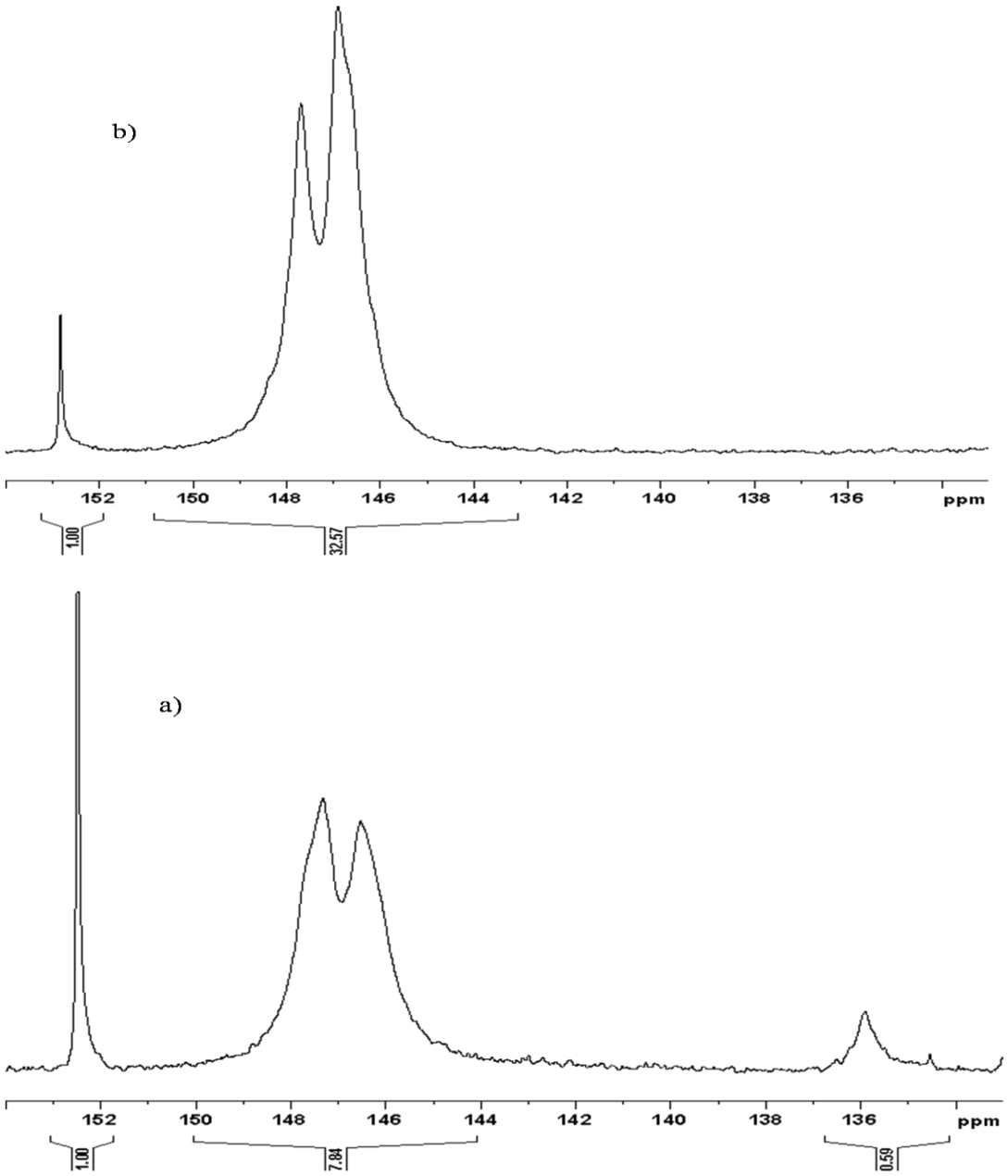

Figure 6.4 ^{31}P NMR spectra of phosphitylated TEMPO-oxidized cellulose nanocrystals (a) and cellulose nanocrystals (b)

As discussed above, the maximum amount of the hydroxyl groups in cellulose is 18.52 mmolg^{-1}. This value can be used for the determination of the maximum amount accessible

primary hydroxyl groups (carboxymethyl) for TEMPO-oxidation. As known, in cellulose molecule, each glucose unit carries three hydroxyl groups consisting of two secondary and one primary hydroxyl group. The maximum amount of carboxymethyl groups is thus approximately 6.2 $mmolg^{-1}$ (18.52/3). However, the maximum amount of carboxymethyl groups accessible for the oxidation is 3.1 $mmolg^{-1}$ because of the two fold screw axis of cellulose molecule which makes half of the carboxymethyl groups inaccessible. The quantitative ^{31}P NMR experiments revealed 0.57 $mmolg^{-1}$ of carboxylic acid groups in TEMPO-oxidized CNCs. The degree of oxidation (DO) can now be calculated by dividing the experimental number with the theoretical value, i.e., 0.57/3.1 leading to a DO value of 0.18 which is in good agreement with the values achieved from the acid-base titrations (0.19) and FTIR experiments (0.21). Overall, the measured DO values correlate well with the 8 x 8 packing model of cotton crystallite (maximum DO of 0.22).

6.4.4 Grafting onto TEMPO-oxidized Cellulose Nanocrystals

As the main goal was to selectively graft the carboxylate groups on the surface of the CNCs the coupling chemistry originally designed for the carboxylic acids was the approach of choice. It has been known for a long time that *N*-hydroxysuccinimide (NHS) converts carboxyl groups to amine-reactive NHS-esters. This is accomplished by mixing the NHS with a carboxyl-containing molecule and a dehydrating agent such as the 1-Ethyl-3-(3-dimethylaminopropyl)-carbodiimide (EDC). EDC by itself is not particularly efficient in

crosslinking reactions because failure to react quickly with an amine will result in hydrolysis and regeneration of the carboxyl moiety.

EDC reacts with a carboxyl group on molecule #1, forming an amine-reactive *O*-acylisourea intermediate (Scheme 6.3). This intermediate may react with an amine on molecule #2, yielding a conjugate of the two molecules joined by a stable amide bond. However, the intermediate is also susceptible to hydrolysis, making it unstable and short-lived in aqueous solution. The addition of NHS stabilizes the amine-reactive intermediate by converting it to an amine-reactive NHS-ester, thus increasing the efficiency of EDC-mediated coupling reactions.[34,35]

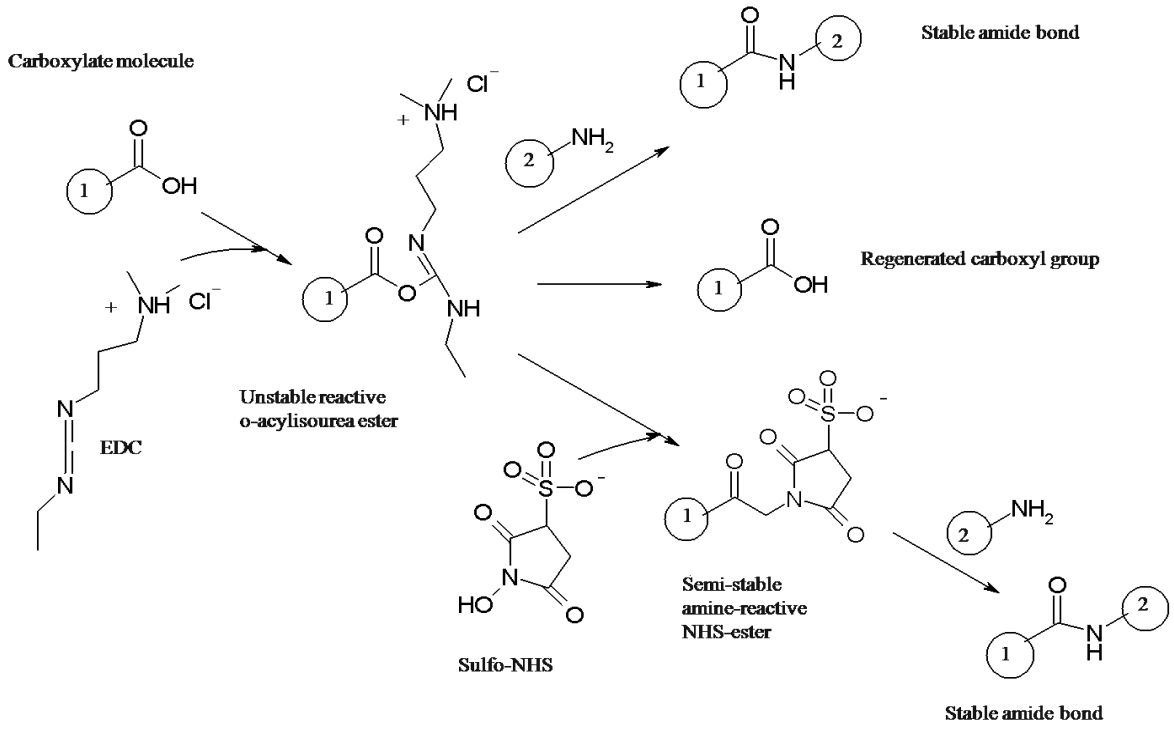

Scheme 6.3 General mechanism for the EDC/NHS mediated coupling reaction of carboxylates and amines

6.4.5 Model Experiments with Octadecylamine

As a starting step, it was reasonable to verify the reactivity of carboxylate groups with a primary amine reagent forming an amide functional group. Therefore, TEMPO-oxidized CNCs were subjected for a reaction with simple amine-terminated model compound, octadecylamine, in a synthetic process as shown in Scheme 6.4.

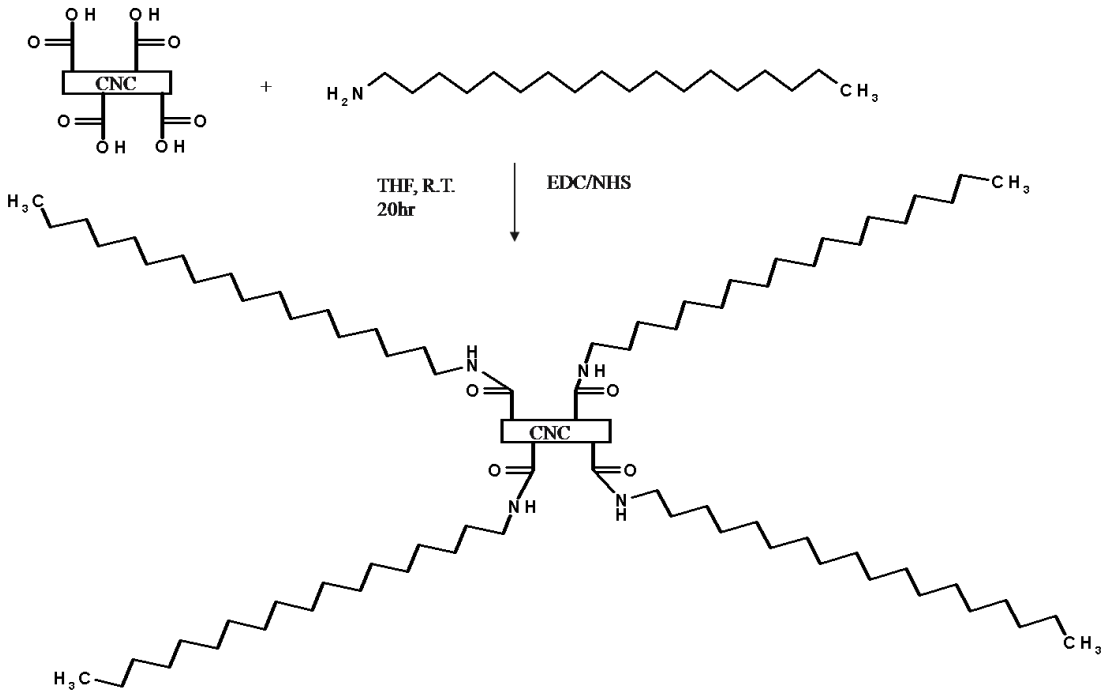

Scheme 6.4 Derivatization of oxidized (TEMPO) cellulose nanocrystals with octadecylamine.

As can be seen from the FT-IR spectra of the product, Figure 6.5, TEMPO-oxidized CNCs were successfully derivatized with octadecylamine. The comparison of the spectrum of unreacted TEMPO-oxidized CNCs (Figure 2) to that of the reaction product revealed the

characteristic octadecyl hydrocarbon aliphatic –CH2, –CH3 stretch in the derivatized cellulose nanocrystals at 2917.8 and 2850.3 cm^{-1}, respectively. Moreover, the C=O stretching frequency of carboxyl groups at 1730 cm^{-1} has disappeared indicating the formation of amide linkage between the carboxylic groups of TEMPO-oxidized CNCs and octadecylamine. The amide band appears at 1650 cm^{-1} and is thus overlapping with the signal from the associated water (1620-1650 cm^{-1}) making it invisible in FTIR spectrum.

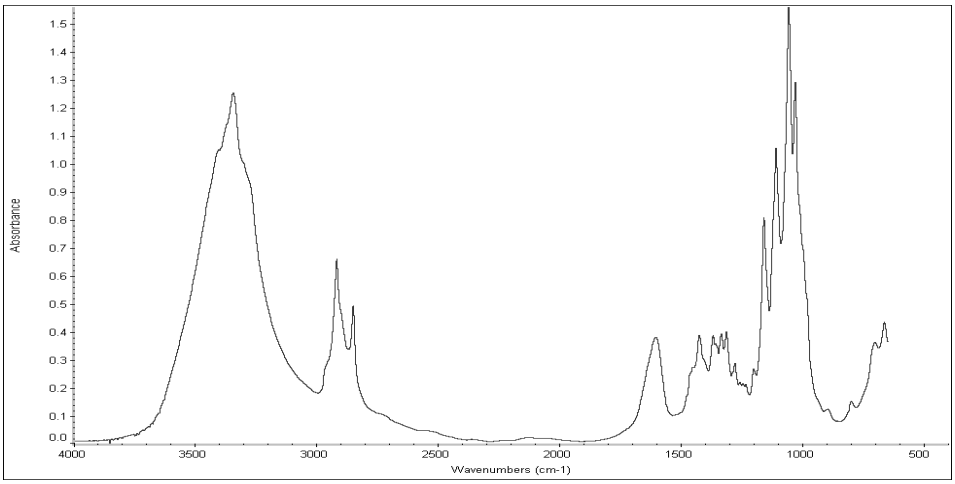

Figure 6.5 FTIR spectrum of octadecylamine grafted oxidized (TEMPO) cellulose nanocrystals

The data from ^{1}H NMR spectroscopy further support the formation of a product that was successfully derivatized from carboxylate groups of cellulose nanocrystals. In Figure 6.6, the ^{1}H spectra of the octadecylamine (6a) and the reaction product (6b) are compared. It shows the appearance of chemical shifts for methyl and methylene protons of octadecylamine in the derivatized cellulose nanocrystals at δ/ppm = 1.235, 0.825 and 2.695, respectively. It is important to note here that the modified CNC sample was not completely

dissolved in deuterated chloroform ($CDCl_3$) but appeared as a suspension. This explains the absence of the proton signals from the cellulose backbone.

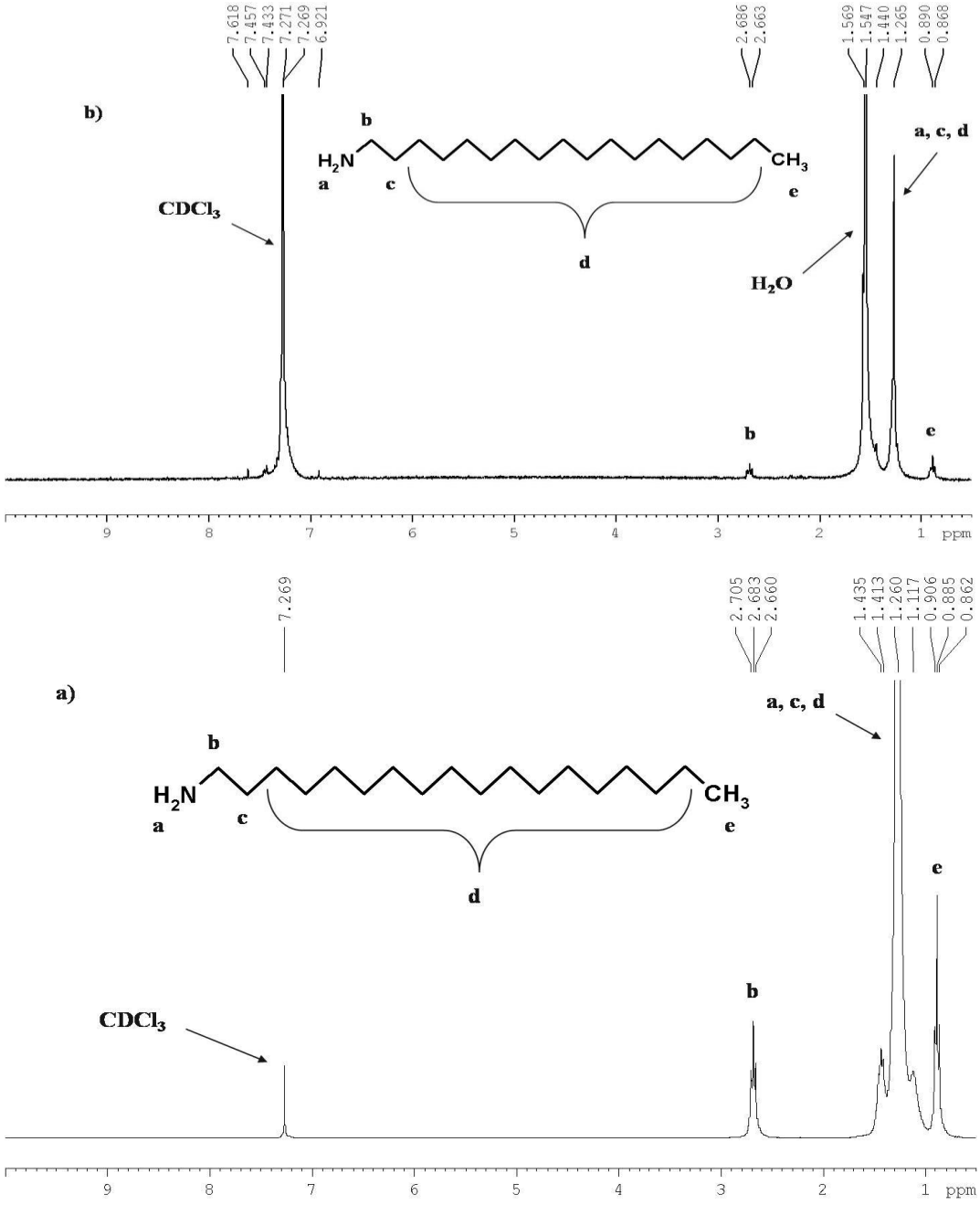

Figure 6.6 ^{1}H NMR spectra of octadecylamine (a) and octadecylamine grafted oxidized (TEMPO) cellulose nanocrystals (b)

6.4.6 Grafting of Amine-terminated Polystyrene (PS-NH_2) onto TEMPO-oxidized Cellulose Nanocrystals

After successfully investigating the synthetic strategy to create an amide linkage between the carboxylic groups of oxidized cellulose nanocrystals (CNCs) and an amine, the same approach was applied for the grafting of amine-terminated polystyrene onto the surface of TEMPO-oxidized CNCs. Figure 6.7 shows the ^{1}H NMR spectrum of amine-terminated polystyrene (PS-NH_2). The signals for the aromatic and aliphatic protons are well defined, at the regions of 7.2-6.5 ppm and 2.2-1.4 ppm, respectively.

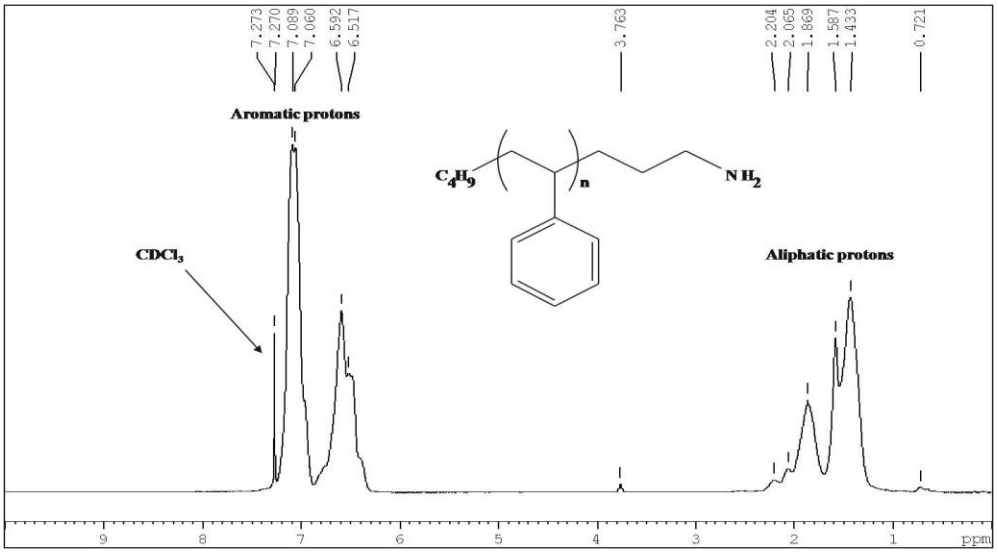

Figure 6.7 ^{1}H NMR spectrum of amine terminated polystyrene (PS-NH_2) in $CDCl_3$

^{1}H NMR spectra of the PS-NH_2 grafted TEMPO-oxidized CNCs are shown in Figure 6.8. The samples were dispersed in deuterated dimethylsulfoxide (DMSO-d_6) and chloroform

($CDCl_3$). It is worth to mention here that neither of the solvents were able to completely dissolve the derivatized CNCs. However, the NMR measurements of the suspensions revealed the presence of aromatic moieties.

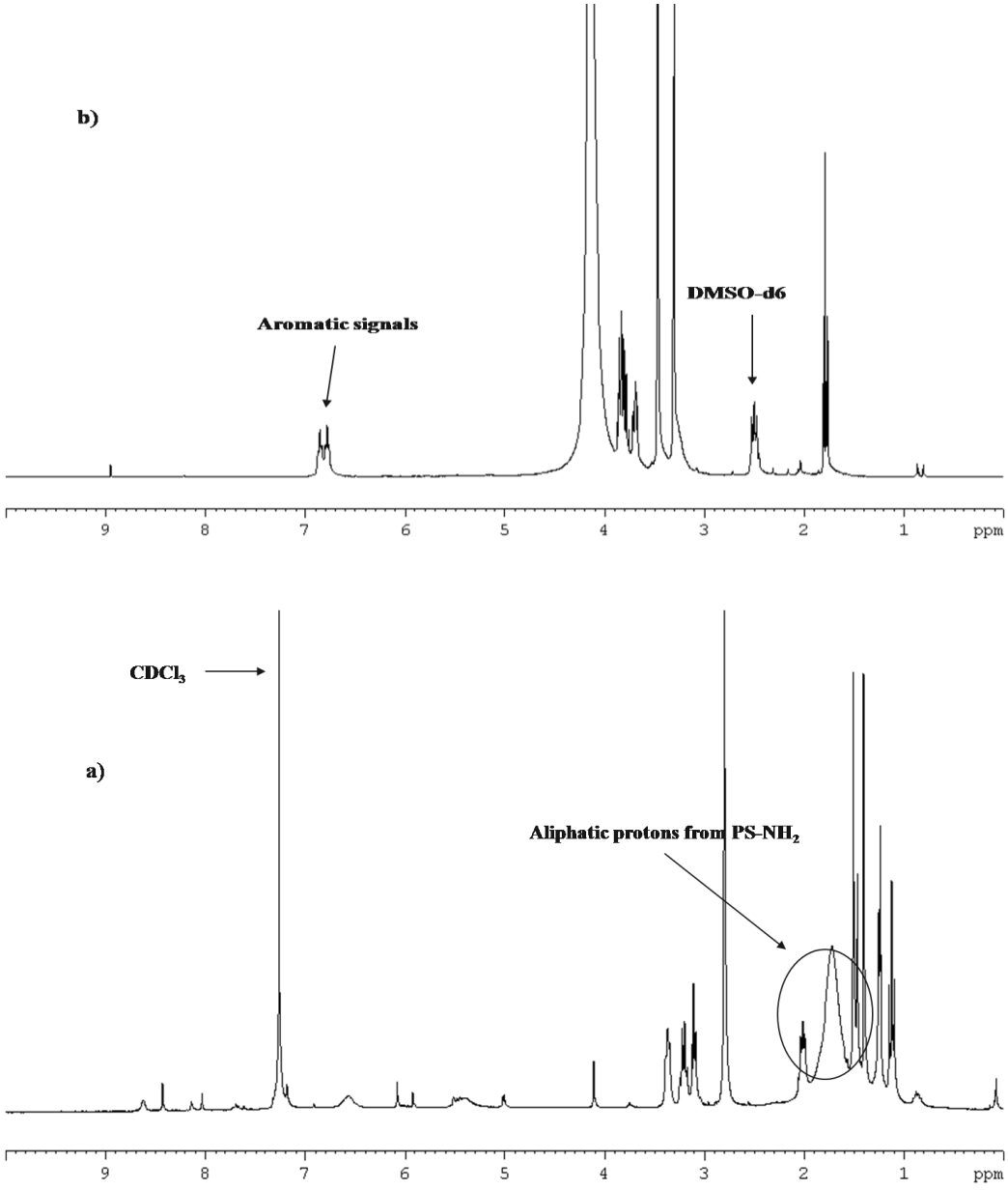

Figure 6.8 ^{1}H NMR spectra of PS-NH_2 grafted oxidized (TEMPO) cellulose nanocrystals dispersed in $CDCl_3$ (a) or DMSO-d_6 (b)

Thermogravimetric analysis further supported the formation of the PS-NH_2 grafted CNCs. Figure 6.9 shows decomposition temperatures of amine-terminated polystyrene (PS-NH_2), TEMPO-oxidized cellulose nanocrystals, and PS-NH_2 grafted CNCs. The thermal decomposition data of PS-NH_2 grafted CNCs shows two decomposition temperatures. A lower temperature correspond to component TEMPO-oxidized CNCs and higher to PS-NH_2, respectively. However, the grafting density of PS-NH_2 on the surface of CNCs seemed to be rather low probably due to the steric reasons. To overcome the steric limitations the use of grafting from approach, such as atom transfer radical polymerization (ATRP), would be of importance to achieve more complete grafting of polystyrene.

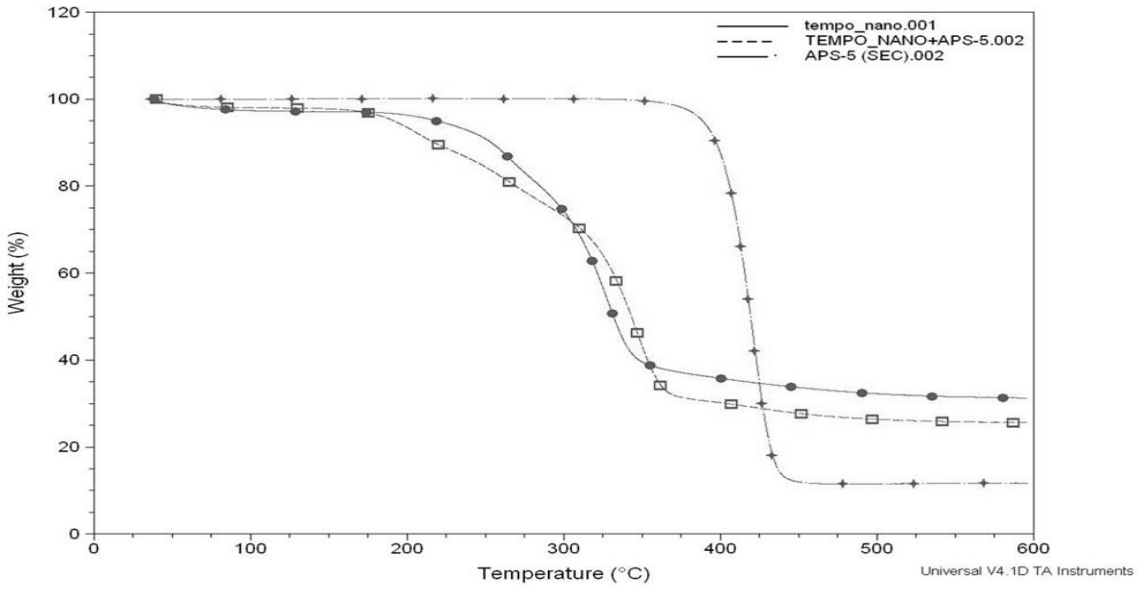

Figure 6.9 TGA curves of tempo-oxidized nanocrystals (circle markers), amine terminated polystyrene (cross markers) and polystyrene grafted cellulose nanocrystals (open square markers)

6.5 Conclusions

The primary hydroxyl groups on the surface of cellulose nanocrystals can be selectively oxidized, thus introducing negative charges or reaction anchors in a patterned fashion. TEMPO-oxidized cellulose nanocrystals were characterized with three different methods, by acid-base titration, FTIR and ^{31}P NMR spectroscopy, respectively. The achieved degree of oxidation (DO) values for the same sample, analyzed with different techniques, were within 0.03 units ranging from 0.18-0.21. Moreover, the carboxylate groups on oxidized CNCs were grafted with amine terminated compounds using succinimide assisted coupling chemistry. However, incomplete grafting of amine-terminated polystyrene suggested that the grafting from approach, such as atom transfer radical polymerization (ATRP), would be more feasible for such derivatization reactions.

6.6 References

1. Battista, O. A., Coppick, S., Howsmon, J. A., Morehead, F. F., and Sisson, W.A. (1956). "Level-Off Degree of Polymerization," *Ind. Eng. Chem., 48(2),* 333-335.

2. Orts, W. J., Godbout, L., Marchessault, R. H., and Revol, J.-F. "Enhanced Ordering of Liquid Crystalline Suspensions of Cellulose Microfibrils: A Small Angle Neutron Scattering Study," *Macromolecules* 1998, 31(17), 5717-5725.

3. Imai, T., Boisset, C., Samejima, M., Igarashi, K., and Sugiyama, J. (1998). "Unidirectional processive action of cellobiohydrolase Cel7A on *Valonia* cellulose microcrystals," *FEBS Lett.*, 432(3), 113-116.

4. Araki, J., Wada, M., Kuga, S., and Okano, T. (1998). "Flow properties of microcrystalline cellulose suspension prepared by acid treatment of native cellulose," *Colloid Surf. A.,* 1998, 142(1), 75-82.

5. Dong, X. M., Revol, J. F., and Gray, D. G. (1998). "Effect of microcrystallite preparation conditions on the formation of colloid crystals of cellulose," *Cellulose,* 5(1), 19-32

6. Dong, X. M. and Gray, D. G. (1997). "Effect of Counterions on Ordered Phase Formation in Suspensions of Charged Rodlike Cellulose Crystallites," *Langmuir,* 13(8), 2404-2409.

7. Araki, J., Wada, M., Kuga, S., and Okano, T. (1999). "Influence of surface charge on viscosity behavior of cellulose microcrystal suspension," *J. Wood Sci.,* 45(3), 258-261.

8. Revol, J.-F., Bradford, H., Giasson, J., Marchessault, R. H., and Gray, D. G. (1992). "Helicoidal self-ordering of cellulose microfibrils in aqueous suspension," *Int. J. Biol. Macromol.,* 14(3), 170-172.

9. Dong, X. M., Kimura, T., Revol, J.-F., and Gray, D. G. (1996). "Effects of Ionic Strength on the Isotropic−Chiral Nematic Phase Transition of Suspensions of Cellulose Crystallites," *Langmuir,* 12(8), 2076-2082.

10. Araki, J., Wada, M., Kuga, S., Okano, T. (2000). "Birefringent Glassy Phase of a Cellulose Microcrystal Suspension," *Langmuir,* 16(6), 2413-2415.

11. De Nooy, A. E., Besemer, A. C., and van Bekkum, H. (1994). "Highly selective tempo mediated oxidation of primary alcohol groups in polysaccharides," *Recl. Trav. Chim. Pays-Bas,* 113(3), 165-166.

12. Saito, T. and Isogai, A. (2005). "Novel method to improve wet strength of paper", *TAPPI J.,* 4(3), 3-8.

13. Tahiri, C. and Vignon, M. (2000). "TEMPO-oxidation of cellulose: Synthesis and characterisation of polyglucuronans," *Cellulose,* 7(2), 177-188.

14. Montanari, S., Roumani, M., Heux, L., and Vignon, M. (2005). "Topochemistry of Carboxylated Cellulose Nanocrystals Resulting from TEMPO-Mediated Oxidation," *Macromolecules,* 38(5), 1665-1671.

15. Saito, T., Shibata, I., Isogai., A., Suguri, N., and Sumikwa, N. (2005). "Distribution of carboxylate groups introduced into cotton linters by the TEMPO-mediated oxidation," *Carbohydr. Polym.,* 61(4), 414-419.

16. Saito, T. and Isogai, A. (2004). "TEMPO-Mediated Oxidation of Native Cellulose. The Effect of Oxidation Conditions on Chemical and Crystal Structures of the Water-Insoluble Fractions," *Biomacromolecules,* 5(5), 1983-1989.

17. Araki, J., Wada, M., and Kuga, S. (2001). "Steric Stabilization of a Cellulose Microcrystal Suspension by Poly(ethylene glycol) Grafting," *Langmuir,* 17(1), 21-27.

18. Ueda, K., Hirao, A., and Nakahama, S. (1990). "Synthesis of polymers with amino end groups. 3. Reactions of anionic living polymers with α-halo-ι-aminoalkanes with a protected amino functionality," *Macromolecules,* 23(4), 939-945.

19. Da Silva Perez, D., Montanari, S., and Vignon, M. R. (2003). "TEMPO-Mediated Oxidation of Cellulose III," *Biomacromolecules,* 4(5), 1417-1425.

20. Habibi, Y., Chanzy, H., and Vignon, M. R. (2006). "TEMPO-mediated surface oxidation of cellulose whiskers," *Cellulose,* 13(6), 679-687.

21. Saito, T., Nishiyama, Y., Putaux, J. L., Vignon, M., and Isogai, A. (2006). "Homogeneous Suspensions of Individualized Microfibrils from TEMPO-Catalyzed Oxidation of Native Cellulose," *Biomacromolecules,* 7(6), 1687-1691.

22. Fan, L. T., Gharpuray, M. M., and Lee, Y.-H. (1987). Biotechnology Monographs: Cellulose Hydrolysis, Springer-Verlag, Berlin.

23. Leppänen, K., Andersson, S., Torkkeli, M., Knaapila, M., Kotelnikova, N., and Serimaa, R. (2009). "Structure of cellulose and microcrystalline cellulose from various wood species, cotton and flax studied by X-ray scattering," *Cellulose,* ASAP Article, Published online 13 may 2009.

24. Argyropoulos, D. S. (1994). "Quantitative phosphorus-31 NMR analysis of lignin: a new tool for the lignin chemist," *J. Wood Chem. Technol,* 1, 45–63.

25. Granata, A. and Argyropoulos, D. S. (1995). "2-Chloro-4,4,5,5-tetramet-hyl-1,3,2-dioxaphospholane a reagent for the accurate determination of the unecondensed and condensed phenolic moieties in lignins," *J. Agric. Food Chem.,* 43(6), 1538–1544.

26. Guerra, A.; Filpponen, I.; Lucia, L. A.; Argyropoulos, D. S. (2006). "Comparative Evaluation of Three Lignin Isolation Protocols for Various Wood Species," *J. Agric. Food Chem.,* 26, 9696–9705.

27. Guerra, A.; Filpponen, I.; Lucia, L. A.; Saquing, C.; Baumberger, S.; Argyropoulos, D. S. (2006). "Toward a Better Understanding of the Lignin Isolation Process from Wood," *J. Agric. Food Chem.,* 54, 5939–5947.

28. Crestini, C.; Argyropoulos, D. S. (1997). "Structural Analysis of Wheat Straw Lignin by Quantitative ^{31}P and 2D NMR Spectroscopy. The Occurrence of Ester Bonds and a-O-4 Substructures," *J. Agric. Food Chem.,* 45, 1212-1219.

29. King, A. W. T., Kilpelainen, I., Heikkinen, S., Jarvi P., and Argyropoulos, D. S. (2009). "Hydrophobic Interactions Determining Functionalized Lignocellulose Solubility in Dialkylimidazolium Chlorides, as Probed by ^{31}P NMR," *Biomacromolecules,* 10(2), 458–463.

30. Granstrom, M., Kavakka, J., King, A. W. T., Majoinen, J., Makela, V., Helaja, J., Hietala, S., Virtanen, T., Maunu, S., Argyropoulos, D. S., and Kilpelainen, I. (2008). "Tosylation and acylation of cellulose in 1-allyl-3-methylimidazolium chloride," *Cellulose, 3,* 481–488.

31. Zhang, H., Wu, J., Zhang, J., and He, J. (2005). "1-allyl-3-methylimidazolium chloride room temperature ionic liquid: A new and powerful nonderivatizing solvent for cellulose," *Macromolecules, 38,* 8272– 8277.

32. Wu, J., Zhang, J., Zhang, H., He, J., Ren, Q., and Guo, M. (2004). "Homogeneous Acetylation of Cellulose in a New Ionic Liquid," *Biomacromolecules,* 5(*2),* 266–268.

33. Cao, Y., Wu, J., Meng, T., Zhang, J., He, J., Li, H., and Zhang, Y. (2007). "Acetone-soluble cellulose acetates prepared by one-step homogeneous acetylation of cornhusk cellulose in an ionic liquid 1-allyl-3-methylimidazolium chloride (AmimCl)," *Carbohydr. Polym., 4,* 665–672.

34. Grabarek, Z. and Gergely, J. (1990). "Zero-length crosslinking procedure with the use of active esters," *Anal. Biochem.,* 185(1), 131-135.

35. Staros, J. V., Wright, R. W., and Swingle, D. M. (1986). "Enhancement by *N*-hydroxysulfosuccinimide of water-soluble carbodiimide-mediated coupling reactions," *Anal. Biochem.,* 156(1), 220-222.

7. 1,3-Dipolar Cycloaddition ("Click"-Reaction) of Cellulose Nanocrystals-Formation of Nano-Platelet Gels

7.1 Abstract

Over a number of years work in our laboratory has been exploring the use of cellulose nanocrystals (CNC) as scaffolds for the creation of novel nanomaterials with unique and stimuli responsive characteristics.

In this communication a method for the grafting of amine-terminated monomers onto surface-modified cellulose nanocrystals (CNCs) followed by 'click chemistry' is demonstrated. In the first step, the primary hydroxyl groups on the surface of the CNCs were converted to carboxylic acids by using TEMPO-mediated hypohalite oxidation. The grafting reactions of TEMPO-oxidized CNCs were carried out via carbodiimide-mediated formation of an amide linkage between monomers carrying an amine functionality and carboxylic acid groups on the surface of the TEMPO-oxidized CNCs. Furthermore, the crosslinking reactions of CNCs were investigated by means of a "Click"-chemistry reaction, i.e., the Cu(I)-catalyzed Huisgen 1,3-dipolar cycloaddition between an azide derivative and an alkyne derivative of TEMPO-oxidized CNCs obtained by aforementioned carbodiimide-mediated amidation.

7.2. Introduction

The modification of polysaccharides plays a central role in the field of sustainable chemistry.[1] By the virtue of their huge abundancy and the structural and superstructural diversity polysaccharides are ideal starting materials for defined modifications and specific

applications. The chemical modification of polysaccharides provides a versatile route for the structure and property design of such materials.[2] Due to the chemical functionality of polysaccharides (bearing hydroxyl and/or carboxylic acid groups) the esterification and etherification are the most common approaches for the modification reactions of polysaccharides. Moreover, the oxidation and homogenous nucleophilic substitution reactions are applied but to a lesser extent. Cellulose and dextran are the most commonly used starting materials for the creation of highly engineered nanoparticles.[3,4,5,6]

In general, 1,3-dipolar cycloaddition reactions have long been popular in the generation of carbohydrate mimetics in homogeneous reaction environment.[7] More precisely, the thermally induced cycloaddition (Huisgen reaction) occurs between an azide and a triple bond and is nowadays often referred as a member of the click-reaction family because of its robustness.[8] The reaction has gained increasing attention after discovering that the 1,3-dipolar cycloaddition between azides and terminal alkynes can be catalysed by CuI salts.[9,10,11,12,13] In fact, the Huisgen reaction has become the most popular click reaction to date by the virtue of its high yields, rapidity, high regio- and stereoselectivity, mild reaction conditions and experimental simplicity. Several authors have described the use of this novel click-chemistry concept for the generation of carbohydrate mimetics and derivatives.[10,14,15,16,17]

In 2001, Araki and coworkers demonstrated a method for grafting amine-terminated poly(ethylene glycol) to surface-modified (TEMPO-oxidized) cellulose microcrystals, thus

improving the stability of the microcrystal suspensions through steric stabilization.[18] In 2007, Crescenzi *et al.* extended Araki's approach by modifying hyaluronic acid with the alkyne and azido groups to achieve suitable precursor for the 1,3-dipolar cycloaddition reaction.[19] They modified hyaluronic acid with the alkyne and azido groups to achieve suitable precursor for the 1,3-dipolar cycloaddition reaction.[9,14,15,20,21,22] Once these precursors were mixed in the aqueous media substantial gel formation was observed. Recently, similar methodology has been successfully applied for cellulose modifications in heterogeneous media.[23,24]

Gel-like nanomaterials have been formed using cellulose nanocrystals (CNC) as a starting material. First, the primary hydroxyl groups on the surface of the CNCs were converted to carboxylic acids by using TEMPO-mediated hypohalite oxidation. In the next step, compounds carrying terminal amine functionality were grafted on to oxidized CNCs via carbodiimide-mediated formation of an amide linkage between an amine and the carboxylic groups on the CNC's surface. The grafted amines were also bearing either alkyne or azide functionalities which were then used for the further reactions. Finally, the modified CNCs were subjected to "Click"-chemistry reaction, i.e., the Cu(I)-catalyzed Huisgen 1,3-dipolar cycloaddition between an azide and an alkyne derivative of TEMPO-oxidized CNCs. Produced crosslinked nanomaterials were characterized by FTIR, elemental analysis, GPC, thermal analysis and TEM.

7.3 Materials and Methods

Materials. Whatman #1 filter paper was used as a starting material for the cellulose nanocrystals. 11-azido-3,6,9-trioxaundecan-1-amine (technical, ≥90%) was purchased from Fluka and propargylamine (98%) from Sigma-Aldrich. All other chemicals were purchased from Sigma-Aldrich or Fisher and used as received unless otherwise stated.

7.3.1 Acid Hydrolysis of Cellulose to Produce Cellulose Nanocrystals (CNC). The cellulose nanocrystals were formed by acidic hydrolysis similar to the procedure used by Araki *et al.*[18,25,26] A typical procedure was as follows. 2.0 g of cellulose pulp obtained from Whatman #1 filter paper (98% α-cellulose, 80% crystallinity) was blended by a 10 Speed Osterizer® Blender. Resulting pulp was hydrolyzed with 100 mL of 2.5 M HBr at 100°C for 3 hours. The ultrasonication was applied during (every 60 minutes) the reaction (Omni-Ruptor 250W ultrasonic homogenizer, 50% power, 5 min). The resulting mixture was diluted with de-ionized (D.I) water followed by five cycles of centrifugation at 1500g for 10 min. (IEC Centra-CL3 Series) to remove excess acid and water soluble fragments. The fine cellulose particles became dispersed in the aqueous solution approximately at pH 4. The turbid supernatant containing the polydisperse cellulose particles was then collected for further centrifugation at 15000 g for 45 min (Automatic Servall® Superspeed Centrifuge) to remove ultra-fine particles. Ultra-fine particles with small aspect ratio were removed from the upper layer, and the precipitation (after the high-speed centrifugation) was dried using a lyophilizing system (Labconco, Kansas City, MU).

7.3.2 TEMPO-mediated Oxidation of CNCs. 648 mg (4 mmol of glucosyl units) of cellulose nanocrystals were suspended in water (50 mL) containing 10 mg of 2,2,6,6-tetramethyl-1-piperidinyloxy-radical (TEMPO, 0.065 mmol) and 200 mg of sodium bromide (1.9 mmol) at room temperature for 30 min. The TEMPO-mediated oxidation of the cellulose nanocrystals was initiated by slowly adding 4.90 mL of 13% NaClO (8.6 mmol) over 20 min at room temperature under gentle agitation. The reaction pH was monitored using a pH meter and maintained at 10 by incrementally adding 0.5 M NaOH. When no more decrease in pH was observed, the reaction was considered complete. About 5 mL of methanol was then added to react and quench with the extra oxidant. After adjusting the pH to 7 by adding 0.5 M HCl, the TEMPO-oxidized product was washed with D.I. water by centrifugation and further purified by dialysis against D.I. water for two days. 550 mg of solid was recovered after freeze-drying. FTIR measurements showed a carboxylic acid peak at 1730 cm^{-1}.

7.3.3 Synthesis of "Click"-Precursors. A 50 mg amount of TEMPO-oxidized CNCs were mixed in 6 mL of MES [2-(*N*-morpholino)-ethanesulfonic acid buffer (50 mM, pH = 4)]. Resulting suspension was further treated with ultrasound treatment (5 min, 20% power (50W) with 30% pulser on; Omni-Ruptor 250 Ultrasonic Homogenizer, Omni International Inc.) to break down the cellulose aggregates. In typical synthesis, 120 mg of EDC·HCl [*N*-(3-dimethylaminopropyl)-*N'*-ethylcarbodiimide hydrochloride)], 72 mg of NHS (*N*-hydroxysuccinimide), and 200 μL of 11-azido-3,6,9-trioxaundecan-1-amine, respectively, were added to the CNC suspension. The reaction was performed at room temperature under

stirring for 24 h. The resulting mixture was dialyzed (cutoff = 12 kDa) against aqueous saturated NaCl for 1 day and then against distilled water for 3 days. Finally, the solutions were dried using a lyophilizing system to recover the CNC-AZ derivatives (see Scheme 7.1).

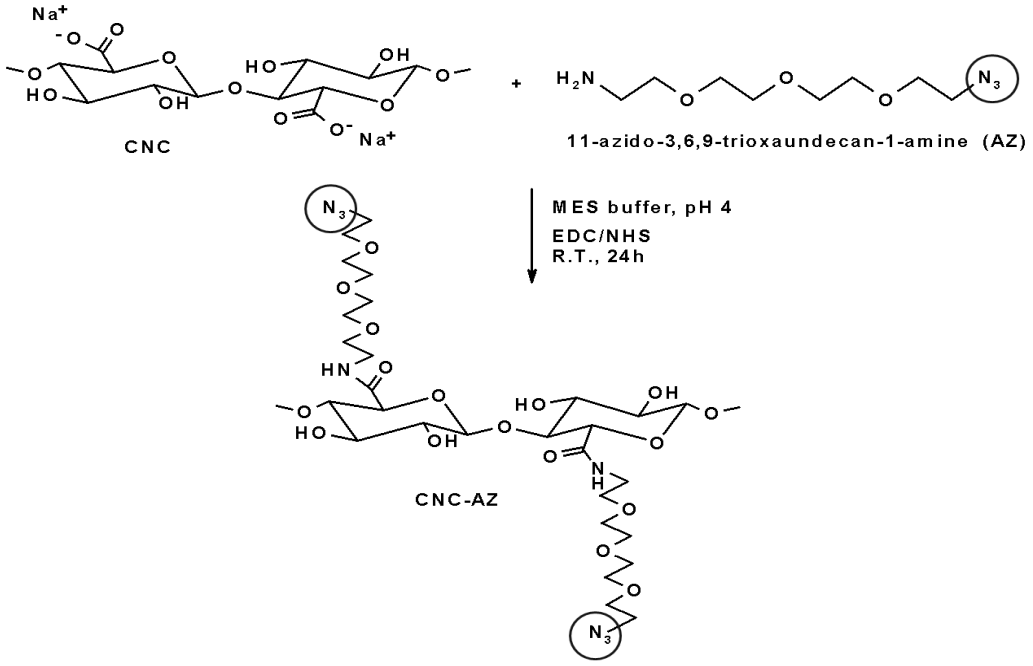

Scheme 7.1 Schematic representation of the reaction between cellulose nanocrystals (CNC) and 11-azido-3,6,9-trioxaundecan-1-amine (AZ)

TEMPO-oxidized CNCs (50mg) were mixed in 6 mL of MES [2-(*N*-morpholino)-ethanesulfonic acid buffer (50 mM, pH = 4). Resulting suspension was further treated with ultrasound treatment (5 min, 20% power with 30% pulser on; Omni-Ruptor 250 Ultrasonic Homogenizer, Omni International Inc.) to break down the cellulose aggregates. In typical synthesis, 120 mg of EDC·HCl [*N*-(3-dimethylaminopropyl)-*N'*-ethylcarbodiimide hydrochloride)], 72 mg of NHS (*N*-hydroxysuccinimide), and 60 μL of propargylamine,

respectively, were added to the CNC suspension. The reaction was performed at room temperature under stirring for 24 h. The resulting mixture was dialyzed (cutoff = 12 kDa) against a saturated NaCl solution for 1 day and then against distilled water for 3 days. Finally, the CNC-PR derivatives (see Scheme 7.2) were recovered by freeze-drying.

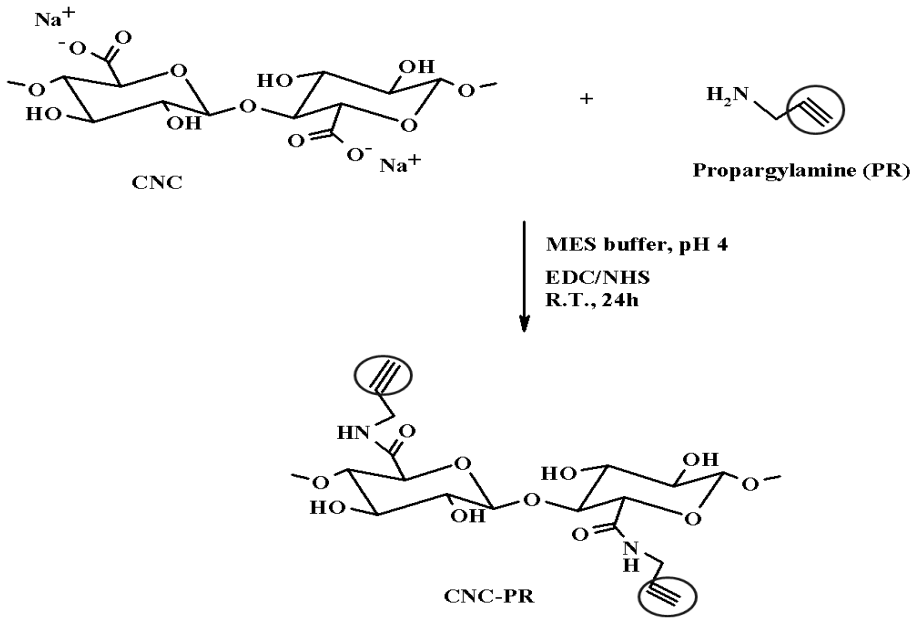

Scheme 7.2 Schematic representation of the reaction between cellulose nanocrystals (CNC) and propargylamine (PR)

7.3.4 Synthesis of "Click"-Product. A 25 mg amount of CNC-AZ and 25 mg of CNC-PR were mixed in 3.0 mL of distilled water. Next, 25 μL of $CuSO_4$ x $5H_2O$ aqueous solution (7.5% w/v) and 30 μL of ascorbic acid (1M sol.) were added and the mixture was vigorously stirred leading to a formation of a stable gel (click-gel: Scheme 7.3). The gel was left at rest overnight and then dialyzed against EDTA solution (10 mM) for 12 h and finally against distilled water until constant weight.

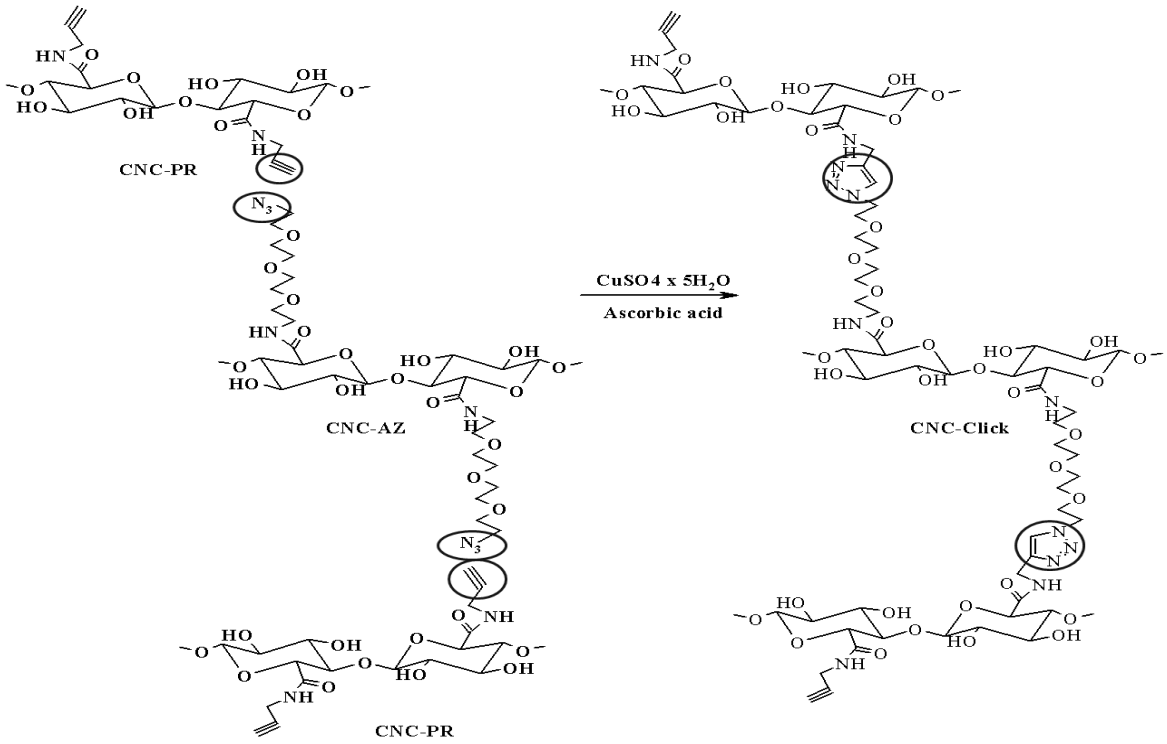

Scheme 7.3 Schematic representation of the formation of CNC-based nano-platelet gels

7.3.5 Benzoylation of CNCs and "Click"-Products. Ionic liquid, 1-allyl-3-methylimidazolium chloride ([Amim]Cl, 950 mg) were added to CNC (50 mg) in a 15 ml sample flasks, vortexed until all solid particles had dispersed and heated at 80°C with magnetic stirring until the solutions were transparent (2 hrs). Pyridine (330 µl, 3.7 mmol) was added and the solution vortexed until homogeneous and allowed to cool down to room temperature. Benzoyl Chloride (380 µl, 3.3 mmol) was added in one portion and the resulting mixture was vortexed until the formation of homogeneous white paste. The sample was then heated at 55 °C for 3 hrs with magnetic stirring and then allowed to cool down to the room temperature. Next, the mixture of deionized water (2.5 ml) and EtOH

(7.5 ml) was added and the mixture vigorously shaken and vortexed for 5 mins. The solid was filtered off through a sintered funnel (grade M), washed further with EtOH and purified with MeOH (stirred overnight without heating). Finally, the resulting solid was filtered off to give a white powder (84 mg).

7.3.6 Infrared Spectroscopy. FTIR spectra were measured on a Thermo Nicolet NEXUS 670 FT-IR infrared spectrophotometer. Spectra in the range of 4000 – 650 cm^{-1} were obtained with a resolution of 4 cm^{-1} by cumulating 64 scans. Degree of oxidation (DO) measurements were carried out by comparing the intensities of absorption band near 1730 cm^{-1} (carbonyl stretching frequency) to that of 1050 cm^{-1} (cellulose backbone).[27]

7.3.7 Acid-base Titration. The carboxylic acid content of the oxidized CNCs was determined by acid-base titration following the procedure developed for the conductometric titrations of such materials.[28] In this procedure TEMPO-oxidized CNC samples (50mg) were suspended into 0.01 M hydrochloric acid (HCl) solutions (15 ml) with stirring. The resulting suspensions were then titrated with 0.01 M sodium hydroxide (NaOH) solution. The degree of oxidation (DO) values were calculated as already published and very reproducible results were obtained.[28]

7.3.8 GPC Analysis. Gel permeation chromatographic (GPC) measurements were carried out with a Waters GPC 510 pump equipped with UV and RI detectors using THF as the eluent at a flow rate of 0.7 mL/min at 40^{o}C. Two Ultrastyragel linear columns (Styragel HR

1 and Styragel HR 5E), connected in series, were used for the measurements. Standard mono-disperse polystyrenes with molecular weight ranges from 0.82 to 1860 kg/mol were used for calibration. The number- and weight-average molecular weights were calculated using the Millenium software of Waters.

7.3.9 Transmission Electron Microscopy. Suspensions (0.01% w/v in water) of unmodified cellulose nanocrystal, TEMPO-oxidized cellulose nanocrystals and cellulose nanocrystals after the "Click"-reaction were prepared. Drops of each suspension were deposited on carbon-coated electron microscope grids, negatively stained with uranyl acetate and allowed to dry. The grids were observed with a Hitachi HF2000 microscope (FEI Company, USA) operated at an accelerating voltage of 200 kV.

7.3.10 Elemental Analysis. The percent carbon (C), hydrogen (H) and nitrogen (N) contents (%) of the unreacted TEMPO-oxidized cellulose nanocrystals, its alkyne and azido derivatives and "Click" product were determined by Perkin Elmer element analyzer (Norwalk, CT, USA). The remaining sample was assumed to be oxygen (O).

7.3.11 Thermal Analysis. Thermal decomposition temperatures were determined using a TA Instrument TGAQ500 at a ramp of 10^{o}C/min under N_2 purge.

7.4 Results and Discussion

7.4.1 FTIR Analysis of the TEMPO-oxidized CNCs and "Click"-Derivatives.

The click-reaction of the CNC derivatives was followed by FTIR measurements. Figure 1a shows carbonyl stretching at 1730 cm^{-1} for the TEMPO-oxidized CNCs. The band dissapears during the formation of the azide derivative (CNC-AZ) which in turn has a characteristic azide stretching band at about 2110 cm^{-1} (Figure 1b). The azide stretching is not apparent in the FTIR spectrum of the Click-CNC (Figure 1c) which indicates of the successful 1,3-dipolar cycloaddition reaction between the CNC-AZ and CNC-PR.

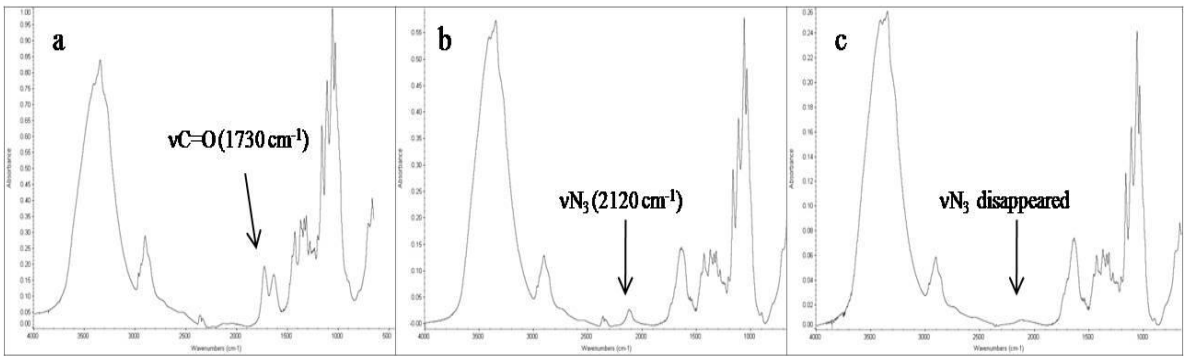

Figure 7.1 FTIR spectra of oxidized (TEMPO) cellulose nanocrystals (a), azido-derivatized cellulose nanocrystals (CNC-AZ) (b) and nano-platelet gels (CNC-Click) (c)

Figure 7.2 demonstrates the formation of a gel as a result of the "Click"-reaction. The addition of water results in a low viscosity suspension of CNC-precursor similar to a

suspension of unmodified cellulose (Figure 7.2b). However, quickly after the addition of the catalysts, copper sulfate and ascorbic acid, stable gel is formed (Figure 7.2c)

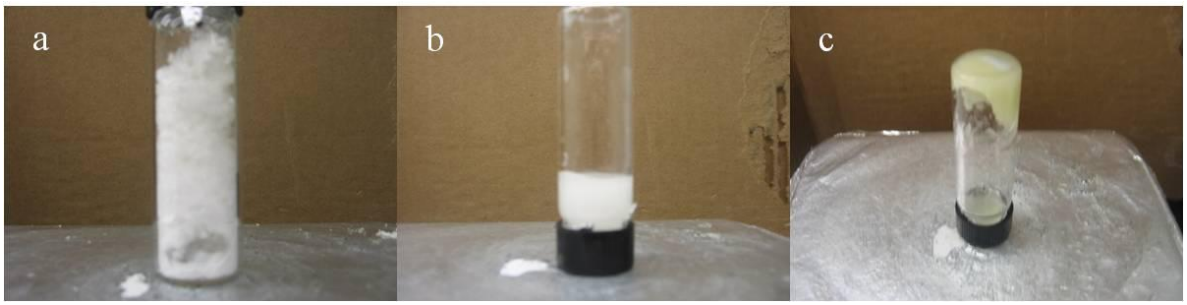

Figure 7.2 “Click”-precursors mixed together (CNC-PR and CNC-AZ) (a), “Click”-precursors after an addition of water (b) and gel formation after adding the catalysts, copper sulfate and ascorbic acid (c).

7.4.2 Elemental Analysis of TEMPO-oxidized CNCs and “Click”-Derivatives.

The nitrogen contents in both of click precursors confirmed the successful grafting reactions (Table 7.1). In order to outsource the possibility of the nitrogen deriving from the used crosslinking agents (1-Ethyl-3-[3-dimethylaminopropyl]carbodiimide hydrochloride and *N*-hydroxysulfosuccinimide) the TEMPO-oxidized CNCs were subjected to identical reaction conditions with the absence of the derivatization compounds (11-azido-3,6,9-trioxaundecan-1-amine and propargylamine). It is worth to mention here that the content of oxygen is elevated in the TEMPO-oxidized CNCs when compared to the CNCs, indicating and further supporting the occurrence of successful oxidation reaction. Moreover, the nitrogen contents for both of the precursors (CNC-PR and CNC-AZ) as well as for the CNC-Click were found to be higher than that of the starting material.

The grafting densities of synthesized precursors were calculated based on the DO value (0.2) of the oxidized CNCs determined by FTIR and acid-base titration. The DO value 0.2 means that 20% of the hydroxymethyl groups on cellulose have been oxidized to corresponding carboxylic acid groups and are thus susceptible for the subsequent grafting reactions. Therefore, the maximum grafting density corresponds to the situation where every fifth of the anhydroglucose units in cellulose contain a grafted propargylamine or 11-azido-3,6,9-trioxaundecan-1-amine moiety. As a result, in the case of propargylamine, the completely grafted TEMPO-oxidized CNCs should contain 1.6% of nitrogen [14 / (5 x 162 + 40)]. Similarly, the complete grafting of 11-azido-3,6,9-trioxaundecan-1-amine should produce modified CNCs with 5.5% nitrogen content (4 x 14 / (5x 162 + 217)]. However, the amount of nitrogen found in the precursors was 0.79% (CNC-PR) and 1.90% (CNC-AZ) which corresponds to the grafting densities of ~50% (CNC-PR) and ~35% (CNC-AZ). Incomplete grafting is not totally surprising since the reactions were carried out under heterogeneous reaction conditions (aqueous suspensions).

Table 7.1 Carbon, hydrogen, oxygen and nitrogen contents of the cellulosic samples.

Sample	% C	% H	% N	% O[a]
Tempo-ox. CNC	41.75	5.76	0.08	52.41
CNCs	43.55	6.11	0.04	50.30
CNC-AZ	42.87	5.20	1.90	50.03
CNC-PR	43.20	5.29	0.79	50.72
CNC-Click	43.28	6.03	1.51	49.18

[a]O = 100 % - C (%) – H (%) – N (%)

7.4.3 Thermal Analysis of TEMPO-oxidized CNCs and "Click"-Derivatives.

In our efforts to investigate the thermal behavior of the formed click products we applied thermogravimetric analysis (TGA) for the determination of thermal decomposition temperature. TGA analysis of the starting materials and the click product indicated significant changes in the decomposition profiles after the click reaction (Figure 7.3). The thermal degradation curves of the TEMPO-oxidized CNCs and both of the derivatives (CNC-AZ and CNC-PR) are almost identical while the click product (CNC-Click) seems to have two degradation temperatures i.e. CNC-Click starts to degrade at similar temperatures (around 225°C) as its precursors but it has significantly elevated second decomposition temperature at 325°C.

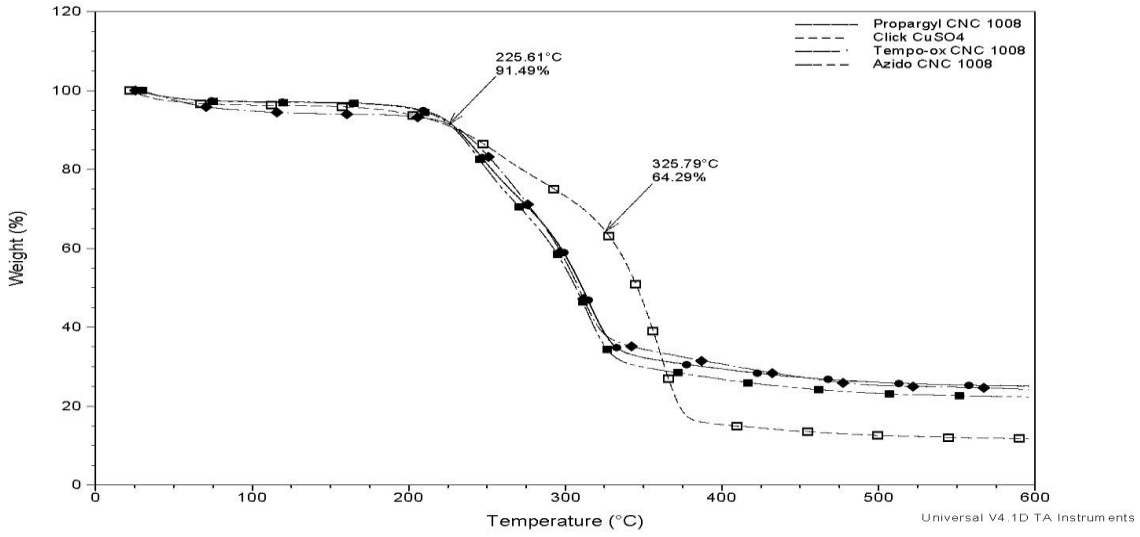

Figure 7.3 TGA curves of tempo-oxidized nanocrystals (circle markers), CNC-PR (cross markers), CNC-AZ (square markers) and CNC-Click (open square markers)

7.4.4 GPC Analysis of "Click"-Derivatives.

The molecular weight distributions of both precursors (CNC-PR and CNC-AZ) and formed click product (CNC-Click) were investigated by the gel permutation chromatography. Due to the insolubility of the cellulosic samples in tetrahydrofuran (THF) samples were benzoylated in prior to the analysis. In order to achieve a high degree of benzoylation, reactions were carried out in ionic liquid, 1-allyl-3-methylimidazolium chloride ([Amim]Cl), that is known to be able to dissolve cellulosic materials.

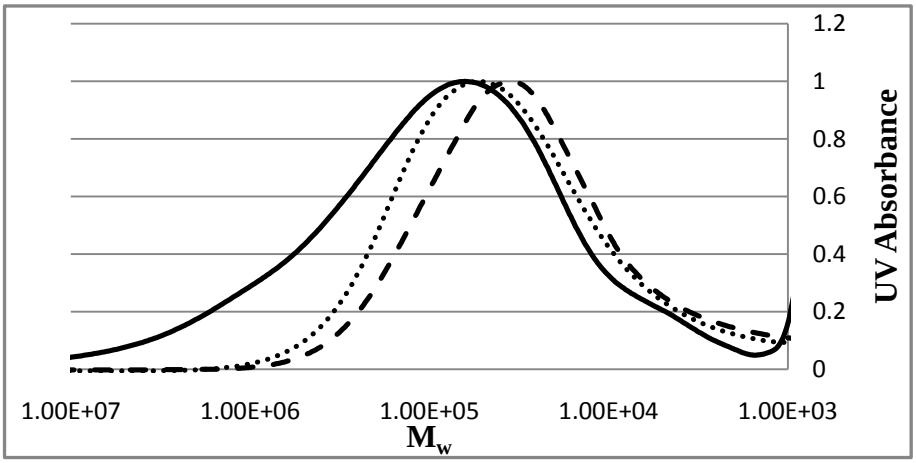

Figure 7.4 Gel permeation chromatograms of CNC precursors (CNC-PR, dotted line) (CNC-AZ, dashed line) and cellulose nano-platelet gel (CNC-Click, solid line)

As expected the molecular weight of click product is considerable higher than those of the starting materials indicating that cross-linking (Huisgen) reaction has occurred (Figure 7.4). As can be seen from the Table 7.2, CNC-Click showed approximately 5 to 6 fold increase in weight average molecular weight (M_w) when compared to its percursors (CNC-PR and

CNC-AZ). Moreover, the significantly elevated polydispersity (PD) value of CNC-Click is characteristic for the highly cross-linked materials.

Table 7.2 Molecular weight distributions of starting precursors (CNC-PR and CNC-AZ) and Click-product (CNC-Click)

Sample	Mw (1 x10^3 $gmol^{-1}$)	Polydispersity (PD)
CNC-PR	72	3.5
CNC-AZ	53	3.4
CNC-Click	335	12.6

7.4.5 TEM Analysis of TEMPO-oxidized CNCs and "Click"-Derivatives.

Electron micrographs of the different cellulose samples are shown in Figure 7.5. It can be seen that the CNCs produced from the HBr hydrolysis of the filter paper are highly aggregated (7.5a) However, after the TEMPO-oxidation of aforementioned CNCs the individualization of the crystals became possible since the oxidation introduces electrostatic repulsion via negatively charged carboxyl groups on the surface of the crystals (Figure 7.5 b). The average size of the crystals was estimated from the well separated oxidized CNCs. The average dimensions of the crystals were found to be approximately 10-20 nm width and 100-200 nm long.

As expected, the TEM image of the crosslinked CNCs revealed significantly larger particles than those obtained from the CNCs (Figure 7.5c). It seems that the cycloaddition reaction has packed the crystals in an organized manner while retaining the rectangular shape of the

starting CNCs. Interestingly, the resulting crosslinked nanoparticles have not only grown one-dimensionally from the derivatized C-6 positions (Figure 7.5c).

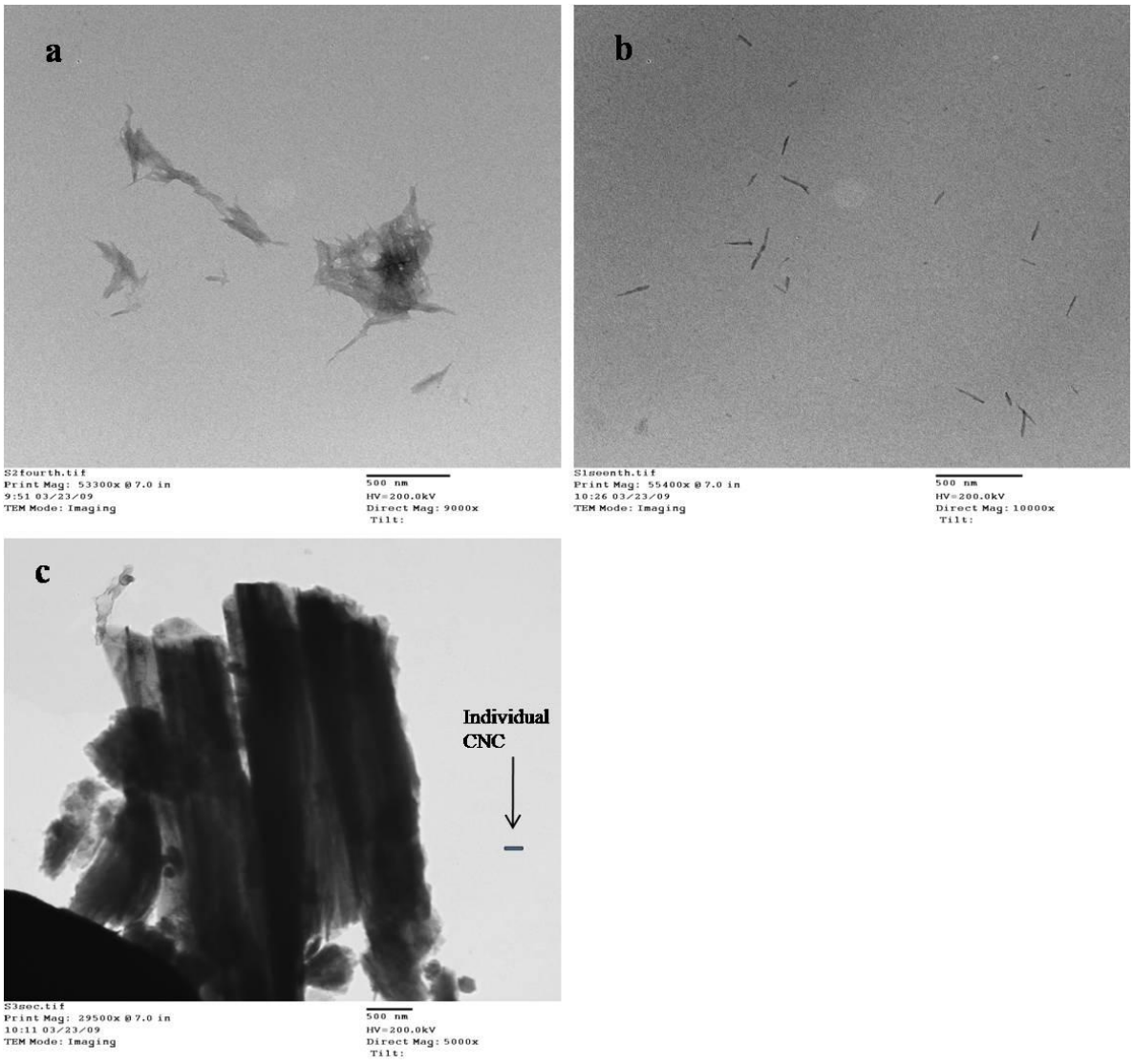

Figure 7.5 TEM images of cellulose nanocrystals (a), TEMPO-oxidized cellulose nanocrystals (b) and cellulose nano-platelet gel (c). Scale bar 500 nm

The insertion of individual CNC reveals the occurrence of two-dimensional growth for the CNC-Click (Figure 7.5c). However, this is not totally surprising when the oxidative

treatment of the starting CNCs is considered. TEMPO-mediated oxidation may introduce carboxylic groups also to the reducing ends of the CNCs.[29,30,31] Therefore, the oxidized reducing end groups can become reactive toward the derivatization conditions that were used to form the alkyne and azido bearing precursors starting from the C-6 position. Subsequently, the modified reducing end groups can also react under the "Click"-chemistry conditions resulting in the two-dimensional growth observed in TEM image.

7.5 Conclusions

"Click"-chemistry has been utilized for the preparation of new gel-like cellulose nanomaterials. The primary hydroxyl groups in cellulose nanocrystals were first selectively oxidized to carboxylic acids. These carboxylic acid functionalities were further used as reactive sites for the amidation reactions to provide the precursors necessary for the "Click"-chemistry reaction. Produced crosslinked nanomaterials were characterized by FTIR, Elemental analysis, GPC, Thermal analysis and TEM.

7.6 References

1. Heinze, T. and Liebert, T. (2001). "Unconventional methods in cellulose functionalization," *Prog. Polym. Sci.*, 26(9), 1689-1762.

2. Klemm, D. K., Heublein, B., Fink, H. P., and Bohn, A. (2005). "Cellulose: Fascinating biopolymer and sustainable raw material," *Angew. Chem. Int. Ed.*, 44(22), 3358-3393.

3. Huang, J. and Kunitake, T. (2003). "Nano-Precision Replication of Natural Cellulosic Substances by Metal Oxides," *J. Am. Chem.Soc.*, 125(39), 11834-11835.

4. Liebert, T., Hornig, S., Hesse, S., and Heinze, T. (2005). "Nanoparticles on the Basis of Highly Functionalized Dextrans," *J. Am. Chem. Soc.,* 127(30), 10484-10485.

5. Huang, J., Ichinose, I., and Kunitake, T. (2006). "Biomolecular Modification of Hierarchical Cellulose Fibers through Titania Nanocoating," *Angew. Chem. Int. Ed.,* 118(18), 2949-2952.

6. Hoffmann, B., Bernet, B., and Vasella, A. (2002). "Oligosaccharide Analogues of Polysaccharides," *Helv. Chim. Acta*, 85(1), 265–287.

7. Gallos, J. K. and Koumbis, A. E. (2003). "1,3-Dipolar Cycloadditions in the Synthesis of Carbohydrate Mimics. Part 1: Nitrile Oxides and Nitronates," *Curr. Org. Chem.*, 7(5), 397–426.

8. Huisgen, R. (1960). "1,3-Dipolar cycloadditions," *Proc. Chem. Soc.*, 357–369.

9. Tornøe, C. W., Christensen, C., and Meldal, M. (2002). "Peptidotriazoles on Solid Phase: [1,2,3]-Triazoles by Regiospecific Copper(I)-Catalyzed 1,3-Dipolar Cycloadditions of Terminal Alkynes to Azides," *J. Org. Chem.*, 67(9), 3057–3064.

10. Rostovtsev, V. V., Green, L. G., Fokin V. V., and Sharpless, K. B. (2002). "A Stepwise Huisgen Cycloaddition Process: Copper(I)-Catalyzed Regioselective "Ligation" of Azides and Terminal Alkynes," *Angew.Chem., Int. Ed.*, 41(14), 2596–2599.

11. Lewis, W. G., Green, L. G., Grynszpan, F., Radic, Z., Carlier, P. R., Taylor, P., Finn, M. G., and Sharpless, K. B. (2002). "Click Chemistry In Situ: Acetylcholinesterase as a Reaction Vessel for the Selective Assembly of a Femtomolar Inhibitor from an Array of Building Blocks," *Angew. Chem.,* 114(6), 1095-1099.

12. Lewis, W. G., Green, L. G., Grynszpan, F., Radic, Z., Carlier, P. R., Taylor, P., Green, M. G., Fokin, V. V., and Sharpless, K. B. (2002). "Click Chemistry In Situ: Acetylcholinesterase as a Reaction Vessel for the Selective Assembly of a Femtomolar Inhibitor from an Array of Building Blocks," *Angew. Chem. Int. Ed.*, 41(6), 1053-1057.

13. Kolb, H. C., Finn, M. G., and Sharpless, K. B. (2001). "Click-Chemie: diverse chemische Funktionalität mit einer Handvoll guter Reaktionen," *Angew. Chem.,* 113(11), 2056-2075.

14. Huisgen, R. (1989). "Kinetics and reaction mechanisms: selected examples from the experience of forty years," *Pure Appl. Chem.*, 61(4), 613−628.

15. Kolb, H. C., Finn, M. G., and Sharpless, K. B. (2001). “Click Chemistry: Diverse Chemical Function from a Few Good Reactions,” *Angew. Chem., Int. Ed.*, 40(11), 2004−2021.

16. Wu, P., Feldman, A. K., Nugent, A. K., Hawker, C. J., Scheel, A., Voit, B., Pyun, J., Fréchet, J. M. J., Sharpless, K. B., and Fokin, V. V. (2004). “Efficiency and Fidelity in a Click-Chemistry Route to Triazole Dendrimers by the Copper(I)-Catalyzed Ligation of Azides and Alkynes,” *Angew. Chem., Int. Ed.*, 43(30), 3928 −3932.

17. Gupta, N., Vestberg, R., Malkoch, M., Hikita, S. T., Thibault, R. J., Lingwood, M., McCarney, E., Han, S., Clegg, O. D., and Hawker, C. J. (2006). “Characterization of poly(ethylene glycol) hydrogels formed via click chemistry,” *Polym. Prepr.*, 47(2), 25−26.

18. Araki, J., Wada, M., and Kuga, S. (2001). “Steric Stabilization of a Cellulose Microcrystal Suspension by Poly(ethylene glycol) Grafting,” *Langmuir*, 17(1), 21-27.

19. Crescenzi, V., Cornelio, L., Di Meo, C., Nardecchia, S., and Lamanna, R. (2007). “Novel Hydrogels via Click Chemistry: Synthesis and Potential Biomedical Applications,” *Biomacromolecules*, 8(6), 1844–1850.

20. Hasegawa, T., Umeda, M., Numata, M., Li, C., Bae, A.-H., Fujisawa, T., Haraguchi, S., Sakuraib, K., and Shinkaia, S. (2006). “‘Click chemistry’ on polysaccharides: a convenient, general, and monitorable approach to develop (1→3)-β-d-glucans with various functional appendages,”*Carbohydr. Res.*, 341(1), 35−40.

21. Ossipov, D. A. and Hilborn, J. (2006). “Poly(vinyl alcohol)-Based Hydrogels Formed by “Click Chemistry”,” *Macromolecules*, 39(5), 1709−1718.

22. Dìaz, D. D., Rajagopal, K., Strable, E., Schneider, J., and Finn, M. G. (2006). ““Click” Chemistry in a Supramolecular Environment: Stabilization of Organogels by Copper(I)-Catalyzed Azide−Alkyne [3 + 2] Cycloaddition,” *J. Am. Chem. Soc.*, 128(18), 6056−6057.

23. Liebert, T., Hänsch, C., and Heinze, T. (2006). “Click Chemistry with Polysaccharides,” *Macromol. Rapid Commun.*, 27(3), 208-213.

24. Hafrén, J., Zou, W., and Córdova, A. (2006). “Heterogeneous ‘Organoclick’ Derivatization of Polysaccharides,” *Macromol. Rapid Commun.*, 27(16), 1362–1366.

25. Araki, J., Wada, M., Kuga, S., and Okano, T. (1999). “Influence of surface charge on viscosity behavior of cellulose microcrystal suspension,” *J. Wood Sci.*, 45(3), 258-261.

26. Araki, J., Wada, M., Kuga, S., and Okano, T. (1998). "Flow properties of microcrystalline cellulose suspension prepared by acid treatment of native cellulose," Colloids *and Surfaces A: Physicochemical and Engineering Aspects*, 142(1), 75–82.

27. Habibi, Y., Chanzy, H., and Vignon, M. R. (2006). "TEMPO-mediated surface oxidation of cellulose whiskers," *Cellulose*, 13(6), 679-687.

28. Da Silva Perez, D., Montanari, S., and Vignon, M. R. (2003). "TEMPO-Mediated Oxidation of Cellulose III," *Biomacromolecules*, 4(5), 1417-1425.

29. Shibata, I. and Isogai, A. (2003). "Depolymerization of cellouronic acid during TEMPO-mediated oxidation," *Cellulose,* 10(2), 151-158.

30. Ibert, M., Marsais F., and Merbouh, N. (2002). "Determination of the side-products formed during the nitro-mediated bleach oxidation of glucose to glucaric acid," *Carbohydr. Res.* 337, 1059–1063.

31. Kato, Y., Matsuo, R., and Isogai A. (2003). "Oxidation process of water-soluble starch in TEMPO-mediated system," *Carbohydr. Polym.*, 51, 69–75.

8. Photoresponsive Coumarin Modified Cellulose Nanocrystals

8.1 Abstract

In this communication a method for the creation of fluorescent cellulose nanoparticles using "Click"-chemistry is demonstrated. In the first step, the primary hydroxyl groups on the surface of the CNCs were converted to carboxylic acids by using TEMPO-mediated hypohalite oxidation. The alkyne groups essential for the "Click"-reaction were introduced into the surface of TEMPO-oxidized CNCs via carbodiimide-mediated formation of an amide linkage between monomers carrying an amine functionality and carboxylic acid groups on the surface of the TEMPO-oxidized CNCs. Finally, the reaction of surface-modified TEMPO-oxidized cellulose nanocrystals and azido-bearing coumarin monomer was carried out by means of a "Click"-chemistry, i.e., the Cu(I)-catalyzed Huisgen 1,3-dipolar cycloaddition to produce higly fluorescent cellulose nanoparticles.

8.2 Introduction

Cellulose is the most abundant and low-cost natural polymer. By virtue of its non-toxicity, biocompatibility and degradability cellulose has a broad application in food, pharmaceutical and chemical industries. However, economically feasible and environmentally friendly chemical processes are required for more efficient utilization of cellulose.[1] Therefore, scientists are constantly seeking new pathways to expand the application range of cellulose while retaining its prominent properties. For example, in the field of photo-luminescence, the cellulose needs to be chemically modified to achieve desirable optical properties.[2]

Typically, this is accomplished by covalently attaching fluorescent dyes on the surface of cellulose either directly or by using cross-linking agents.[3,4]

Cellulose and cellulose derivatives offer several advantages as backbones for photo-responsive polymers. The presence of optically active centers is of particular interest with respect to the formation of a cholesteric state of liquid crystalline properties and interactions with chromophoric molecules.[5,6,7,8] Cellulose derivatives that are soluble in some solvents can be used for the preparation of high quality thin film.[9,10] Thus, if these photoresponsive molecules can be introduced into cellulose and cellulose derivatives, these cellulose and cellulose derivatives could be novel materials for photoresponsive polymers. Furthermore, they might be used as photoreactive materials for applications such as photorecording devices, liquid crystal displays, and other light-sensitive applications.

Efforts have been made to make photoresponsive cellulose derivatives. To date, there are several papers that attempt to prepare the photoresponsive cellulosic polymers with the goal of preparing new materials with the advantages of both starting materials. Most photoresponsive molecules introduced into cellulose derivatives are azobenzene, cinnamate and stilbene molecules.[11,12,13,14,15] The cellulose derivatives containing azobenzene were found to show photoreactivity by UV light irradiation and to form lyotropic liquid crystalline phase.[16,17] However, there are no trials on cellulose derivatives containing coumarin molecules, although they can be expected to possess photoreactivity and to form a liquid crystalline phase.

In this paper, we report a synthesis of fluorescent cellulose nanocrystals (CNCs) by covalently linking of fluorescence chromophore to the cellulose. First, the primary hydroxyl groups on the surface of the CNCs were converted to carboxylic acids by using TEMPO-mediated hypohalite oxidation. In the next step, a compound (propargylamine) carrying a terminal amine functionality was grafted on to the oxidized CNCs via carbodiimide-mediated formation of an amide linkage between an amine and the carboxylic groups on the CNC's surface. The grafted amine was also bearing an alkyne functionality which was then used as a reaction site for the further modification. Finally, the modified CNCs were subjected to "Click-chemistry reaction" i.e. the Cu(I)-catalyzed Huisgen 1,3-dipolar cycloaddition with an azide-bearing fluorescent chromophore resulting in a highly fluorescent cellulose material.

8.3 Materials and Methods

Materials. Whatman #1 filter paper was used as a starting material for the cellulose nanocrystals. Propargylamine (98%) was purchased from Aldrich. All other chemicals were purchased from Aldrich or Fisher and used as received unless otherwise stated.

8.3.1 Acid Hydrolysis of Cellulose to Produce Cellulose Nanocrystals (CNC). The cellulose nanocrystals were formed by acidic hydrolysis similar to the procedure used by Araki *et al.*[18,19,20] A typical procedure was as follows. 2.0 g of cellulose pulp obtained from Whatman #1 filter paper (98% α-cellulose, 80% crystallinity) was blended by a 10 Speed

Osterizer® Blender. Resulting pulp was hydrolyzed with 100 mL of 2.5 M HBr at 100°C for 3 hours. The ultrasonication was applied during (every 60 minutes) the reaction (Omni-Ruptor 250W ultrasonic homogenizer, 50% power, 5 min). The resulting mixture was diluted with de-ionized (D.I) water followed by five cycles of centrifugation at 1500g for 10 min. (IEC Centra-CL3 Series) to remove excess acid and water soluble fragments. The fine cellulose particles became dispersed in the aqueous solution approximately at pH 4. The turbid supernatant containing the polydisperse cellulose particles was then collected for further centrifugation at 15000 g for 45 min (Automatic Servall® Superspeed Centrifuge) to remove ultra-fine particles. Ultra-fine particles with small aspect ratio were removed from the upper layer, and the precipitation (after the high-speed centrifugation) was dried using a lyophilizing system (Labconco, Kansas City, MU).

8.3.2 TEMPO-mediated Oxidation of CNCs. 648 mg (4 mmol of glucosyl units) of cellulose nanocrystals were suspended in water (50 mL) containing 10 mg of 2,2,6,6-tetramethyl-1-piperidinyloxy (TEMPO, 0.065 mmol) and 200 mg of sodium bromide (1.9 mmol) at room temperature for 30 min. The TEMPO-mediated oxidation of the cellulose nanocrystals was initiated by slowly adding 4.90 mL of 13% NaClO (8.6 mmol) over 20 min at room temperature under gentle agitation. The reaction pH was monitored using a pH meter and maintained at 10 by incrementally adding 0.5 M NaOH. When no more decrease in pH was observed, the reaction was considered complete. About 5 mL of methanol was then added to react and quench with the extra oxidant. After adjusting the pH to 7 by adding 0.5 M HCl, the TEMPO-oxidized product was washed with D.I. water by centrifugation

and further purified by dialysis against D.I. water for two days. 550 mg of solid was recovered after freeze-drying. FTIR measurements showed a carboxylic acid peak at 1730 cm^{-1}.

8.3.3 Preparation of 6-((6-hydroxyhexyl)oxy)coumarin (1). A solution of 6-bromohexanol (2g, 12.3mmol), 6-hydroxycoumarin (2.23g, 12.3mmol), and K_2CO_3 (6.82g, 49.3mmol) in 40 mL of butanone was heated at 80℃ for overnight. The reaction solution was filtered to remove inorganic material and then evaporated. The crude product was purified using flash chromatography on silica gel (70% ethyl acetate in hexane, r.f=0.4) to give the compound **1** as a yellow solid (1.65g, 55% yield). ^{1}H NMR (300 MHz, $CDCl_3$) δ 1.47 (m, 4H, $HOCH_2CH_2\mathit{CH_2CH_2}CH_2CH_2O$), 1.60 (quintet, 2H, J=6.6Hz, $\mathit{CH_2}CH2O$), 1.81 (quintet, 2H, J=6.6Hz, $HOCH_2\mathit{CH_2}$), 3.66 (t, 2H, J=6.6Hz, $HO\mathit{CH_2}$), 3.97 (t, 2H, J=6.6Hz, $\mathit{CH_2}O$), 6.40 (d, 1H, J=9.6Hz, $C\mathit{CH}$=CHCOO), 6.88 (d,1H, J=3.0Hz, CCH=CHCOO), 7.08 (d.d, 1H, J=3.0Hz, J=9.0Hz, Ar), 7.24 (d, 1H, J=9.0Hz, Ar), 7.62 (d, 1H, J=9.6Hz, Ar).

8.3.4 Preparation of 6-((6-bromohexyl)oxy)coumarin (2). To a solution of 6-((6-hydroxyhexyl)oxy)coumarin (100 mg, 0.38mmol) and 1,2-bis(diphenylphosphino)ethane (DIPHOS, 182 mg 0.46 mmol) in 3 mL of dried CH_2Cl_2 was slowly added dropwise a solution of carbon tetrabromide (152 mg. 0.46 mmol) in 1 mL of dried CH_2Cl_2 at 0℃ under argon. The reaction mixture was stirred for 1 hour at 0℃ under argon, and then diluted with CH_2Cl_2. The resulting solution of the reaction mixture was filtered through celite. The filtrate was evaporated at reduced pressure and the residue was purified by flash

chromatography on silica gel (33% ethyl acetate in hexane, r.f=0.5) to give compound **2** (111mg, 90% yield). ^{1}H NMR (300 MHz, $CDCl_3$) δ 1.52 (m, 4H, $BrCH_2CH_2\mathit{CH_2CH_2}CH_2CH_2O$), 1.60 (quintet, 2H, J=6.6Hz, $\mathit{CH_2}CH2O$), 1.88 (m, 4H, $BrCH_2\mathit{CH_2}CH_2CH_2\mathit{CH_2}CH_2O$), 3.44 (t, 2H, J=6.6Hz, $Br\mathit{CH_2}$), 3.97 (t, 2H, J=6.6Hz, $\mathit{CH_2}O$), 6.43 (d, 1H, J=9.6Hz, $C\mathit{CH}$=CHCOO), 6.92 (d,1H, J=3.0Hz, CCH=CHCOO), 7.11 (d.d, 1H, J=3.0Hz, J=9.0Hz, Ar), 7.26 (d, 1H, J=9.0Hz, Ar), 7.65 (d, 1H, J=9.6Hz, Ar).

8.3.5 Preparation of 6-((6-azidohexyl)oxy)coumarin (3). A stock solution of 0.25M NaN_3 in dry DMSO was prepared by stirring the solution for 24 hours at 25°C. To a 10 ml round-bottom flask equipped with a magnetic stir bar, was added a 0.25M solution of NaN_3 (24.4mg, 0.38mmol) in DMSO (1.5mL) at 25°C. To this solution was added 6-((6-bromohexyl)oxy)coumarin (100 mg, 0.31mmol), and the mixture was stirred 3 hours at room temperature. The reaction was quenched with D.I. H_2O (3.0 mL) [slightly exothermic] and stirred until it cooled to room temperature. The reaction was extracted with Et_2O (3x15mL); the Et_2O extracts were washed with H_2O (2x15mL) and once with brine (15mL). The organic layer was dried ($MgSO_4$) filtered, and the solvent removed under vacuo (20 Torr) to afford the pure alkyl azide **3** in almost quantitative yield. ^{1}H NMR (300 MHz, $CDCl_3$) δ 1.49 (m, 4H, $N_3CH_2CH_2\mathit{CH_2CH_2}CH_2CH_2O$), 1.59 (quintet, 2H, J=6.6Hz, $\mathit{CH_2}CH2O$), 1.77 (m, 4H, $N_3CH_2\mathit{CH_2}CH_2CH_2\mathit{CH_2}CH_2O$), 3.26 (t, 2H, J=6.6Hz, $N_3\mathit{CH_2}$), 3.96 (t, 2H, J=6.6Hz, $\mathit{CH_2}O$), 6.43 (d, 1H, J=9.6Hz, $C\mathit{CH}$=CHCOO), 6.90 (d,1H, J=3.0Hz, CCH=CHCOO), 7.12 (d.d, 1H, J=3.0Hz, J=9.0Hz, Ar), 7.26 (d, 1H, J=9.0Hz, Ar), 7.65 (d, 1H, J=9.6Hz, Ar).

8.3.6 Synthesis of Alkyne Bearing CNC-Derivative. TEMPO-oxidized CNCs (50mg) were mixed in 6 mL of MES [2-(*N*-morpholino)-ethanesulfonic acid buffer (50 mM, pH = 4). Resulting suspension was further treated with ultrasound treatment (5 min, 20% power with 30% pulser on; Omni-Ruptor 250 Ultrasonic Homogenizer, Omni International Inc.) to break down the cellulose aggregates. In typical synthesis, 120 mg of EDC·HCl [*N*-(3-dimethylaminopropyl)-*N'*-ethylcarbodiimide hydrochloride)], 72 mg of NHS (*N*-hydroxysuccinimide), and 60 μL of propargylamine, respectively, were added to the CNC suspension. The reaction was performed at room temperature under stirring for 24 h. The resulting mixture was dialyzed (cutoff = 12 kDa) against a saturated NaCl solution for 1 day and then against distilled water for 3 days. Finally, the CNC-PR derivatives (see Scheme 8.1) were recovered by freeze-drying.

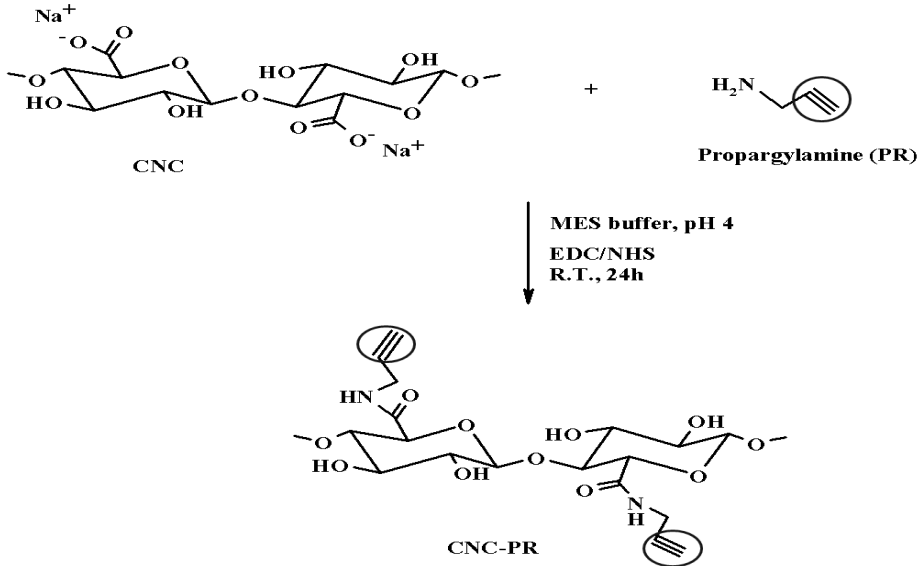

Scheme 8.1 Schematic representation of the reaction between cellulose nanocrystals (CNC) and propargylamine (PR)

8.3.7 Synthesis of "Click"-Product. A 25 mg amount of CNC-PR and a 25 mg of azidocoumarin were mixed in 3.0 mL of distilled water. Next, 25 μL of $CuSO_4$ x $5H_2O$ aqueous solution (7.5% w/v) and 30 μL of Ascorbic acid (1M sol.) were added and the mixture was vigorously stirred in the dark overnight at the room temperature leading to a formation of coumarin modified CNCs (Scheme 8.2). Finally, the CNC-Coumarin was extensively washed with cold water and dichloromethane to remove the inorganic catalyst and the excess azidocoumarin.

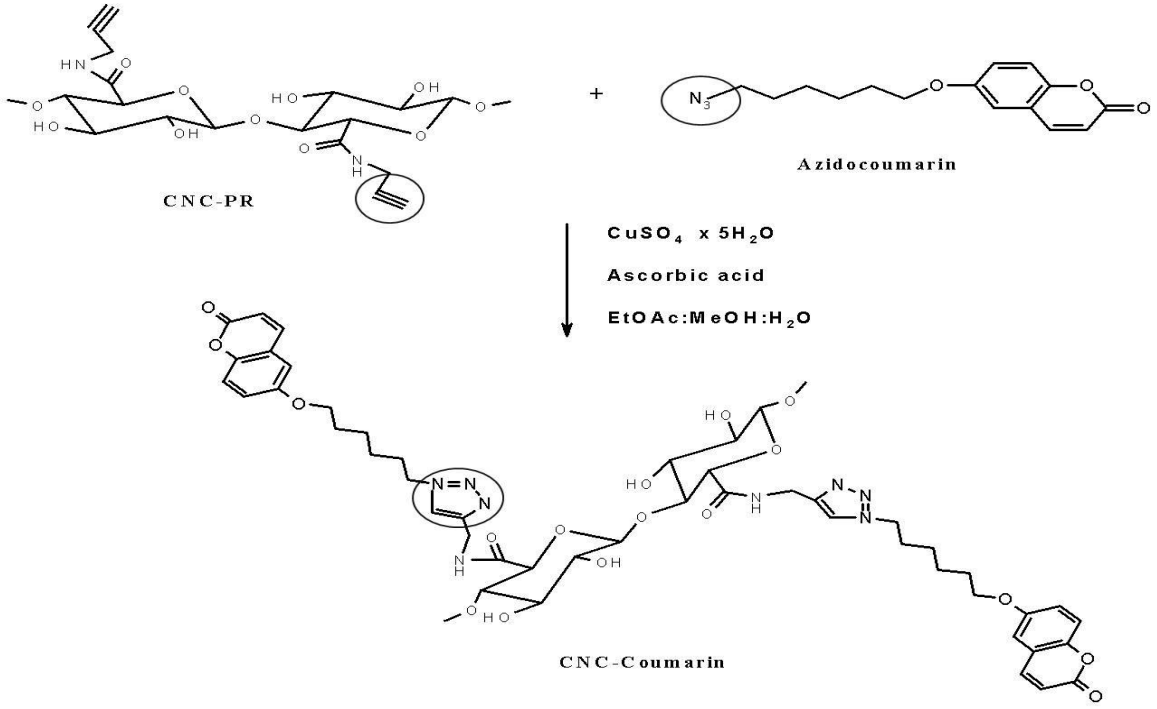

Scheme 8.2 Schematic representation of the reaction between cellulose nanocrystals (CNC) and azidocoumarin

8.3.8 Infrared Spectroscopy. FTIR spectra were measured on a Thermo Nicolet NEXUS 670 FT-IR infrared spectrophotometer. Spectra in the range of 4000 – 650 cm^{-1} were

obtained with a resolution of 4 cm^{-1} by cumulating 64 scans. Degree of oxidation (DO) measurements were carried out by comparing the intensities of absorption band near 1730 cm^{-1} (carbonyl stretching frequency) to that of 1050 cm^{-1} (cellulose backbone).[21]

8.3.9 Acid-base Titration. The carboxylic acid content of the oxidized CNCs was determined by acid-base titration following the procedure developed for the conductometric titrations of such materials.[22] In this procedure tempo-oxidized CNC samples (50mg) were suspended into 0.01 M hydrochloric acid (HCl) solutions (15 ml) with stirring. The resulting suspensions were then titrated with 0.01 M sodium hydroxide (NaOH) solution. The degree of oxidation (DO) value was calculated as already published and very reproducible results were obtained.[22]

8.3.10 Fluorescence Microscopy. Microscope: Olympus BX 51, Objective 40x 0.75 NA, Camera: Q-Imaging Micropublisher 3.3 Excitation: 350/50nm Emission: 460/50 nm Dichroic Beamsplitter: 400 DCLP. The 3D images were taken using Zeiss LSM 710 confocal microscope with the 20x 0.8 NA objective.

8.3.11 Elemental Analysis. The percent carbon (C), hydrogen (H) and nitrogen (N) contents (%) of unreacted TEMPO-oxidized cellulose nanocrystals and the its alkyne derivative were determined by Perkin Elmer element analyzer (Norwalk, CT, USA). The remaining sample was assumed to be oxygen (O).

8.3.12 ^{1}H NMR Spectroscopy. NMR measurements were acquired using on a Bruker 300 MHz spectrometer equipped with a Quad probe dedicated to ^{31}P, ^{13}C, ^{19}F, and ^{1}H acquisition.

8.4 Results and Discussion

TEMPO-oxidized cellulose nanocrystals (CNCs) have been reacted with propargylamine in the presence of the coupling agent N-hydroxysuccinimide to form a precursor suitable for a "Click"-chemistry reaction (Scheme 8.1). The "Click"-reaction was performed with the modified azide-bearing coumarin chromophore which was synthesized starting from 6-hydroxycoumarin (Scheme 8.3).

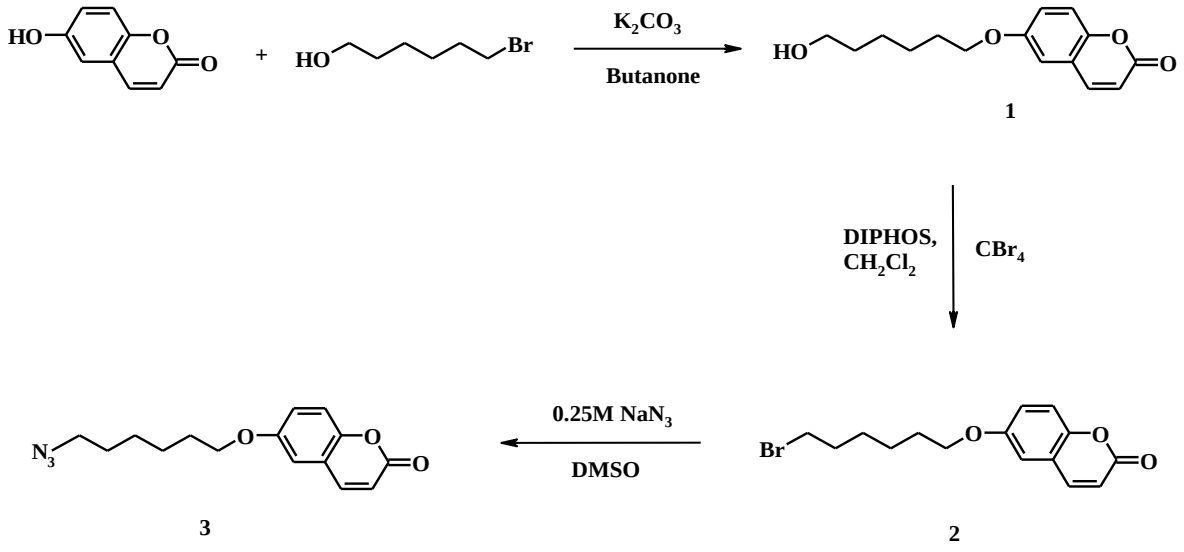

Scheme 8.3 Synthetic route for the preparation of the fluorescent probe **3**

8.4.1 FTIR Analysis of the TEMPO-oxidized CNCs.

In the first step, cellulose nanocrystals were oxidized by using TEMPO-mediated hypohalite oxidation. TEMPO-oxidation selectively converts the primary hydroxyl groups of cellulose to carboxylic acids. Therefore, TEMPO-oxidation provides known pattern of reactive sites for further derivatization reactions. FTIR spectra of TEMPO-oxidized cellulose nanocrystals contains a band around 1730 cm^{-1} which corresponds to the C=O stretching frequency of carboxyl groups in their acidic forms. The degree of oxidation (DO) values can be roughly estimated by comparing the intensity of the new band at 1730 cm^{-1} to that near 1050 cm^{-1} which derives from the cellulose backbone.[21] For example, the corresponding band intensities in Figure 6.2 are 0.23 and 1.10 leading to a DO value of 0.21 (0.23/1.10). This value is in good agreement with the DO value of 0.19 achieved by the acid-base titration of TEMPO-oxidized CNCs.

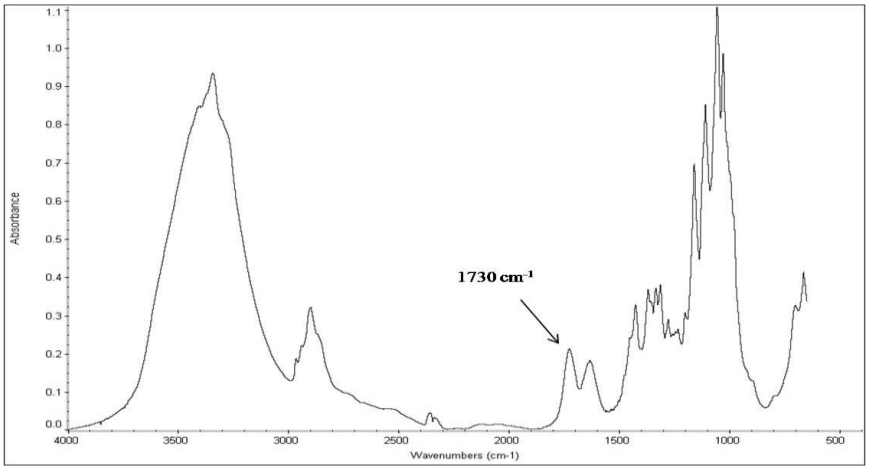

Figure 8.1 FTIR spectra of TEMPO-oxidized cellulose nanocrystals

8.4.2 Elemental Analysis of the Fluorescence "Click"-Derivative.

The nitrogen content of CNC-PR confirmed the successful grafting reaction (Table 8.1). In order to outsource the possibility of the nitrogen deriving from the used crosslinking agents (1-Ethyl-3-[3-dimethylaminopropyl]carbodiimide hydrochloride and *N*-hydroxysulfosuccinimide) the TEMPO-oxidized CNCs were subjected to identical reaction conditions with the absence of the derivatization compound (propargylamine). It is worth to mention here that the content of oxygen is elevated in TEMPO-oxidized CNCs when compared to the CNCs, indicating the successful oxidation reaction. Moreover, the nitrogen content of CNC-PR was found to be higher than that of the starting material (TEMPO-ox. CNCs).

The grafting density of synthesized precursor (CNC-PR) was calculated based on the DO value (0.2) of the oxidized CNCs. The DO value 0.2 means that 20% of the hydroxymethyl groups on cellulose have been oxidized to corresponding carboxylic acid groups and are thus susceptible for the subsequent grafting reactions. Therefore, the maximum grafting density corresponds to the situation where every fifth of the anhydroglucose units in cellulose contain a grafted propargylamine moiety. As a result, the completely grafted TEMPO-oxidized CNCs should contain 1.6% of nitrogen [14 / (5 x 162 + 40)]. However, the amount of nitrogen found in the precursor (CNC-PR) was 0.79% which corresponds to the grafting density of ~50% i.e. half of the available carboxyl groups were grafted with

propargylamine. Incomplete grafting is not totally surprising since the reactions were carried out under heterogeneous conditions.

Table 8.1 Carbon, hydrogen, oxygen and nitrogen contents of cellulosic samples. The amount of protein was calculated from the nitrogen content.

Sample	% C	% H	% N	% O[a]
CNCs	43.55	6.11	0.04	50.30
Tempo-ox. CNCs	41.75	5.76	0.08	52.41
CNC-PR	43.20	5.29	0.79	50.72

[a]O = 100 % - C (%) – H (%) – N (%)

The decision to perform the click reaction between propargyl-modified CNCs (CNC-PR) and azidocoumarin **3** is based on the fact that already fluorescent azidocoumarin **3** will provide additional fluorescence upon a formation of 1,2,3-triazole product as a result of the CuI-catalyzed 1,3-dipolar cycloaddition reactions with terminal alkynes.[23,24] Subsequently, the resulting product (CNC-Coumarin) should be highly fluorescent, and a successful derivatization will be clearly demonstrated. The reaction between modified CNCs (CNC-PR) azidocoumarin **3** proceeds smoothly in aqueous media and gives the corresponding highly fluorescent triazole-modified CNCs (CNC-Coumarin, Scheme 8.2). De-amidation of the CNC-Coumarin with aqueous NaOH produces a highly fluorescent solution, which is a result of the liberation of the triazole coumarin amine probe (Figure 8.2b, left vial). In comparison, the solution from the de-amidation of propargyl modified CNCs (CNC-PR) does not show blue fluorescence (Figure 8.2b, right vial). Thus, the fluorescence of CNC-Coumarin is due to the triazolecoumarin modification.

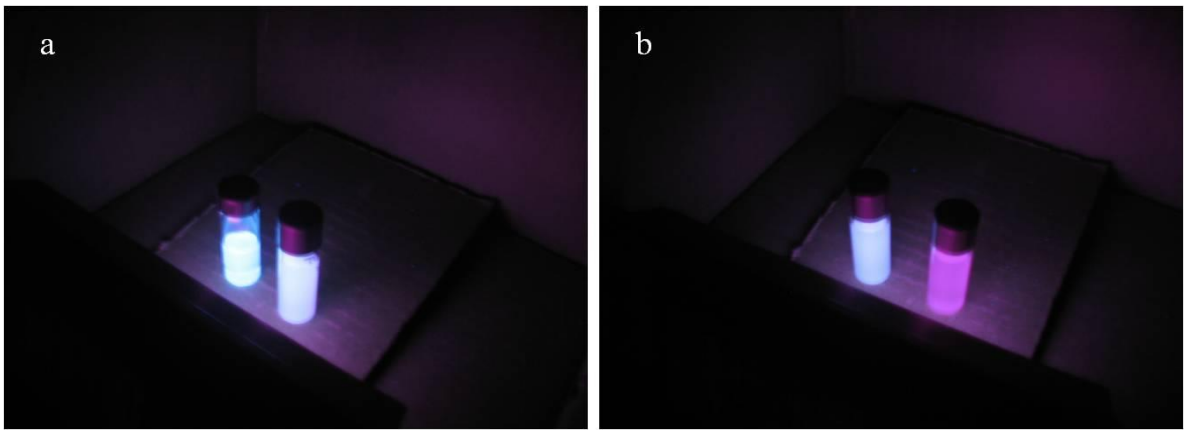

Figure 8.2 a) The left vial contains azidocoumarin **3** dispersed in water, the right vial contains CNC-Coumarin dispersed in water under UV-light. b) The left vial contains the aqueous phase after treatment of CNC-Coumarin with aqueous NaOH under UV light (right vial negative control). Excitation wavelength 366 nm.

8.4.3 Fluorescence Microscopy of the Fluorescence "Click"-Derivative.

The modified CNCs (CNC-Coumarin) are intensely blue fluorescent, as shown by a fluorescence photomicrograph (Figure 8.3c). It is worth to mention here that both succinimide assisted amidation and the CuI-catalyzed 1,3-dipolar cycloaddition are relatively mild reaction conditions for the cellulose nanocrystal modifications. Moreover, the click reaction confirms that CNCs has been grafted with propargylamine, since the copper catalyzed cycloaddition between unmodified TEMPO-oxidized CNCs and azidocoumarin **3** does not provide a fluorescent CNC product (Figure 8.3b). In fact, it appears as non-fluorescent as TEMPO-oxidized CNCs (Figure 8.3a).

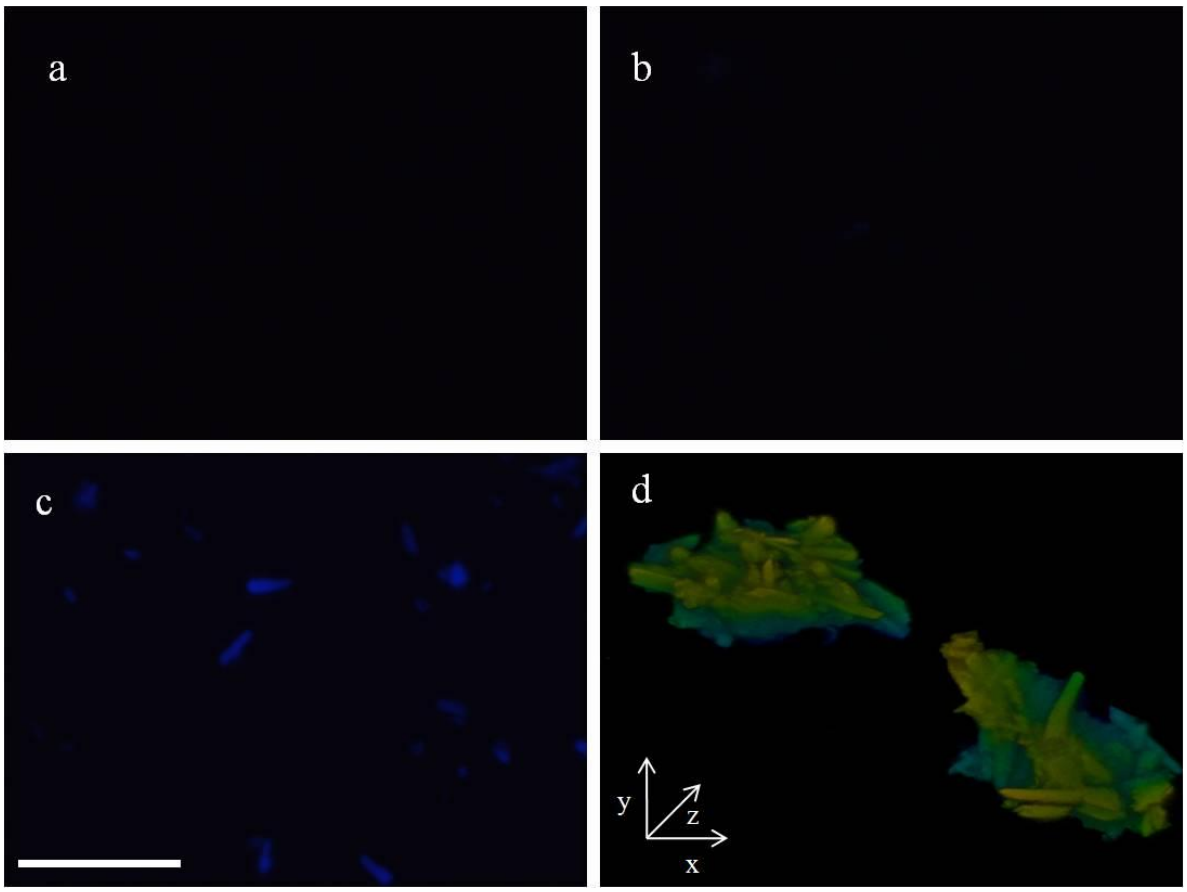

Figure 8.3 a) Fluorescence photomicrograph of TEMPO-oxidized cellulose nanocrystals. b) Fluorescence photomicrograph of the cellulose material after the reaction between TEMPO-oxidized cellulose nanocrystals and azidocoumarin **3** (negative control). c) Fluorescence photomicrograph of CNC-Coumarin dispersed in water. d) 3D reconstructions of 45 images taken at different focus levels (CNC-Coumarin). (scale bars: 50 µm in Figure 8.3c and 20 µm in Figure 8.3d)

The size distribution of the fluorescent cellulose particles (CNC-Coumarin) in water dispersion is rather broad varying from 2 to 15 µm in length and 2 to 5 µm in width (Figure 8.3c). It is important to note that the fluorescent particles are significantly larger than the starting Tempo-oxidized CNCs that possessed nanometer dimensions. This could be due to the aggregation of the derivatized cellulose particles and/or possible [2+2] cycloaddition

between the grafted coumarin side chains which can connect individual nanocrystals to larger particles. The 3D confocal microscopic image of dry state CNC-Coumarin revealed even larger particles having approximate dimensions of 60 x 30 x 20 μm (Figure 8.3d). Moreover, the 3D constructions clearly displayed the formation of bulkier cellulose components as a result of the aggregation of the smaller particles.

8.5 Conclusions

"Click"-chemistry has been utilized for the preparation of new fluorescence cellulose nanomaterials. The primary hydroxyl groups in cellulose nanocrystals were first selectively oxidized to carboxylic acids. These carboxylic acid functionalities were further used as reactive sites for the amidation reactions to provide the precursors necessary for the "Click"- chemistry reaction. Based on this mild, robust and environmentally friendly methodology, highly fluorescent cellulose particles were prepared.

8.6 References

1. Yin, C.Y., Li, J. B., Xu, Q., Peng, Q., Liu, Y. B., and Shen, X. Y. (2007). "Chemical modification of cotton cellulose in supercritical carbon dioxide: Synthesis and characterization of cellulose carbamate," *Carbohydrate Polymers*, 67, 147-154.

2. Dong, S. P and Roman, M. (2007). "Fluorescently labeled cellulose nanocrystals for bioimaging applications," *J. Am. Chem. Soc.*, 129(45), 13810-13811.

3. Siegel, E. Reactive dyes: Reactive groups. (1972). In: Venkataraman K, ed. The Chemistry of Synthetic Dyes, vol. 6, Chapter 1. New York: Academic Press.

4. Hensel, H. R., and Luetzel, G. (1965). "Reactions of metal acetylacetonates," *Angew Chem Int Ed.*, 4(2), 312-318.

5. Gilbert, R. D. and Patton, P. A. (1983). "Liquid-crystal formation in cellulose and cellulose derivatives," *Progress in Polymer Science,* 9(2-3), 115-131.

6. Haurand, P. and Zugenmaier, P. (1991). "Structure and phase behavior of a lyotropic mesophase system: cellulose tricarbanilate-methyl acetoacetate," *Polymer,* 32(16), 3026-3037.

7. Yoshiyuki, N. and Ryotaro, C. (2003). "Structural characteristics and novel functionalization of liquid-crystalline polysaccharides and cholesterol derivatives," *Ekisho,* 7(3), 218-227.

8. Yim, C. T., Gilson, D. F. R., Kondo, T., and Gray, D. G. (1992). "Order parameters and side-chain conformation in ethyl cellulose/chloroform liquid crystal phases," *Macromolecules,* 25(13), 3377-3380.

9. Burchard, W. (2003). "Solubility and Solution Structure of Cellulose Derivatives," *Cellulose,* 10(3), 213-225.

10. Akira, I. Atsushi, I., and Junzo, N. (1984). "Preparation of tri-O-substituted cellulose ethers by the use of a nonaqueous cellulose solvent," *Journal of Applied Polymer Science,* 29(12), 3873-3882.

11. Arai, K. and Udagawa, H. (1988). "Application of photoresponsive groups-containing cellulose as an adsorbent for thin layer chromatography," *Makromolekulare Chemie, Rapid Communications,* 9(12), 797-800.

12. Tang, X., Gao, L., Fan, X., and Zhou, Q. (2007). "Controlled grafting of ethyl cellulose with azobenzene-containing polymethacrylates via atom transfer radical polymerization," *Journal of Polymer Science, Part A: Polymer Chemistry,* 45(9), 1653-1660.

13. Yang, K., Yang, S., and Kumar, J. (2006). "Formation mechanism of surface relief structures on amorphous azo-polymer films," *Physical Review B: Condensed Matter and Materials Physics*, 73(16), 1-14.

14. Arai, K. (1992). "Development of cellulosic optically functional materials," *Kami Pa Gikyoshi*, 46(8), 969-980.

15. Yashima, E., Noguchi, J., and Okamoto, Y. (1995). "Photocontrolled Chiral Recognition by [4-(Phenylazo)phenyl]carbamoylated Cellulose and Amylose Membranes," *Macromolecules,* 28(24), 8368-74.

16. Wu, C., Gu, Q., Huang, Y., and Chen, S. (2003). "The synthesis and thermotropic behaviour of an ethyl cellulose derivative containing azobenzene-based mesogenic moieties," *Liquid Crystals,* 30(6), 733-737.

17. Arai, K. and Udagawa, H. (1990). "Photoregulation of liquid crystalline phase of cellulose containing azobenzene moiety," *Sen'i Gakkaishi,* 46(4), 150-154.

18. Araki, J., Wada, M., Kuga, S., and Okano, T. (1999). "Influence of surface charge on viscosity behavior of cellulose microcrystal suspension," *J. Wood Sci.,* 45(3), 258-261.

19. Araki, J., Wada, M. and Kuga, S. (2001). "Steric stabilization of a cellulose microcrystal suspension by polyethylene glycol (PEG) grafting," *Langmuir*, 17(1), 21-27.

20. Araki, J., Wada, M., Kuga, S., and Okano, T. (1998). "Flow properties of microcrystalline cellulose suspension prepared by acid treatment of native cellulose," Colloids *and Surfaces A: Physicochemical and Engineering Aspects,* 142(1), 75–82.

21. Habibi, Y., Chanzy, H., and Vignon, M. R. (2006). "TEMPO-mediated surface oxidation of cellulose whiskers," *Cellulose,* 13(6), 679-687.

22. Da Silva Perez, D., Montanari, S., and Vignon, M. R. (2003). "TEMPO-Mediated Oxidation of Cellulose III," *Biomacromolecules,* 4(5), 1417-1425.

23. Sivakuman, K., Xie, F., Cash, B. M., Long, S., Barnhill, H. N., and Wang, Q. (2004). "A Fluorogenic 1,3-Dipolar Cycloaddition Reaction of 3-Azidocoumarins and Acetylenes," *Org. Lett.,* 6(24), 4603-4606.

24. Beatty, K. E., Xie, F., Wang, Q., and Tirrell, D. A. (2005). "Selective Dye-Labeling of Newly Synthesized Proteins in Bacterial Cells," *J. Am. Chem. Soc.,* 127(41), 14150-14151.

9. Future Work

In the present research a methodology for the determination of the reactive hydroxyl groups on cellulose using quantitative ^{31}P NMR has been developed (Chapter 4). The technique was successfully used for monitoring the reactivity changes in cotton cellulose during mechanical treatments. However, the methodology was not yet optimized for the CNCs. Therefore, future work should be conducted with CNCs to further verify the validity of the new ^{31}P NMR method.

Grafting reactions to the reducing end groups of cellulose nanocrystals (CNCs) were demonstrated with small molecules (Chapter 5). However, the experiments with larger molecules (amine-terminated polystyrene) were more controversial and indisputable evidence of coupling reaction could not be provided. The difficulties encountered in the coupling of amine-terminated polystyrene are most likely due to the entropic reasons i.e. likelihood of the hydrophopic amine-terminated polystyrene to find the reducing end aldehyde in hydrophilic CNCs is rather low. However, so called grafting from approach may offer one way to overcome the entropic barriers. For this purpose, N-(2-Amino-ethyl)-2-bromo-2-methyl-propionamide, has already been synthesized (Figure 9.1). It can be used as an initiator in atom transfer radical polymerization (ATRP) reactions. Owing to its amine functionality it can be coupled with the reducing end groups and/or with the carboxylic acid groups in the TEMPO-oxidized CNCs as demonstrated with the other amine bearing

compounds (Chapters 5, 6, 7 and 8). Once successfully coupled with CNCs the ATRP reaction can be commenced from the tertiary bromine functionality of the grafted initiator.

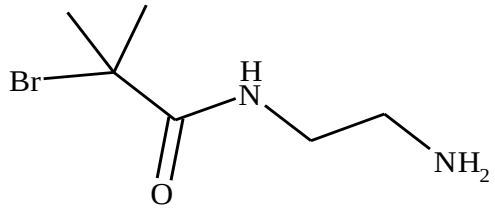

Figure 9.1 ATRP-initiator N-(2-Amino-ethyl)-2-bromo-2-methyl-propionamide

TEMPO-oxidized CNCs were investigated by means of "Click"-chemistry reaction (Chapter 7). It was demonstrated that the CNCs can be modified to produce suitable precursors for the 1,3-dipolar cycloaddition reaction. Moreover, the "Click"-reaction was used to form gel-like materials starting from CNCs (Chapter 7). Future work should include the preparation of the "Click"-precursors with different grafting densities in order to study the cross-linking reaction of CNCs in more details. Furthermore, the physico-chemical properties, such as swelling and viscosity, of formed gel-like materials deserve more attention.

The "Click"-chemistry approach was used for the formation of highly fluorescent CNCs (Chapter 8). It was shown that the coumarin molecules can be introduced as fluorescence dyes in CNCs. However, the possible [2+2] cycloaddition reaction between the coumarin side chains should be investigated. The reversible nature of the cyclodimerization could lead in design of new stimuli photoresponsive nanomaterials such as photorecording devices, liquid crystal displays, and other light-sensitive applications.